TECHNISCHE UNIVERSITÄT MÜNCHEN

Fakultät für Medizin

Inhibition of autocrine signaling of the Epithelial-Mesenchymal Transition in breast cancer

Diana Dragoi

Vollständiger Abdruck der von der Fakultät für Medizin der Technischen Universität München zur Erlangung des akademischen Grades eines

Doktors der Naturwissenschaften

genehmigten Dissertation.

Vorsitzende:	Prof. Dr. Gabriele Multhoff
Prüfer der Dissertation:	1. Prof. Dr. Heiko Lickert
	2. Prof. Dr. Fabian Theis

Die Dissertation wurde am 05.11.2015 bei der Technischen Universität München eingereicht und durch die Fakultät für Medizin am 26.05.2016 angenommen.

Table of Contents

1. Abbreviations

1D/2D/3D	1/2/3 dimensional
7-AAD	7-Aminoactinomycin D
α6-integrin	α6-int
A83	A83-01
ADAM	A Disintegrin And Metalloproteinase
ALK1	Transforming Growth Factor Beta Activin Receptor-like Kinase 1
AP-1	activator protein 1
APS	ammonium persulfate
ATP	adenosine triphosphate
Ax	Axitinib
β-cat	β-catenin
bHLH	basic helix-loop-helix
BIO	6-bromoindirubin-3'-oxime
BRCA1	Breast Cancer 1
BRD4	Bromodomain Containing 4
BRG1	Brahma-related gene-1
BSA	bovine serum albumin
CBP	CREB-binding protein
cDNA	complementary DNA
ChIP	Chromatin Immunoprecipitation Assay
CNS	central nervous system
COPD	chronic obstructive pulmonary disease
CTBP	C-terminal-binding protein
CTC	circulating tumor cell
Ctrl	control
DAPI	4',6-diamidino-2-phenylindole
Dkk-1	Dickkopf-1
DMEM	Dulbecco's Modified Eagle Medium
DMSO	dimethyl sulfoxide
dpi	days post induction
DNA	deoxyribonucleic acid
E-cad	E-cadherin
ECL	enhanced chemiluminescence
EDTA	ethylenediaminetetraacetic acid
e.g.	for example
EGF	epidermal growth factor
EGFR	epidermal growth factor receptor
EGTA	ethylene glycol tetraacetic acid
EMT	Epithelial-Mesenchymal Transition
EndMT	endothelial-mesenchymal transition

ER	estrogen receptor
ERBB2	EGF receptor 2
FACS	fluorescence-activated cell sorting
FCS	fetal calve serum
FGF	fibroblast growth factor
FN	fibronectin
FOX	forkhead box
FZD	Frizzled
G3BP2	GTPase Activating Protein (SH3 Domain) Binding Protein 2
GFP	green fluorescent protein
GSK3β	glycogen synthase kinase 3 β
h	hour(s)
HC	Hemacolor
HDAC	histone deacetylase
HEPES	4-(2-hydroxyethyl)-1-piperazineethanesulfonic acid
HER2	human epidermal growth factor receptor 2
HMEC	Human Mammary Epithelial Cells
HMGA2	high mobility group A2
HMLE	Immortalized Human Mammary Epithelial Cells
HRP	horseradish peroxidase
hTERT	human telomerase reverse transcriptase
ICB	Institute for Computational Biology
ID	inhibitor of DNA binding
i.e.	id est: that is
IGF	insulin growth factor
IPF	Idiopathic Pulmonary Fibrosis
IWP2	inhibitors of Wnt production 2
JAG1	Jagged1
JNK	c-Jun N-terminal kinase
KLF8	Krüppel-like factor 8
Lam	Laminin-1
LB	lysogeny broth
LEF1	lymphocyte enhancer binding factor 1
LGR5	Leucine-rich repeat-containing G-protein coupled receptor 5
LOL2	lysyl oxidase-like 2
LRP	low-density lipoprotein receptor–related protein
MAPK	Mitogen-activated protein kinase
MBOAT	membrane-bound O-acyltransferase
MC	methylcellulose
MDCK	Madin-Darby Canine Kidney Epithelial Cells
MET	Mesenchymal-Epithelial Transition
min	minute(s)
miRNA	micro RNA
MMP	matrix metalloproteinase

mRNA	messenger RNA
MRTF	myocardin-related transcription factors
NaCl	sodium chloride
N-cad	N-cadherin
NICD	Notch intracellular domain
ON	over night
OVOL	OVO-like
PBS	phosphate-buffered saline
Pc2	polycomb 2
PCAF	p300/CBP-associated factor
pCR	pathological complete response
PDGF	platelet-derived growth factor
PDGF receptor α	PDGFRα
PDK1	protein kinase D1
PDL	Poly-D-Lysine
PEI	polyethyleneimine
Pen/Strep	Penicillin/Streptomycin
PFA	paraformaldehyde
PR	progesterone receptor
Prrx1	Paired Related Homeobox 1
PVDF	polyvinylidene fluoride
RBP-Jk	Recombination Signal Binding Protein For Immunoglobulin Kappa J Region
RIPA	radioimmunoprecipitation assay
RIPK2	receptor-interacting serine/threonine-protein kinase 2
RLU	relative light units
RNA	ribonucleic acid
RT	room temperature
RT-PCR	Real-Time Polymerase Chain Reaction
SBE	smad binding elements
SDS	sodium dodecyl sulfate
SDS-Page	Sodium Dodecyl Sulfate Polyacrylamide Gel Electrophoresis
sec	second(s)
SFE	sphere forming efficiency
shRNA	small hairpin RNA
SIP1	Smad-interacting protein 1
SP	SP600125
sm	small-molecule
SWI/SNF	SWItch/Sucrose Non-Fermentable
TAK1	TGFβ-associated kinase 1
TAM	4-hydroxytamoxifen
TAT	Timm’s Acquisition Tool
TBS	Tris-buffered saline
TCF	T cell factors
TEMED	tetramethylendiamine

TF	transcription factor
TGFBR/TGFR	Transforming Growth Factor beta Receptor (gene/protein)
TGFβ	Transforming Growth Factor beta
TIC	tumor-initiating cell
TNBC	triple-negative breast cancer
TNS	Trypsin Neutralizing Solution
TRAF6	tumor necrosis factor (TNF)-receptor-associated factor 6
TTT	Timm's Tracking Tool
uPA	urokinase-type plasminogen activator
VEGF	vascular endothelial growth factor
VEGFR1	VEGF receptor 1
Vim	Vimentin
Wnt	Wingless-Type MMTV Integration Site Family Members
WR	tryptophan/arginine
WST-1	water soluble tetrazolium 1
XAV	XAV939
ZEB1/2	Zinc Finger E-Box Binding Homeobox 1/2

2. Introduction

This work investigated molecular mechanisms governing the Epithelial-Mesenchymal Transition (EMT) in breast cancer and functional outcomes of blocking EMT-inducing signaling pathways. The corresponding theoretical background is provided in the introduction. Thus, clinical features of breast cancer are presented, followed by a description of the role of EMT in development and disease. Subsequently, the regulation of EMT, including signaling pathways and transcriptional, as well as post-transcriptional regulators are reported on. Finally, current therapeutic strategies targeting EMT in breast cancer are described.

2.1 Breast cancer

2.1.1 Epidemiology and clinical subtypes

Worldwide, breast cancer has the highest incidence of all cancer types in women, registering 1,677,600 new patients every year (Torre et al., 2015). Likewise striking is the fact that breast cancer is the most common cause of death amongst all cancer types in women (Torre et al., 2015). Classifications of breast tumors with impact on therapeutic strategies are mainly based on clinical parameters (age, node status, tumor size, histological grade) and the pathological markers Estrogen Receptor (ER), Progesterone Receptor (PR) and Human Epidermal Growth Factor Receptor 2 (HER2) (Valentin et al., 2012; Prat and Perou; 2011). For example, patients bearing ER positive (ER+) tumors often receive adjuvant treatment with tamoxifen, an ER inhibitor, or aromatase inhibitors, which block estrogen production. Indeed, it has been shown that tamoxifen or aromatase inhibitors decrease the risk of cancer recurrence and mortality by up to 30 % in patients suffering from ER+ breast cancer (Early Breast Cancer Trialists' Collaborative Group, 1998; Mauri et al., 2006). Similarly, in patients overexpressing HER2, administration of the anti-HER2 antibody trastuzumab in combination with chemotherapy resulted in improved survival rates (Piccart-Gebhart et al., 2005; Perez et al., 2014).

Triple Negative Breast Cancer (TNBC)

Tumors which do not express any of the receptors ER, PR or HER2 are termed 'triple-negative breast cancers' (TNBC). Although TNBCs account for only 15 – 20 % of all breast cancers (Carey et al., 2006), they are the most difficult to treat because of their aggressive phenotype, poor prognosis and the lack of targeted therapies (Podo et al., 2010). Additionally, albeit the mean age of overall breast cancer patients at diagnosis is around 57 years, the number of women diagnosed with TNBC increases with younger ages (Parise and Caggiano, 2014). Thus, more than 21 % of women are younger than 40 years when diagnosed with TNBC. The occurrence of TNBC at early ages is partially due to the fact that two in nine women with TNBC harbor a BRCA1 mutation, resulting in deficient DNA repair, which causes genetic aberrations that drive carcinogenesis (Tun et al., 2014). In addition, the aggressive phenotype of TNBC is reflected by high tumor grades based on a majority of poorly differentiated and undifferentiated cancer cells (Parise and Caggiano, 2014).
Due to the absence of hormone receptors expression (ER, PR, HER2), TNBC is often treated by means of chemotherapy rather than targeted therapies (Amos et al., 2012). Although TNBC initially displays significantly higher pathological complete response (pCR) rates to chemotherapy compared to ER+ breast tumors (27 % versus 7 %), patients suffering from TNBC show worse survival due to higher rates of relapse among those with residual disease after chemotherapy (Carey et al., 2007; Liedtke et al., 2008). In fact, TNBC has increased likelihood of distant recurrence and death within 5 years of diagnosis compared to other breast cancer phenotypes (Dent et al., 2007). The poor prognosis associated with TNBC and heterogeneous responsiveness to chemotherapy call for targeted, individualized therapies (Prat et al., 2010).

2.1.2 Molecular subtypes

To better understand the biological heterogeneity of breast tumors, Perou, Sørlie and colleagues have performed global gene expression analysis of human breast carcinomas and identified five different molecular subtypes (Luminal A, Luminal B, HER2-enriched, Basal-like and Normal breast-like) (Perou et al., 2000; Sørlie et al., 2001). Later, a sixth distinct subtype, called 'Claudin-low', was discovered in both mouse and human samples (Herschkowitz et al., 2007). Cells from the luminal group

(Luminal A and Luminal B) are ER+ and express a set of genes that encode typical proteins of luminal epithelial cells. HER2 positive tumors express high levels of HER2 and genes related to the HER2 amplicon (Perou et al., 2000; Sørlie et al., 2001). Similarly to the definition of the luminal subtype, which is based on the genetic profile of developmental cell lineages in the mammary gland, Basal-like tumors express the same markers as the basal/myoepithelial cell population, such as cytokeratin (CK) 5/14/17 and laminin (Valentin et al., 2012). However, whether Basal-like tumors actually arise from the basal/myoepithelial compartment is still debated, since it was shown that deletion of the BRCA1 gene (which is associated with Basal-like tumors) in luminal progenitors resulted in Basal-like breast cancer, whereas its deletion in basal cells did not (Molyneux et al., 2010). Normal breast-like tumors where named this way due to their genetic clustering with normal breast specimens (Perou et al., 2000). Finally, Claudin-low breast tumors are characterized by low expression of the tight junction proteins Claudin 3, 4, 7 and Occludin, and the cell-cell adhesion protein E-cadherin (Herschkowitz et al., 2007). Hierarchical clustering analysis of human breast tumors places the Claudin-low group next to the Basal-like subtype, indicating that both tumor types share some gene expression features (Prat and Perou, 2011). Indeed, these two groups mostly lack ER, PR and HER2 expression, thus constituting 79 % of the TNBC phenotype (Prat and Perou, 2011). Both groups exhibit mesenchymal traits, albeit the Claudin-low subtype correlates much stronger with an EMT-related gene expression profile compared to Basal-like tumors (Prat et al., 2010; Sarrió et al., 2008; Marchini et al., 2010). Thus, Claudin-low tumors show the highest gene expression of the mesenchymal markers vimentin and fibronectin, and of several EMT transcription factors (ZEB1/2, Snail1/2, Twist1) acting as E-cadherin repressors compared to other tumor subtypes (Prat et al., 2010). Additionally, EMT induction in a Neu-transgenic-mouse-derived epithelial cell line led to a Claudin-low gene expression profile (Asiedu et al., 2011). These findings were corroborated by experiments showing that combined expression of Ras and Twist1 in luminal-committed cells resulted in the development of Claudin-low breast tumors *in vivo* (Morel et al., 2012). The contribution of EMT to generation of Claudin-low tumors extends from *in vivo* observations to breast cancer cell lines. More precisely, several mesenchymal breast cancer cell lines, including the highly tumorigenic MDA-MB-231 cells, cluster with the Claudin-low gene signature (Prat et al., 2010). Thus,

understanding the molecular mechanisms governing EMT might reveal new therapeutic targets for patients suffering from TNBC.

2.2 The Epithelial-Mesenchymal Transition (EMT)

Epithelial cells are characterized by an apico-basal polarity and cobblestone-like morphology. These are arranged in well-organized clusters, based on strong cell-cell adherens junctions. Through the process of Epithelial-Mesenchymal Transition (EMT), epithelial cells lose expression of cell-cell junction proteins, such as E-cadherin, detach from their neighboring cells and aquire a front-to-back polarity with high expression of mesenchymal markers, such as N-cadherin, fibronectin and the intermediate filament vimentin. By gaining migratory abilities, cells then detach from their original site of residence and colonize distant territories (Hay and Zuk, 1995). Importantly, for this last step of colonization, cells need to revert back to their epithelial state by undergoing MET (Mesenchymal-Epithelial Transition), the reverse of the EMT process. EMT and MET have first been discovered during embryonic development (Hay, 1968 and 1991) and only in the past decade they have also been shown to play a key role in cancer formation and progression (Kalluri and Weinberg, 2009; Polyak and Weinberg, 2009; Peinado et al, 2007; Thiery et al., 2009). Additionally, the EMT program mediates pathological fibrosis upon inflammation or injury (O'Connor JW and Gomez EW, 2014).

2.2.1 Embryonic development and other physiological processes require EMT

During embryonic development, multiple rounds of EMT and its counterplayer MET lead to the formation of germ layers, the nervous system and finally, whole organs (Hay, 1968). The first EMT event in the embryo occurs during gastrulation, when cells from the epiblast detach from the epithelial layer and internalize to form two additional layers, the mesoderm and the endoderm. The epithelial cells remaining in the epiblast give rise to the ectoderm, part of which thickens during neurulation to form the so-called neural plate. As a next step, the neural plate folds on itself into the neural tube, a precursor of the brain and spinal cord. Cells deriving from the neural folds, residing between the neural tube and the overlying epidermis, emerge to the neural crest. In a second EMT event, these neural progenitor cells start migrating and

produce components of the peripheral nervous system. Similarly, cells from the mesoderm and the endoderm pass through several EMT and MET cycles, thereby contributing to the generation of new tissue entities, such as the heart, skeletal muscles, bones and the digestive system (Acloque et al., 2009).
Other physiological processes that employ EMT are wound healing upon injury and the menstrual cycle (Thiery et al., 2009).

2.2.2 EMT in pathological processes

Tumor formation and propagation

In several solid cancer types, malignant cells were found to recapitulate the otherwise developmentally restricted EMT program to facilitate tumor progression and metastasis. When EMT is triggered in epithelial cells from a primary tumor, these start loosing adherence to the neighbouring cells and become highly migratory and invasive. By breaking through the basement membrane, cancer cells gain the ability to penetrate surrounding blood vessels, leading to a systemic dissemination of the tumor. At distant sites, cancer cells can then extravasate and give rise to secondary tumors by undergoing MET (Fig. 1; Scheel and Weinberg, 2012).

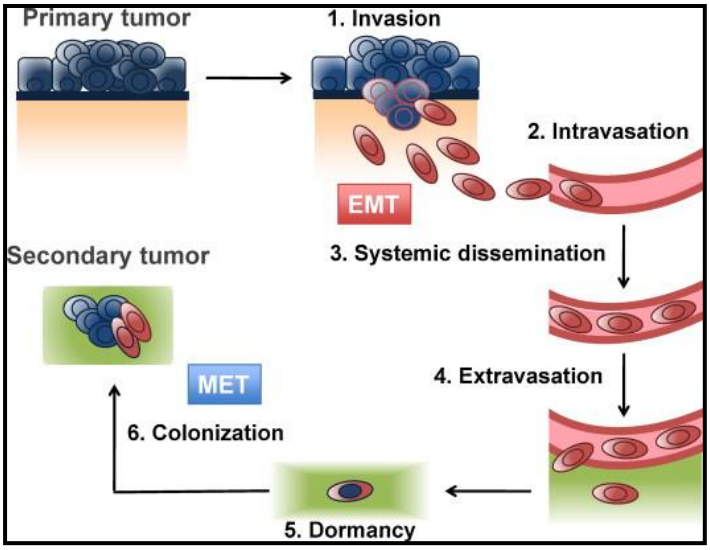

Figure 1: EMT in tumor progression and metastasis.
(from Scheel and Weinberg, 2012)

Very often, single-cells undergo a full EMT at the invasive front of a tumor, thereby losing the epithelial marker E-cadherin and delaminating into single migratory cells (Prall, 2007; Brabletz et al., 2001). Nevertheless, studies done in breast cancer reveal that the original acquisition of invasive properties is not strictly linked to a complete EMT. Thus, cancer cells can also disseminate by undergoing only a partial EMT and retaining an epithelial morphology, including E-cadherin expression (Shamir et al., 2014; Aceto et al., 2015). While whether a complete initial epithelial-

mesenchymal switch is required for distant metastasis or not is still debated (Giampieri et al., 2009; Cheung and Ewald, 2004), there is strong evidence that cancer cells depend on epithelial properties for colonization of a secondary site (Nieto 2013). This might be explained by the fact that mesenchymal cells show reduced proliferation capacity compared to epithelial cells and relocate resources for an efficient migration program, thereby losing their colonization abilities (LeBleu et al., 2014; Schmidt et al., 2015). Thus, if EMT transcription factors (EMT-TFs) are downregulated after initial tumor dissemination, cancer cells regain proliferative capacity and can form metastasis more efficiently compared to a sustained mesenchymal state (Schmidt et al., 2015; Tsai et al., 2012; Ocana et al., 2012).

Fibrosis

Besides tumor development, another pathological process involving EMT is organ degeneration, accompanied by pathological fibrosis. Analysis of samples from patients suffering from Ideopathic Pulmonary Fibrosis (IPF) and chronic obstructive pulmonary disease (COPD) showed that EMT is implicated in the deposition of excess collagen fibers in the surroung tissue, therby compromising organ function and leading to its failure (Bartis et al., 2014). Also in the kidney it was observed that during renal fibrosis epithelial cells convert to interstitial myofibroblasts through EMT. These myofibroblasts are then responsible for building the fibrotic collagen network (Iwano et al., 2002; Boutet et al, 2006).

2.3 Regulation of the EMT program

The EMT program is regulated at different cellular levels (Lamouille et al., 2014). Exogenously, growth factors and signaling molecules such as Transforming Growth Factor beta (TGFβ) and Wingless-Type MMTV Integration Site Family members (Wnt) bind to cellular membrane receptors and propagate the signal inside the cell. These signaling pathways then activate the transcriptional machinery of EMT, orchestrated by EMT-TFs. On a post-transcriptional level, the homeostasis of EMT-TFs and of their target genes is balanced by micro RNAs (miRNAs) and proteasomal degradation (Nieto, 2011). In the following, all three regulation levels will be exemplified.

2.3.1 Transcriptional regulators of EMT

EMT is orchestrated by a set of pleiotropic transcription factors from the basic helix-loop-helix (Twist, E proteins, IDs), Snail (Snail, Slug) and ZEB (ZEB1, ZEB2) families. Depending on tissue and signaling context, these factors are employed differentially and/or sequentially to elicit EMT, as they generate unique expression profiles (Peinado et al., 2007). In general, EMT-TFs repress transcription of epithelial genes, while upregulating mesenchymal markers (De Craene and Berx, 2013). Often, the factors control each other's transcription or cooperate at the promoters of target genes (Lamouille et al., 2014).

Basic Helix-loop-helix family transcription factors

The basic helix-loop-helix (bHLH) family comprises transcription factors that act either as homodimers or as heterodimers to determine transcription of target genes. Amongst these bHLH factors, the Twist proteins Twist1 and Twist2, the E proteins E12/E47 (representing two different splicing products of the E2A gene), and inhibitor of DNA binding (ID) proteins 1-4 are known to be involved in EMT (Xu et al., 2009). As this work focuses on Twist1 and its role in EMT and cancer, this factor will be described more in detail in the following.

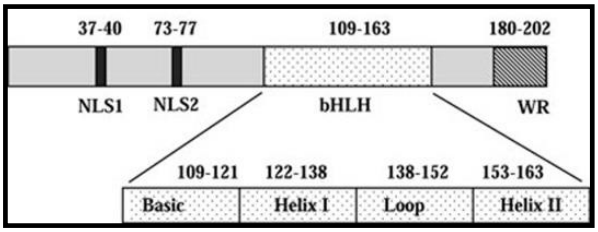

Figure 2: Molecular structure of the human Twist1 protein. NLS, nuclear localization signal; WR, tryptophan/arginine motif (modified from Qin et al., 2012)

Twist1 was first discovered in *Drosophila*, where it was shown to be essential for mesoderm specification and dorsal-ventral patterning (Simpson, 1983). Mouse embryos lacking Twist1 failed to form the cranial neural tube and died before birth, thereby attributing Twist1 a key role during embryonic development (Chen and Behringer, 1995). Consequently, mutations of the Twist1 gene resulted in the Saetrhe-Chotzen syndrome, the most common autosomal dominant disorder of craniosynostosis in humans (Howard et al., 1997; el Ghouzzi et al., 1997). The Twist1 protein consists of a bHLH domain, two nuclear localization domains and a tryptophan/arginine (WR) motif (Fig. 2; Qin et al., 2012). The basic region is the main domain responsible for DNA binding, while the two alpha helices mediate dimerization with E proteins. Typically, Twist1 forms heterodimers with E proteins

and together they bind to E-box regulatory sequences of target genes (Massari and Murre, 2000). The WR motif, also known as Twist box (Spring et al., 2000), has been demonstrated to function as a transactivation domain and therefore increase Twist1-driven transcription independently of and more potently than the E protein activation domain (Laursen et al., 2007). The stability of Twist1 protein is enhanced by phosphorylation through MAPK signaling, which prevents Twist1 ubiquitination and degradation (Hong et al., 2011). Another factor affecting Twist1 protein activity is its cytoplasmic binding partner GTPase Activating Protein (SH3 Domain) Binding Protein 2 (G3BP2), which impedes Twist1 nuclear translocation (Wei et al., 2015). With increasing matrix stiffness, as observed during cancer progression, G3BP2 releases Twist1, thus promoting EMT and invasion (Wei et al., 2015). Indeed, it was shown that Twist1 induces EMT and enhances metastatic potential by upregulation of the mesenchymal marker N-cadherin and transcriptional repression of E-cadherin (Yang et al., 2010; Yang et al. 2012). Moreover, Twist1 was found to be upregulated in various human cancers and it conferred breast cancer cells the ability to metastasize from the mammary gland to the lung (Ansieu et al., 2008; Yang et al., 2004). A detailed examination of cytoskeletal changes revealed that Twist1 regulates invasion by promoting invadopodia formation and extracellular matrix degradation (Eckert et al., 2011). Nevertheless, evidence emerges that Twist1 levels have to be reduced after initial EMT induction in order for metastasis to occur. More precisely, continuous Twist1 activation in a squamous cell carcinoma model inhibited proliferation of disseminated tumor cells at distant sites, while turning off Twist1 allowed re-epithelialization and metastatic outgrowth (Tsai et al., 2012). Similar observations were made in breast epithelial cells, where transient Twist1 activation was required for acquisition of colonization abilities (Schmidt et al., 2015).

Accompanying Twist1 in its role as an EMT inducer, the E proteins E12/E47 directly bind to the E-cadherin promoter, thereby repressing gene transcription (Perez-Moreno et al., 2001). Besides E-cadherin, E47 also represses the cell-cell adhesion protein desmoplakin and contributes to the acquisition of a mesenchymal phenotype by inducing N-cadherin and the matrix-associated proteins SPARC and α5-integrin (Moreno-Bueno et al., 2006). In addition, E47 stabilized Twist1 by formation of heterodimer complexes, an effect which was reversed by ectopic expression of ID1, which sequestered E47, resulting in Twist1 degradation (Hayashi et al., 2007). ID

proteins lack the DNA binding domain, but can functionally interact with other bHLH factors, such as E proteins and antagonize them (Norton, 2000; Kondo et al., 2004).

Snail transcription factors

The Snail family consists of 3 members, Snail (also known as Snail1), Slug (also known as Snail2) and the newly discovered Smuc (also known as Snail3). While Snail and Slug have well-established functions during EMT in both development and cancer, Smuc has proven to be a rather weak inducer of EMT, hence suggesting other roles for this novel Snail family member (Nieto, 2002; Gras et al., 2014; Zhuge et al., 2005). Snail proteins are zinc-finger transcription factors, with zinc fingers functioning as DNA-binding domains which recognize E-box elements. Like Twist1, Snail and Slug preferentially act as transcriptional repressors (Nieto, 2002). Different post-transcriptional modifications can interfere with Snail activity as a transcription factor (Peinado et al., 2007). For example, glycogen synthase kinase 3 β (GSK3β) phosphorylates Snail thus marking it for proteasomal degradation (Zhou et al., 2004). Snail protein stability and nuclear localization is enhanced by interaction with lysyl oxidase-like 2 (LOL2) enzyme (Peinado et al., 2005), whereas phosphorylation by protein kinase D1 (PDK1) triggers nuclear export of Snail (Du et al., 2010).

Both Snail and Slug play crucial roles in EMT during development and disease. Gastrulation depends on Snail-mediated cell movements for mesoderm formation and Snail was shown to promote migration of neural crest cells (Nieto, 2002). Similarly, Slug supports mesodermal cell migration from the primitive streak and is indispensable in neural crest development (Nieto et al., 1994). The function of Snail/Slug as EMT transcription factors is best characterized by their ability to repress E-cadherin. Upon binding of E-box elements in the E-cadherin promoter, Snail/Slug recruits co-repressors such as histone deacetylases (HDACs) or Sin3A to repress E-cadherin (Hemavathy et al., 2000; Peinado et al., 2004). Besides E-cadherin, Snail and Slug also inhibit expression of other cell-cell adhesion proteins, such as claudins, occludins and desmosome proteins (desmoplakin, plakophilin), while at the same time inducing the mesenchymal markers vimentin, fibronectin and N-cadherin (Xu et al., 2009). Together, these changes in gene expression drive the EMT program and promote tumorigenesis. Thus, Snail proteins favor delamination from primary tumor and confer selective advantage to migratory cells for metastasis

formation by preventing cell death (Barrallo-Gimeno and Nieto, 2005). In concordance with a cancer-propagating role, Snail is activated at the invasive front of tumors and correlates with a decreased E-cadherin expression, and with dedifferentiation and invasiveness (Barrallo-Gimeno and Nieto, 2005). In addition to repression of E-cadherin, Snail employs Ets1 to induce expression of matrix metalloproteinases (MMP2 and MMP9), thus promoting EMT and invasive properties (Jorda et al., 2005; Taki et al., 2006).

ZEB transcription factors

Two Zinc Finger E-Box Binding Homeobox (ZEB) family transcription factors are known in vertebrates: ZEB1, also known as δEF1 and ZEB2, also known as Smad-interacting protein 1 (SIP1). Structurally, both proteins have two zinc-finger clusters at each end and a homeodomain in the middle (Peinado et al., 2007). The zinc-finger motifs typically bind to bipartite E-boxes as the ones found in the E-cadherin promoter (Remacle et al., 1999). The central domain contains a Smad-interaction sequence which allows ZEB proteins to form complexes with ligand-activated Smads (Postigo, 2003). The recruitment of either coactivators (p300 and PCAF- p300/CBP-associated factor) or corepressors (CTBP- C-terminal-binding protein) determines whether ZEB factors enhance or repress Smad-mediated transcription (Postigo et al., 2003). On a post-transcriptional level, ZEB factors are regulated by microRNAs (miRNAs; see also section *2.3.2 Non-coding miRNAs as post-transcriptional regulators of EMT-TFs*). Additionally, Pc2-mediated sumoylation of ZEB2 prevents it from binding CTBP and consequently downregulating E-cadherin (Long et al., 2005).
ZEB proteins are expressed in the heart, skeletal muscle, central nervous system (CNS) and hematopoietic cells during development. While ZEB1 and ZEB2 have redundant functions in skeletal muscle and CNS, they show different expression patterns in lymphocytes (Postigo and Dean, 2000). Moreover, mouse embryos lacking ZEB2 have lethal defects in the migration of neural crest cells, suggesting crucial implications for ZEB2 in neurulation (Van de Putte et al., 2003). Besides their role during development, ZEB proteins also induce cancer-related EMT. ZEB1 and ZEB2 repress E-cadherin expression and promote migration and invasion in tumor cell lines (Shirakihara et al., 2007; Comijn et al., 2009). Additionally, ZEB1 was found to enhance colorectal cancer cell metastasis and loss of cell polarity (Spaderna et al.,

2008). The mechanisms through which ZEB proteins regulate E-cadherin expression very often involve recruitment of the transcriptional repressor CTBP (Peinado et al., 2007). However, ZEB1 is not entirely dependent on CTBP for E-cadherin repression (van Grunsven et al., 2003) and can also exert its function by recruiting the SWI/SNF chromatin-remodeling protein BRG1 (Sanchez-Tillo et al., 2010). In addition to E-cadherin, ZEB2 also downregulates tight junction proteins (claudin-4, ZO-3) and the desmosomal protein plakophilin-2, as well as induces vimentin and N-cadherin, resulting in increased migratory abilities (Vandewalle et al., 2005; Bindels et al., 2006). Similar to Snail, ZEB2 employs Ets1 to induce MMP2 expression (Taki et al., 2006).

Other EMT-TFs

There are several less well characterized transcription factors complementing the master regulators Twist, Snail and ZEB in inducing EMT. Some of them are forkhead box (FOX) transcription factors with a helix-turn-helix domain binding to DNA (Carlsson and Mahlapuu, 2002). For example, FoxC2 is sufficient to induce EMT, although it does not mainly suppress E-cadherin, as do the master regulators, but it rather induces mesenchymal markers, such as vimentin, fibronectin and N-cadherin (Mani et al., 2007). In addition, overexpression of FoxC2 enhances the metastatic ability of mouse mammary carcinoma cells, which correlates with elevated levels of FoxC2 in highly aggressive basal-like breast cancers (Mani et al., 2007). Two other factors involved in developmental EMT, Krüppel-like factor 8 (KLF8) and Goosecoid also induce invasive growth of breast cancer cells and promote metastasis (Wang et al., 2007; Wang et al., 2011; Hartwell et al., 2006). Recently, the homeobox factor Prrx1 was shown to have similar dynamics to Twist1 in uncoupling EMT and stemness in cancer. More precisely, Prrx1 induced a full EMT in canine kidney cells (MDCK), but, just like Twist1, it had to be turned off again to allow metastatic colonization of human breast carcinoma cells (Ocana et al., 2012).

Cross-regulations between EMT-TFs

EMT transcription factors not only drive an epithelial-mesenchymal transdifferentiation on their own, but they also collaborate with each other and, most

importantly, they positively regulate each other's expression to enhance the EMT program. As a major EMT orchestrator, Snail was shown to induce transcription of both ZEB1 and ZEB2 (Guaita et al., 2002; Taki et al., 2006). Snail also cooperates with Twist1 to activate ZEB1 expression, as Snail induces Ets1, which then binds together with Twist1 to the ZEB1 promoter, albeit to different elements (Dave et al., 2011). Additionally, Slug drives Twist1 transcription (Moreno-Bueno et al., 2006), while Twist1 was reported to directly induce Snail and Slug expression (Ip et al., 1992; Casas et al., 2011). Finally, FoxC2 has been proposed to lie downstream of Twist1, Snail and Goosecoid in the EMT signaling cascade (Mani et al., 2007).

2.3.2 Non-coding miRNAs as post-transcriptional regulators of EMT-TFs

miRNAs are non-coding RNAs of approximately 23 nucleotides that pair to complementary sequences of protein-coding mRNAs, thus inhibiting their translation or promoting their degradation (Bartel, 2009). Several miRNAs inhibit EMT by post-transcriptionally silencing EMT-TFs (Lamouille et al., 2013). The most prominent miRNA family associated with EMT is miR-200, which consists of 5 members (miR-200a, miR-200b, miR-200c, miR-429 and miR-141) and has been found to be downregulated in various types of cancer (De Craene and Berx, 2013). miR-200 members bind to the 3' untranslated regions of ZEB1 and ZEB2, thereby inhibiting their activity (Burk et al., 2008; Korpal et al., 2008). This inhibition results in increased E-cadherin expression, accompanied by a reduction in migration and invasion of cancer cells (Burk et al., 2008; Korpal et al., 2008). Additionally, miR-200 and ZEB proteins reside within a feed-forward loop, where ZEB factors downregulate miR-200 as a prerequisite for an epithelial-mesenchymal transdifferentiation (Burk et al., 2008). Of note, miR-141 and miR-200c also attenuate expression of the EMT inducer TGFβ and its downstream effectors (Burk et al., 2008; Perdigão-Henriques et al., 2015). In reverse, TGFβ is known to silence the miR-200 loci by DNA-methylation (Gregory et al., 2011). Similar to miR-200 and ZEB, a double-negative feedback mechanism between Snail and miR-34 and miR-203 governs the EMT process (Siemens et al., 2011; Moes et al., 2012). Additionally, miR-29b and miR-30a also target Snail mRNA (Ru et al., 2012; Zhang et al., 2012). The closely related EMT-TF Slug is negatively regulated by miR-1 and miR-200b, while itself repressing the

expression of the same miRNAs (Liu et al., 2013). Finally, Twist1 employs miR-10b to mediate breast cancer metastasis (Ma et al., 2007).

2.3.3 Signaling pathways inducing EMT

TGFβ signaling

As a main EMT inducer, TGFβ binds to a tetrameric serin/threonine kinase receptor consisting of two type I and two type II receptors (TGFRI and TGFRII). Upon TGFβ binding, the type II receptors transphosphorylate type I receptors, which then propagate the signal by recruitment and phosphorylation of Smad2 and Smad3 (Massague, 2008). Once activated, Smad2/3 form a complex with Smad4 and translocate into the nucleus, where they associate with other DNA binding transcription factors, thus activating or repressing transcription of target genes (Shi and Massague, 2008). Additionally, TGFβ also signals through Smad-independent pathways by activating c-Jun N-terminal kinase (JNK) and p38 mitogen-activated protein kinase (MAPK), amongst other factors (Derynck and Zhang, 2003).

TGFβ is a strong EMT inducer both in development and disease (Derynck and Akhurst, 2007; Thiery et al., 2003). In breast cancer, tumor-initiating cell populations expressing the cell surface marker $CD44^+$ (associated with stem cell-like properties and a mesenchymal state) were shown to be enriched in TGFβ pathway components. Conversely, treatment with a TGFRI/II inhibitor promoted $CD44^+$ cells to adopt a more epithelial phenotype, suggesting a role for TGFβ-induced EMT in cancer (Shipitsin et al., 2007). Moreover, murine mammary epithelial NMuMG cells expressing a constitutively active TGFRI exhibited full epithelial to mesenchymal transdifferentiation (Piek et al., 1999; Valcourt et al., 2005), while interference with TGFRI resulted in impaired EMT during cardiac valve formation (Mercado-Pimentel et al., 2007). Similarly, overexpression of a dominant negative TGFRII inhibited EMT in a mouse skin carcinoma model (Portella et al., 1998) and reduced tumorigenicity of Ha-Ras-transformed mammary epithelial cells (EpRas) and highly metastatic mesenchymal mouse colon carcinoma cells (CT26) by preventing EMT (Oft et al., 1998). In addition, dominant-negative forms of the TGFβ downstream effectors Smad2, Smad3, or Smad4 blocked TGFβ-induced EMT, thus indicating that TGFβ promotes EMT through Smad-dependent mechanisms (Valcourt et al., 2005).

In response to TGFβ, Smad complexes can induce transcription of EMT-TFs in both direct and indirect ways. TGFβ has been shown to indirectly regulate expression of Snail and Twist1 by Smad-mediated upregulation of high mobility group A2 (HMGA2). Thus, overexpression of HMGA2 resulted in increased Snail and Twist1 promoter activity, whereas HMGA2 knock-down attenuated TGFβ-induced transcription of the same factors (Thuault et al., 2006; Thuault et al., 2008). TGFβ may also promote epithelial mesenchymal transdifferentiation by reducing levels of the E2A antagonizers ID1, ID2 and ID3 (Kang et al., 2003; Kondo et al., 2004). TGFβ-mediated ID inhibition therefore restores E2A activity and promotes downregulation of the epithelial marker E-cadherin. Furthermore, given the role of E2A as a Twist1 dimerization partner enhancing Twist1 activity (Hayashi et al., 2007), it is conceivable that inhibition of ID proteins by TGFβ might result in the negative regulation of Twist1 as well. With respect to other EMT-TFs, TGFβ employs Smad3 to directly induce transcription of Snail (Dang et al., 2011) and indirectly activates Slug by triggering the nuclear translocation of myocardin-related transcription factors (MRTFs), which then associate with Smad3 and bind to the Slug promoter (Morita et al., 2007). TGFβ also induces the expression of the two-handed zinc-finger factor ZEB1, mediated by Ets1 (Shirakihara et al., 2007). Beyond activating downstream EMT-TFs, Smad complexes also directly interact with factors like ZEB1, ZEB2 and Snail to promote TGFβ-induced EMT (Vincent et al., 2009; Nishimura et al., 2006; Postigo et al., 2003). Additionally, TGFβ facilitates an epithelial mesenchymal transdifferentiation in a Smad-dependent manner and without requiring EMT-TFs, by directly upregulating mesenchymal markers, such as fibronectin and vimentin (Nawshad et al., 2007).

Complementing Smad-dependent signaling, TGFβ can also induce EMT by non-smad pathways, most prominently by activating Erk MAP kinases, Rho GTPases, JNK and the PI3 kinase/Akt complex (Xu et al., 2009). Most of these signaling molecules influence cell proliferation, dissolution of tight junctions, migratory abilities and degradation of the extracellular matrix (Moustakas and Heldin, 2005). Since this work focuses on the TGFβ – JNK pathway, this link will be described more in detail. TGFβ-induced JNK activation starts with the association of the Ubiquitin ligase tumor necrosis factor (TNF)-receptor-associated factor 6 (TRAF6) with the TGFβ receptors, followed by recruitment of the TGFβ-associated kinase 1 (TAK1), which then phosphorylates and activates JNK (Yamashita et al., 2008). JNK elicits its function by

phosphorylating c-Jun, a member of the AP-1 complex, which has been found to be required for induction of the mesenchymal markers fibronectin, vimentin and urokinase-type plasminogen activator (uPA), and for acquisition of invasive properties (Wang et al., 2010; Santibanez, 2006). Indeed, chemical inhibition of JNK or its gene silencing prevented A549 lung cancer cells and airway epithelial cells from undergoing EMT (Chen et al., 2013; Alcorn et al., 2008). Only recently, a model has been proposed that attributes Smad and non-Smad TGFβ signaling to different stages of the tumorigenic process (Sahu et al., 2015). According to this model, Smad complexes are required for the initiation of TGFβ-induced EMT, while JNK sustains the progression towards acquisition of mesenchymal properties and determines a gene signature associated with metastasis.

In conclusion, TGFβ contributes to developmental changes and cancer formation through a diversity of EMT-inducing mechanisms, which rely on both Smad-dependent, as well as Smad-independent signaling cascades.

Receptor Tyrosin Kinases (RTKs)

Apart from TGFβ, there are also other growth factors that have been reported to induce EMT, including the epidermal growth factor (EGF), insulin growth factor (IGF), fibroblast growth factor (FGF), vascular endothelial growth factor (VEGF) and the platelet-derived growth factor (PDGF) (Thiery et al., 2009). These signaling molecules typically bind to RTKs, thereby propagating the signal inside the cell. For example, EGF has been shown to cause endocytosis of E-cadherin and to induce transcription of Snail and Twist1, leading to increased invasiveness and metastatic potential (Lu et al., 2003; Lo et al., 2007). Also, activation of the EGF receptor 2 (ERBB2) in mammary epithelial cells promotes tumorigenesis and cancer recurrence by inducing Snail (Moody et al., 2005). VEGF is required for the transdifferentiation of endocardial cells to mesenchymal cells during heart valve development (Stankunas et al., 2010) and enhances malignant transformation and invasion of prostate cancer cells (Gonzalez-Moreno et., 2010). In addition, VEGF receptor 1 (VEGFR1) activation led to an increase in nuclear localization of Snail and induced migratory properties in epithelial breast cancer cells, while shRNA-mediated knock-down of VEGFR1 reduced the metastatic ability of invasive MDA-MB-231 breast cancer cells (Ning et al., 2013). Finally, PDGF was shown to induce EMT by promoting β-catenin nuclear

translocation (Yang et al., 2006) and PDGF receptor α (PDGFRα) activation was required for Twist1-induced invadopodia formation and tumor metastasis (Eckert et al., 2011). Both VEGF and PDGF might constitute the link between EMT and endothelial-mesenchymal transition (EndMT), a process that facilitates angiogenesis and tumor vascularization along with metastasis (Potenta et al., 2008).

Wnt signaling

Wnt signals are transduced across the cell membrane by Frizzled (FZD) and low-density lipoprotein receptor–related protein (LRP) transmembrane receptors. In canonical, β-catenin-dependent Wnt signaling, binding of Wnt ligands to their receptors prevents phosphorylation of β-catenin by GSK3β, which would otherwise mark β-catenin for ubiquitination, resulting in proteasomal degradation. In response to Wnt signaling, β-catenin translocates into the nucleus, where it associates with T cell factors (TCF) or lymphocyte enhancer binding factor 1 (LEF1), two closely related transcription factors, and regulates transcription of target genes (Niehrs 2012). Non-canonical Wnt signaling is mediated by intracellular calcium ions and JNK. The latter is being referred to as the planar cell polarity pathway and directs asymmetric localization of cytoskeletal components and coordinated polarization of cells within the plane of epithelial sheets (Habas and Dawid, 2005). Wnt signals contribute to EMT induction both in development and cancer (Gonzales and Medici, 2014). During gastrulation, Wnt signaling controls the formation of the primitive streak in chick and mouse embryos (Skromne and Stern, 2001; Liu et al., 1999). Later on in embryogenesis, canonical as well as non-canonical Wnt signaling induces EMT-dependent neural crest formation and delamination of migratory neural crest cells (Garcia-Castro et al., 2002; Carmona-Fontaine et al., 2008).

It is known that Wnt elicits its activity through transcriptional regulation of EMT-TFs, such as Twist1, Snail and Slug (Howe et al., 2003; Bachelder et al., 2005; Vallin et al., 2001) and also stabilizes Snail protein by inhibition of GSK3β, thus promoting EMT (Zhou et al., 2004). Moreover, β-catenin-TCF/LEF1 complexes directly repress E-cadherin promoter activity (Jamora et al., 2003) and upregulate the mesenchymal marker fibronectin (Gradl et al., 1999). By analyzing the role of Wnt-induced EMT in cancer, recent studies have shown that Wnt/β-catenin signaling promotes stem-like properties and invasiveness in colon cancer cells (Han et al., 2013), while the Wnt-

antagonist Dickkopf-1 (Dkk-1) reduces EMT-associated tumor-initiating ability of colon cancer cells (Qi et al., 2012). These results confirm the observation of increased β-catenin-mediated gene expression at the invasive front of colorectal tumors (Brabletz et al., 2001). In addition, knock-down of β-catenin in lung cancer cells reduced ZEB1 and Snail transcript levels, thereby inhibiting invasion (Yang et al., 2015a). In the breast it was shown that LGR5 promoted cell mobility, tumor formation, and epithelial-mesenchymal transition in cancer cells by activating Wnt/β-catenin signaling (Yang et al., 2015b). Also, Wnt5a-mediated non-canonical Wnt signaling has been implicated in tumor formation and has been reported to induce EMT in several cancer types, leading to increased invasiveness and metastasis (Gujral et al., 2014; Quin et al., 2015).

Beyond its singularly role in EMT regulation, Wnt also collaborates with TGFβ in development and pathological events (Nishita et al., 2000; Nelson and Nusse 2004; Nawshad et al., 2007). For example, Smad2 and Smad4 form a transcriptional complex with LEF1 to repress E-cadherin gene expression in palate medial-edge epithelial cells (Nawshad et al., 2007).

Notch signaling

Ligands from the families Delta and JAG/Serrate bind to Notch receptors (Notch1-Notch-4), thereby triggering cleavage of the Notch receptor by the proteases ADAM and γ-secretase, followed by nuclear translocalization of the Notch intracellular domain (NICD). NICD releases the transcription factor RBP-Jk from its repressors, thus inducing transcription of target genes, such as Hes and Hey (Zhou et al., 2013). Notch signaling contributes to EMT both during development and cancer progression. Notch induces Snail during endocardial cushion formation (Timmerman et al., 2004) and is required for neural crest induction (Cornell and Eisen, 2005). Additionally, Slug is directly upregulated by Notch during cardiac cushion EMT and in invasive breast cancer (Niessen et al., 2008; Shao et al., 2015). It was recently shown that Notch overexpression induces EMT in epithelial breast cancer cells and leads to acquisition of stem cell-like properties (Zhang et al., 2015). In lung cancer cells, Notch promoted EMT, while its silencing inhibited colony-formation (Xie et al., 2012). Notch also collaborates with TGFβ for epithelial-mesenchymal transdifferentiation and enhancement of tumorigenic potential. In epithelial cells,

TGFβ activated expression of Hey1 in a Smad3-dependent manner and Hey1 depletion blocked TGFβ-induced EMT (Zavadil et al., 2004). Moreover, Notch3 was reported to regulate TGFβ-induced EMT by directly binding to the ZEB1 promoter, resulting in increased invasion and metastasis of non-small cell lung cancer cells (Liu et al., 2014).

2.4 Inhibitors of EMT as candidate drugs in TNBC therapy

In concordance with EMT promoting invasive and aggressive tumor growth (Thiery et al., 2009), several EMT markers were found to be elevated in TNBC (Jeong et al., 2012; Sethi et al., 2011). Thus, inhibition of signaling pathways driving EMT appears to be a promising therapeutic strategy for TNBC patients. Current approaches in this field include antibodies against receptor tyrosine kinases or their ligands (e.g.: cetuximab against EGFR, sunitinib against VEGFR or the anti-VEGF antibody bevacizumab) aiming to specifically target the large majority of TNBCs, which indeed overexpress EGFR, and block VEGFR-driven angiogenesis (Podo et al., 2010). However, the combination of monoclonal antibodies with cytotoxic agents showed only moderate improvements in terms of tumor response and progression free survival compared to chemotherapy alone. In addition, the toxicity of these combined therapies was considerable (Podo et al., 2010).

Another EMT pathway driving TNBC is Notch signaling. Preclinical studies have shown that gain-of-function mutations and amplifications of Notch receptors are frequent in TNBC and sensitize tumors to a γ-secretase inhibitor (Wang et al., 2015). Moreover, an ongoing Phase II clinical trial aims to investigate the effect of RO4929097, a γ-secretase inhibitor, in patients suffering from invasive TNBC (NCT01151449 at www.clinicaltrials.gov).

The Wnt signaling pathway is also being considered as targetable in TNBC, as β-catenin has been found to be enriched in invasive TNBC/basal-like breast cancer and was predictive of a poor clinical outcome (Khramtsov et al., 2010; Geyer et al., 2011). Indeed, the porcupine inhibitor LGK974 (Liu et al., 2013) is currently being tested in a Phase I dose-escalation study in patients with advanced or metastatic cancer, including TNBC (Le Du et al., 2015; NCT01351103 at www.clinicaltrials.gov).

Finally, TGFβ expression levels were found to be higher in TNBC cells compared to non-TNBC cells and dual blocking of TGFRI and TGFRII attenuated vimentin and

fibronectin expression, while concomitantly impairing cell motility (Kim et al., 2015). Therefore, another strategy for pathway-directed therapies uses antibodies against TGFβ or small-molecule inhibitors of TGFβ receptors (Calone and Souchelnytskyi, 2012). For example, Fresolumimab (targeting TGFβ 1-3) is currently being tested in a Phase I clinical trial against metastatic breast cancer (NCT01401062 at www.clinicaltrials.gov; Buijs et al., 2012). Additionally, the PF-03446962 compound, an antibody against the Transforming Growth Factor Beta Activin Receptor-like Kinase 1 (ALK1) has just completed Phase I clinical trials in advanced solid tumors (NCT00557856 at www.clinicaltrials.gov; Buijs et al., 2012).

Nevertheless, due to moderate progress during the past decade in increasing life expectancy of patients with TNBC, it still remains a great challenge to develop new and improved therapeutic strategies.

3. Objectives

Worldwide, breast cancer has the highest incidence among all cancer types in women (Torre et al., 2015). Epidemiologic results attributing also the highest mortality rate of all cancer types in women to breast cancer (Torre et al., 2015) suggest that there is an urgent need for the development of new and improved treatment strategies. TNBC, the most aggressive and deadly type of breast cancer is also the most difficult to treat due to lacking expression of targetable hormone receptors (Dent et al., 2007). However, global gene expression analysis of TNBC samples, associating a large majority of TNBC with an EMT signature provided novel insights into targeted therapeutic strategies (Prat et al., 2010; Sarrió et al., 2008). Thus, the goal of this study was to use small-molecule inhibitors against developmental signaling pathways governing EMT to reduce tumorigenicity of TNBC. As the use of single anti-cancer agents has resulted in acquired therapy resistances before (Yamamoto-Ibusuki et al., 2015; Nahta et al., 2006), it was postulated that these resistances can be overcome by combining multiple inhibitors.

Nevertheless, as this study progressed, targeting EMT-related signaling pathways in TNBC neither reversed the mesenchymal phenotype nor completely blocked functional characteristics of aggressive cancer cells, such as migration and clonogenic growth. These observations led to the hypothesis that known developmental signaling pathways may only contribute to EMT induction, but are not required for maintenance of the mesenchymal state resulting from EMT. To test this hypothesis, I set out to determine which signaling pathways are necessary for Twist1-induced EMT and through which molecular mechanisms they operate. In addition, cell state dynamics (epithelial, mesenchymal or intermediate phenotypes) upon inhibition of Twist1-induced EMT were analyzed. Moreover, functional consequences, such as cell motility and proliferation resulting from the concomitant inhibition of signaling pathways and activation of Twist1 were examined.

4. Materials and Methods

4.1 Materials

4.1.1 Buffers and solutions

All buffers and solutions were prepared in MilliQ water unless stated otherwise.

Table 1: Composition of buffers and solutions

Buffer/Solution	Composition
APS	10 % (m/v) APS
Biotinylation buffer	1 mM $NaIO_4$ 500 uM Aminooxy-Biotin 10 mM Aniline in 1xPBS
Blocking Solution for Immunofluorescence	10 % (v/v) Normal Goat Serum in 0.1 % (v/v) BSA in 1x PBS
Collagenase I solution	300 U/ml Collagenase type I in 1xPBS
FACS Buffer	0.1 % (v/v) BSA in 1x PBS
Freezing medium	20 % FCS 10 %DMSO in corresponding growth medium
Laemmli Running Buffer 1x	192 mM Glycine 3.5 mM SDS ultrapure 25 mM Trizma® base
Lysis buffer (Proteomics)	1 % (v/v) NP40 10 mM NaCl 10 mM Tris/HCl pH 7.6 add freshly before use 1x cOmplete™ protease inhibitor cocktail
Milk Powder Solution	5 % (m/v) non-fat dried milk powder in 1x TBS/T
Neutralizing Solution	10 % (v/v) 1 M HEPES in 2xPBS adjust to pH 7.3 with NaOH (1 M)
PBS/$CaCl_2$/$MgCl_2$ Buffer	1 mM CaCl2 500 uM MgCl2 in 1xPBS adjust to pH 6.7 with HCl (1 M)
Permeabilization Buffer for Immunofluorescence	0.2 % (v/v) TritonX-100 in 1xPBS
PFA	4 % (v/v) Paraformaldehyde

Buffer/Solution	Composition
Polyethyleneimine (PEI) Solution for Transfection	40 uM PEI in 1xPBS (pH 4.5), filter sterlized
Protamine Sulfate Solution	980 uM Protamine Sulfate, filter sterilized
RIPA Buffer	20 mM Tris/HCl (pH 7.5) 150 mM NaCl 1 mM Na_2EDTA 1 mM EGTA 1 % (v/v) NP40 1 % (v/v) Sodium Deoxycholate 2.5 mM Sodium Pyrophosphate 1 mM Beta-glycerophosphate add freshly before use 10 % (v/v) Phosphatase Inhibitor Cocktail 2+3 and 1 mM Sodium Orthovanadate Solution
SDS Buffer 5x	30 % (v/v) Glycerol 10 % (v/v) 2-Mercaptoethanol 35 mM SDS 250 mM Tris/HCl (pH 6.8) pinch of Bromophenol Blue
Sodium Orthovanadate Solution	1 M Na_3VO_4
Stripping Buffer	200 mM Glycine 35 mM SDS 1 % (v/v) Tween® 20 adjust to pH 2.2-2.6 with HCL (1 M)
TBS 10x	1.5 M Sodium chloride 0.1 M Trizma® base adjust to pH 7.2-7.4 with HCl (1 M)
TBS/T	10x TBS supplemented with 0.1 % (v/v) Tween® 20
Transfer Buffer	192 mM Glycine 20 % (v/v) Methanol 26 mM Trizma® base
Tris/HCl	1 M Trizma® base adjust to pH 6.8 or 8.8 with HCl (1 M)
Tween20 Lysis Buffer	25 mM HEPES (pH 8) 20 mM NaCl 2 mM EDTA 0.5 % (v/v) Tween® 20 add freshly before use 10 % (v/v) Phosphatase Inhibitor Cocktail 2+3 and 1 mM Sodium Orthovanadate Solution

4.1.2 Reagents

Table 2: Listing of utilized reagents and their suppliers

Reagent	Supplier
4',6-diamidino-2-phenylindole (DAPI)	Sigma
7-Aminoactinomycin D (7-AAD)	BD Biosciences
Aluminum potassium sulfate	Sigma
Aminooxy-Biotin	Biotium
Ampicillin	Sigma
Anilin	Sigma
AQUA-POLY MOUNT	Polysciences
β-Mercaptoethanol	Sigma
Bovine Serum Albumin (BSA) 200mg/ml	Sigma
Carmine	Sigma
Cell Titer Glo	Promega
cOmplete™ protease inhibitor cocktail	Roche
Ethylenediaminetetraacetic acid (EDTA)	Sigma
Ethylene glycol tetraacetic acid (EGTA)	Sigma
Formaldehyde 37 %	Sigma
Glycine	Carl Roth
Hydrochloric acid solution	Applichem
HEPES	Applichem
LB Agar Miller	Sigma
LB-Medium (Lennox)	Carl Roth
Methanol, ROTIPURAN	Carl Roth
Non fat dried milk powder	Carl-Roth
Normal Donor Goat Serum	Biozol
PageRuler Prestained Protein Ladder	Thermo Scientific
Phalloidin-Atto 647N	Sigma
Phosphatase Inhibitor Cocktail 2	Sigma
Phosphatase Inhibitor Cocktail 3	Sigma
Power SYBR green PCR Master Mix	Life Technologies
RNase-Free H2O	Life Technologies
SDS, ultrapure	Carl Roth
Sodium metaperiodate	Merck
Sodium orthovanadate	Sigma
Tris/HCl	Carl Roth
Tetramethylendiamine (TEMED)	Carl Roth
TritonX-100	Sigma
Tween®20	Sigma
WST-1	Roche
XL10-Gold Ultracompetent Cells	Agilent Technologies

4.1.3 Kits

Table 3: Listing of utilized kits and their suppliers

Kit	Supplier
Amersham™ ECL Advance Western Blotting Detection Kit	GE Healthcare
Bio-Rad DC Protein Assay Kit	Bio-Rad
Dual-Luciferase® Reporter Assay System	Promega
EasyScript Plus	Applied Biological Materials
Hemacolor Rapid staining Set	Merck
miRNeasy Mini Kit	Qiagen
miScript Primer Assays	Qiagen
miScript RT Kit	Qiagen
miScript SYBR Green PCR Kit	Qiagen
Plasmid Midi Kit	Qiagen
RNase-Free DNase Set	Qiagen
Rneasy Mini Kit	Qiagen

4.1.4 Primers and vectors

Table 4: Primers used for RT-PCR analysis

Gene	Forward	Reverse
E-cadherin	tgcccagaaaatgaaaaagg	gtgtatgtggcaatgcgttc
Fibronectin	cagtgggagacctcgagaag	tccctcggaacatcagaaac
FoxC2	gcctaaggacctggtgaagc	ttgacgaagcactcgttgag
N-cadherin	acagtggccacctacaaagg	ccgagatggggttgataatg
RPL32	cagggttcgtagaagattcaaggg	cttggaggaaacattgtgagcgatc
Slug	ggggagaagccttttcttg	tcctcatgtttgtgcaggag
TGFBR1	acggcgttacagtgtttctg	gcacatacaaacggcctatctc
Vimentin	gagaactttgccgttgaagc	gcttcctgtaggtggcaatc
Wnt5a	atggctggaagtgcaatgtct	atacctagcgaccaccaagaa
ZEB1	gcacaagaagagccacaagtag	gcaagacaagttcaagggttc
ZEB2	ttcctgggctacgaccatac	tgtgctccatcaagcaattc

Table 5: Primers used for ChIP analysis

Gene	Forward	Reverse
ZEB1 - positive site	gcagaggccatcattccacaa	ttgcaaaatctggcaaacactatca
ZEB1 - negative site	ttccatattgagctgttgccg	aaagcgaacagctctttccga

Table 6: Listing of utilized plasmids

Name	Vector backbone	Gene/Insert name	Source/Citation
GIPZ TGFBR1 shRNA	pGIPZ	shRNA constructs: Non-targeting control shRNA (# RHS4346); V2LHS_42386; V2LHS_55961; V2LHS_55964; V3LHS_305780; V3LHS_305782; V3LHS_305784	GE Healthcare
M50 Super 8x TOPFlash	pTA-Luc	TCF/LEF binding sites	Bob Weinberg Lab; Veeman et al., 2003
M51 Super 8x FOPFlash (TOPFlash mutant)	pGL3	mutant TCF/LEF binding sites	Bob Weinberg Lab; Veeman et al., 2003
pBp-TGFβ1	pBABE-puro	TGFβ1	Bob Weinberg Lab
pBp-Wnt3a	pBABE-puro	Wnt3a	Bob Weinberg Lab
pCMV-dR8.2 dvpr	pCMV-dR8.2 dvpr	none (2nd generation lentiviral packaging plasmid)	Bob Weinberg Lab
pCMV-VSV-G	pCMV-VSV-G	none (Envelope protein for producing lentiviral and MuLV retroviral particles)	Bob Weinberg Lab
pRL-SV40 *Renilla*	pRL-TK	SV40 promoter	Bob Weinberg Lab
pUMVC	pUMVC	none(Packaging plasmid for producing MuLV retroviral particles)	Bob Weinberg Lab
pWZL Blast Twist1-ER	pWZL-Blast	Twist1-ER	Bob Weinberg Lab
SBE4-Luc	pBV-Luc	Smad binding element	Bob Weinberg Lab; Zawel et al., 1998

All plasmids contain an ampicillin resistance for bacterial cloning purposes and were amplified using XL10-Gold Ultracompetent Cells.

4.1.5 Antibodies

Table 7: Primary antibodies

Target protein	Company	Species	Application and dilution
α6-Integrin [GOH3]	Santa Cruz	monoclonal/rat	IF/1:100
α-Tubulin [B-5-1-2]	Sigma-Aldrich	monoclonal/mouse	WB/1:5000
β-actin [AC-15]	Sigma-Aldrich	monoclonal/mouse	WB/1:6000
β-catenin	BD	monoclonal/mouse	IF/1:150
CD24 – FITC [ML5]	BD	monoclonal/mouse	FACS/1:12.5
CD44 – APC [G44-26]	BD	monoclonal/mouse	FACS/1:25
E-cadherin [24E10], Alexa 488 conjugated	NEB	monoclonal/rabbit	IF/1:50
E-cadherin [EP700Y]	Biozol	monoclonal/rabbit	IF/1:250; WB/1:25.000
ERα [HC-20]	Santa Cruz	polyclonal/rabbit	ChIP/1:200
Fibronectin	BD	monoclonal/mouse	WB/1:5000
Histone H3	Abcam	polyclonal/rabbit	WB/1:5000
IgG isotype control	Abcam	polyclonal/rabbit	ChIP/1:5000
Ki-67	Abcam	polyclonal/rabbit	IF/1:300
Laminin-1	Sigma-Aldrich	polyclonal/rabbit	IF/1:100
NF-κB p65 [D14E12] XP	Cell signaling	monoclonal/rabbit	WB/1:1000
Phospho-NF-κB p65 (Ser536) [93H1]	Cell signaling	monoclonal/rabbit	WB/1:1000
Phospho-Smad2 (Ser465/467)/Smad3 (Ser423/425) [D27F4]	Cell signaling	monoclonal/rabbit	WB/1:1000
Slug [C19G7]	Cell signaling	monoclonal/rabbit	WB/1:1000
Smad 2/3 [D7G7] XP	Cell signaling	monoclonal/rabbit	WB/1:1000
Vimentin [D21H3] XP	Biozol	monoclonal/rabbit	WB/1:1000
Vimentin [V9]	abcam	monoclonal/mouse	IF/1:100
ZEB1 [H-102]	Santa Cruz	polyclonal/rabbit	IF/1:100; WB/1:200

Table 8: Secondary antibodies

Secondary antibodies	Company	Labeling	Application and dilution
Goat Anti-Mouse IgG	Life Technologies	Alexa Fluor 594	IF/ 1:250
Goat Anti-Rat IgG		Alexa Fluor 594	
Goat Anti-Rabbit IgG		Alexa Fluor 488	
Goat Anti-Mouse IgG (H+L)	Jackson ImmunoResearch	Peroxidase conjugated	WB/ 1:25 000
Goat Anti-Rabbit IgG (H+L)			

4.1.6 Cell culture

Table 9: Reagents and compounds utilized with cell culture methods

Reagent/Compound	Supplier
1,7-Dichloro-octamethyltetrasiloxane	Santa Cruz
6-bromoindirubin-3'-oxime (BIO)	Stemgent
A83-01	Tocris
B27 (50x)	Life Technologies
Basic FGF, human recombinant	Millipore
Blasticidin 10mg/ml	Gibco Life Technologies
Collagen type I rat tail	Corning
Collagenase type I	Sigma
DAPT	Tocris
Dimethyl sulfoxide Cell culture grade	Sigma
DMEM	Gibco Life Technologies
DMEM/F-12	Gibco Life Technologies
EGF, human recombinant	Millipore
F12/K Nutrient mixture	Gibco Life Technologies
Fetal calve serum (FCS)	Pan Biotech
Heparin sodium salt from porcine intestinal mucosa	Sigma
Hydrocortisone	Sigma
Insulin from bovine pancreas	Sigma
IWP2	Sigma
Mammary Epithelial Cell Growth Medium	PromoCell
Methylcellulose Stock Solution	R&D Systems
PBS, pH 7.4	Gibco Life Technologies
Penicillin/Streptomycin (Pen/Strep)	Invitrogen
Poly-D-Lysine	Sigma
Polyethyleneimine (PEI), linear, 25 kDa	VWR
Protamine Sulfate	Sigma
Puromycin 10mg/ml	ENZO Life Sciences
Recombinant human TGFβ 1	R&D Systems
Recombinant human Wnt3a	R&D Systems
SP600125	Tocris
Trypsin neutralizing solution (TNS)	PromoCell
Trypsin-EDTA	Invitrogen
XAV939	Enzo Life Sciences
X-tremeGENE HP DNA Transfection Reagent	Roche
Wnt Antagonist, C59	Biocat
(Z)-4-Hydroxytamoxifen	Sigma

4.1.7 Cell lines

Table 10: Listing of utilized cell lines and their origins

Cell line	Origin
A549	Human lung carcinoma
A549-Twist1-ER (derived cell line)	A549 cells that were infected with pWZL Blast Twist1-ER plasmid followed by selection with 5 ng/ml blasticidin; HMLE-Twist1-ER cells express an inducible Twist1 protein upon treatment with 4-hydroxytamoxifen (Mani et al., 2008)
HEK293T	Human embryonic kidney cells that express SV40 large-T antigen
HMLE (Immortalized Human Mammary Epithelial Cells)	Cells that were transformed by infection with retroviruses containing the SV40 large T early region (containing the Large and Small T antigen, inactivating tumor suppressor proteins p53 and RB, as well as Protein Phosphatase 2, thereby driving transition through the cell cycle) and hTERT gene (encoding the catalytic subunit of telomerase, sufficient to induce telomerase activity), but which are not tumorigenic and are ER-negative (Elenbaas et al., 2001; Scheel and Weinberg, unpublished)
HMLE-Twist1 (derived cell line)	HMLE cells that were transduced with a constitutively active Twist1 construct (Yang et al., 2004)
HMLE-Twist1-ER (derived cell line)	HMLE cells that were infected with pWZL Blast Twist1-ER plasmid followed by selection with 5 ng/ml blasticidin; HMLE-Twist1-ER cells express an inducible Twist1 protein upon treatment with 4-hydroxytamoxifen (Mani et al., 2008)
MCF7-Ras	Mammary gland, breast; derived from metastatic site: pleural effusion; additionally express Ras
MDA-MB-231	Human breast adenocarcinoma; originally derived from pleural effusion

4.1.8 Laboratory equipment

Table 11: Listing of laboratory materials and their suppliers

Material	Supplier
6-, 24-, 96-well plates	BD
10 cm cell culture dishes	BD
Cell culture inserts with 8 µm pores	BD
Cell scraper	VWR
Cell strainer 40 µm nylon	BD
Cover glass, 13 mm, round	VWR
Conicals Falcon	Corning
Cryotubes	Thermo Scientific
F96 MicroWell white polystyrene plate	Thermo Scientific

Material	Supplier
FACS tube 5 ml with strainer cap 35 µm	BD
KOVA Glasstic SLIDE 10 with GRIDS	VWR
Microscope slides, cut edges, matt strip	Thermo Scientific
Micro cover glasses, 22 mm x 40 mm	VWR
Optical 384-well reaction plate	Life Technologies
Pipette tips filtered and unfiltered	Starlab
PVDF Blotting Membrane	GE Healthcare
PVDF filter pore size 0.45 uM	Millipore
QIAshredder	Qiagen
Reaction Tubes	Eppendorf
Rotilabo® - Blotting papers, thick 1.5 mm, 580x600 mm	Carl Roth
Scalpels	VWR
Stripettes	Greier Bio-One
Ultra-low attachment 96-well plates	Sigma

4.1.9 Instruments

Table 12: Listing of laboratory instruments and their manufacturers

Instrument	Manufacturer
Axioplan 2 Imaging Microscope	Carl Zeiss
Avio Observer.Z1 (including Heating Unit XL S, CO_2 Module S and Temp Module S)	Carl Zeiss
ChemiDoc™ MP System	Bio-Rad
Dounce homogenizer	B. Braun
FACSAria IIIu	BD
FV1000 inverted confocal laser scanning microscope	Olympus
Heracell 240i CO2 incubator	Thermo Scientific
Heraeus Megafuge 40R Centrifuge	Thermo Scientific
iMark™ Microplate Absorbance Reader	Bio-Rad
Leica DM IL LED	Leica
Luminometer Centro XS^3 LB 960	Berthold Technologies
Mastercycler nexus gradient	Eppendorf
Mini-PROTEAN® Tetra Cell Systems	Bio-Rad
NanoDrop® ND 1000 Spectrophotometer	Thermo Scientific
QuantStudio 12K Flex qPCR System	Life Technologies
Sonopuls HD 2070 Sonicator	Bandelin
SteREO Lumar.V12	Carl Zeiss
Thermomixer comfort 1.5 ml	Eppendorf

4.1.10 Software

Table 13: Listing of utilized software and their manufacturers

Software	Manufacturer
Axiovision Rel 4.7	Carl Zeiss
FACS Diva 6.0	BD
FlowJo V10	FlowJo, LLC
FV10-ASW	Olympus
ImageJ 1.48	NIH
Image Lab™	Bio-Rad
MikroWin, Version 4.41	Mikrotek Laborsysteme GmbH
QuantStudio 12K Flex	Life Technologies
Photoshop	Adobe
Timm's Aquisition Tool (TAT)	with the courtesy of Timm Schröder
Timm's Tracking Tool (TTT)	with the courtesy of Timm Schröder

4.2 Methods

4.2.1 Cell biological methods

4.2.1.1 Cell culture

All cell culture steps were performed under a sterile work bench. Cell lines used in this study were cultured in tissue culture dishes at 37°C and 5 % CO_2 in a Heracell 240i incubator. Every two to three days cells were passaged. For passaging, media was removed and the cells were washed with PBS, followed by trypsinization with 0.15 % Trypsin-EDTA. For HMLE cells and their derivatives, trypsinization was stopped by adding TNS in a 3:1 ratio. For all other cell lines the corresponding media containing FCS was used in a 10:1 ratio. The cell suspension was then centrifuged at 1500 rpm for 5 min and the cell pellet was resuspended in fresh media and dispensed into a new culture dish. Cell lines and the corresponding cell culture media are listed in *Table 14*. Additionally, for induction of the Twist1 transcription factor, cells were treated with 4-hydroxytamoxifen (TAM; dissolved in 100 % EtOH) at a final concentration of 20 nM and/or 2 ng/ml TGFβ (dissolved in 4 mM HCl containing 1 mg/ml BSA).

Table 14: Cell lines and corresponding cell culture media

Cell line	Culture Media	Supplements
HEK293T	DMEM	10 % FCS, 1 % Pen/Strep
MCF7-Ras	DMEM	10 % FCS, 1 % Pen/Strep
MDA-MB-231	DMEM/F12	10 % FCS, 1 % Pen/Strep
A549 (Twist1-ER)	F12/K	10 % FCS, 1 % Pen/Strep, (10 µg/ml blasticidin)
HMLE-Twist1 (-ER)	Mammary Epithelial Cell Growth Medium	0.004 ml/ml bovine pituitary extract, 10 ng/ml EGF, 5 µg/ml insulin, 0.5 µg/ml hydrocortisone, (10 µg/ml blasticidin) and 1 % Pen/Strep

4.2.1.2 Cell treatment with small-molecule inhibitors

For *in vitro* experiments, small-molecule (sm) inhibitors were used from a stock solution (10 nM) in dimethyl sulfoxide (DMSO). Inhibitors were added freshly to the media before treatment. Concentrations established during inhibitor titrations were: 1 µM for A83-01, 1 µM for IWP-2, 1 µM for XAV939, 200 nM for SP600125 and 30 nM for Wnt-C59. Untreated cells and cells treated only with DMSO served as controls.

4.2.1.3 Puromycin selection

In order to select successfully transduced cells with a puromycin resistance, the lethal puromycin dose had to be established. For this, $2x10^5$ non-transfected cells per well were disseminated on a 6-well plate. Puromycin was diluted in HEPES buffer to a concentration of 10 mg/ml according to manufacturer's instructions. Cells were treated with different concentrations of the puromycin solution ranging from 0.5 to 5 µg/ml. Media supplemented with puromycin was changed every second day. The lowest concentration that killed 100 % of non-transduced cells in 3 – 5 days after start of the treatment was used for puromycin selection (here: 2 µg/ml).

4.2.1.4 Migration assay

For testing of single-cell migratory abilities, cells were trypsinized and counted. $2.5x10^4$ cells per well were seeded in triplicates in 24-well culture inserts with 8 µm pores (BD). Cells were allowed to squeeze through the pores and attach to the underside of the insert for 24 h. Afterwards, non-migratory cells were removed from the upper side of the insert with a cotton swab. For visualization of the migrated cells, these were fixed and stained with the Hemacolor Rapid staining Set (Merck) according to the manufacturer's instructions (for details see *section 4.2.2.4*). Migrated cells were counted on a light microscope using 10-fold magnification.

4.2.1.5 Mammosphere assay

To determine anchorage-independent clonogenic growth, cells were plated into the mammosphere assay (Dontu et al., 2003). Cells were trypsinized, filtered through a 40 µm strainer and counted in duplicate. Subsequently, cells were seeded into an ultra-low attachment 96-well plate in mammosphere medium (100 µl/well) as indicated in *Table 15*. Mammospheres ≥ 50 µm were counted after 10-12 days of culture. For serial passaging, mammospheres were collected into a 50 ml tube, washed with PBS and trypsinized. To obtain single-cells only, cells were filtered through a 40 µm strainer, counted and reseeded as described above.

Table 15: Receipe of the mammosphere medium

Mammosphere Medium Composition
DMEM/F12
5 ng/ml EGF
20 ng/ml bFGF
0.5 µg/ml hydrocortisone
10 µg/ml insulin
4 µg/ml heparin
1x B27
0.3 % methylcellulose

4.2.1.6 Proliferation assay

To determine the maximum concentration of sm-inhibitors that is not generally cytotoxic, 2500 to 3000 cells per well were seeded in white polystyrene 96-well plates in 100 µl corresponding medium. Starting the following day, cells were drug-treated for 72 h (6 replicates per condition), adding fresh drugs every 24 h. The viability of the cells was measured every day using either WST-1 (Roche) or Cell Titer Glo reagent (Promega). The WST-1 reagent is cleaved by metabolically active cells, which results in a colorimetric reaction. Thus, measurement of the dye intensity correlates with viable, proliferating cells. Similarly, the Cell Titer Glo reagent allows assessment of viable cells by cell lysis and subsequent generation of a luminescent signal proportional to the amount of ATP present, an indicator of metabolically active cells. When using WST-1, 10 µl of the reagent was added to each well and the plate was then returned to the incubator for another hour. Afterwards, absorbance was measured on an iMark™ Microplate Absorbance Reader at 450nm, using the 595nm wavelength as a reference. For Cell Titer Glo measurements, the growth medium of the cells was replaced (50 µl/well), plates were equilibrated to room temperature for 10 min and then 1 volume (50 µl/well) of Cell Titer Glo reagent was added to the wells. Plates were agitated for 2 min on an orbital shaker and then incubated at room temperature for 1 h to allow lysis of cells and luciferase reaction of the Cell Titer Glo reagent. Luminescence was then measured on a BertholdTech plate luminometer using luciferase specific settings and 0.25 sec integration time/well. Data was normalized to respective untreated control.

4.2.1.7 Culture in 3D collagen gels

To model *in vivo* 3D breast tissue environment, cells were cultivated in a compliant collagen-based matrix, termed as 3D collagen gels. 3D collagen gels were prepared according to a published protocol (Linnemann et al., 2015). Briefly, single-cell suspensions were prepared in the corresponding media (Table 14) with desired numbers of cells. The cell suspensions were first quickly mixed with neutralizing solution (1:1 volume of collagen) and then with acidified rat tail collagen type I on ice, so that the final collagen concentration was 1.3 mg/ml. The gel mixture was plated into silioxane-coated 24 (400µl/well) or 6-well (2 ml/well) plates on ice and was allowed to polymerize at 37°C for 1 h. Gels were then loosened from the well using a

pipet tip and 1 ml (24-well) or 2 ml (6-well) cell growth medium (Table 14) was added. Floating of the gels was ensured by carefully shaking the plate, in order to completely release the gel. Media was changed every 2-3 days. To measure proliferation in 3D-collagen cultures, gels were digested with Collagenase I solution (1:100 dilution in growth medium) for 1 h at 37°C, followed by trypsinization to obtain a single-cell suspension. Cells were then counted manually on a light microscope using 10-fold magnification.

4.2.1.8 Live cell imaging

Live cell imaging is a very accurate technique for monitoring cell behavior and real-time modifications, especially when applying drug treatment. In this study, we assessed the impact of Twist1 activation on cell proliferation and migration in the presence or absence of TGFβ signaling. For this, HMLE-Twist1-ER cells that have been treated with TAM alone or in combination with A83-01 for 9 days were plated in triplicates 24 h prior to imaging onto 24-well plates (10,000 cells/well). Media including drugs was changed just before starting live analysis and was not replaced further during the imaging procedure. Cells were monitored via an Axio Observer.Z1 microscope using Timm's Acquisition Tool (TAT) over a period of 72 h. During this time, brightfield pictures were taken automatically at 20-fold magnification every 5 min. Cell tracking and statistical analysis was performed in collaboration with Prof. Fabian Theis and Dr. Carsten Marr at the Institute for Computational Biology (ICB) at the Helmholtz Zentrum München.

Single-cells were tracked manually using Timm's Tracking Tool (TTT) (Eilken et al., 2009; Rieger et al., 2009). Data was displayed as a binary tree, where each node represented one event (spatial displacement, cell division or apoptosis). Following parameters were assessed: cell cyle duration (from origin to division) and cell speed (displacement during the time between two consecutive observations – 5 min). The mean displacement of a cell over all observations was defined as average cell speed. A Kruskal-Willis test with post-hoc pairwise comparisons using Nemenyi-test: $p<001$ was employed for statistical analysis.

4.2.2 Biochemical methods

4.2.2.1 Protein isolation from mammalian cells

To assess protein expression levels, either whole cell lysates containing total proteins or fractioned lysates of the nuclear and cytoplasmic compartment were prepared. Protein extracts were stored at -80°C.

4.2.2.1.1 Whole cell lysate preparation

Isolation of total proteins was performed using RIPA buffer fabricated in concordance with the recipe provided by Cell Signaling Technologies and following the manufacturer's instructions. Cells were washed with PBS and incubated with RIPA buffer (400-600 µl/10-cm plate, depending on cell number, and 250 µl/6-well) for 5 min on ice. The lysed cells were collected by using a cell scraper and were transferred into an Eppendorf tube. Afterwards, the cell suspension was centrifuged for 10 min at 14,000 g and 4°C. The supernatant containing the protein fraction was transferred into a new tube.

4.2.2.1.2 Subcellular fractionation

Nuclear and cytoplasmic cell fractionation was done using Tween 20 lysis buffer as previously described (Klenova et al., 2002), with minor modifications. Cells were grown on 10 cm dishes until they reached 80-90 % confluence. For the cytoplasmic protein extraction, cells were washed with PBS and then 250 µl of Tween 20 lysis buffer was distributed to the cell culture dish. Cells were immediately scraped and transferred to an Eppendorf tube, followed by 30 min incubation on ice. Cells were then lysed by 25 strokes in the dounce homogenizer (B. Braun). Nuclei were pelleted at 2500 rpm for 10 min at 4°C. The supernatant equaled the cytoplasmic protein extract and was transferred to a fresh tube and supplemented with 5 M NaCl to a final concentration of 250 mM.

For the nuclear protein extraction, the previous pellet was washed with 250 µl of Tween 20 lysis buffer and again centrifuged at 2500 rpm for 10 min at 4°C. The supernatant was then fully removed and the pellet was resuspended in 100 µl Tween

20 lysis buffer supplemented with 500 mM NaCl. Following 15 min incubation on ice, nuclear membranes were broken using a Sonopuls HD 2070 sonicator (Bandelin) for 15 impulses at 30 % input. Next, 100 µl Tween 20 lysis buffer were added to each sample and tubes were centrifuged at 10,000 g for 15 min at 4°C. The supernatant containing nuclear protein extract was collected into a new tube.

4.2.2.2 Determination of protein concentration

Proteins were quantified using the Bio-Rad DC Protein Assay Kit following the manufacturer's instructions. Similar to the well-documented Lowry assay (Lowry et al., 1951), this method is based on the reaction of protein with an alkaline copper tartrate solution and Folin reagent. First, copper ions associate with the peptide bond of proteins under alkaline conditions (Biuret-reaction). In a subsequent step, the copper-protein complex leads to the reduction of Folin reagent, which results in a blue color development that can be measured at 750 nm.

For an accurate protein determination a series of protein dilutions was prepared (BSA diluted in RIPA or Tween 20 lysis buffer) , containing following concentrations: 10 mg/ml, 5 mg/ml, 2 mg/ml, 1.5 mg/ml, 1 mg/ml, 0.5 mg/ml, 0.25 mg/ml, 0.125 mg/ml and pure RIPA or Tween 20 lysis buffer as blank. 5 µl of each sample of protein extract or of protein standards was pipetted in duplicate into a 96-well plate. Then, reagent A' was prepared by mixing 20 µl of reagent S with 1 ml of reagent A. 25 µl of reagent A' was added to each well. Subsequently, 200 µl of reagent B was added to each well. Upon 15 min of incubation at RT the absorbance at 750 nm was measured using an iMark™ Microplate Absorbance Reader (Bio-Rad).

4.2.2.3 Sodium Dodecyl Sulfate Polyacrylamide Gel Electrophoresis (SDS-Page)

SDS-Page is a biochemical technique used for protein separation according to their size and charge. Negatively charged SDS binds to proteins and denatures these to their primary structure. Consequently, the protein-SDS complexes migrate to the anode (the positive electrode) during gel electrophoresis.

In this study, acrylamide gels with different concentrations were used to separate proteins depending on their molecular weight (Table 16).

Table 16: Composition of stacking gel and separating gel used for SDS-Page

Reagent	Stacking Gel	Separating Gel (10 %) 30-200 kDa	Separating Gel (12.5 %) 10-120 kDa
30 % Acrylamide	833 µl	3.3 ml	3.9 ml
MilliQ water	3.46 ml	6.1 ml	5.5 ml
1 M Tris pH 8.8	-	2.5 ml	2.5 ml
1 M Tris pH 6.8	625 µl	-	-
10 % SDS	50 µl	100 µl	100 µl
Temed	5 µl	7.5 µl	7.5 µl
10 % APS	25 µl	75 µl	75 µl

An amount of 10-30 µg of each protein sample was mixed with 5x SDS buffer and then incubated for 5 min at 95°C in order for protein denaturation to occur. Afterwards, the samples together with 8 µl of PageRuler Prestained Protein Ladder (Thermo scientific) were loaded on the previously prepared gel. Electrophoresis was performed at 120 V for 60-80 min.

4.2.2.4 Immunoblotting

Immunoblotting (also called Western blot) is a biochemical technique used for protein detection after having these separated in an electrophoretic process like SDS-Page.
In this study, a Tank/Wet Blotting System was used. For this, proteins from the SDS-gel were transferred to a PVDF membrane by electroblotting. First, sponges and filter paper were soaked in transfer buffer. The PVDF membrane was activated for 30 seconds in methanol. Then, sponges and filter papers together with the PVDF membrane and the gel were arranged as a sandwich as shown in *Figure 3*. Since the proteins were still negatively charged from the SDS buffer, these migrated towards the anode. Electroblotting was performed at amperage suitable for the size of the membrane (2 mA/cm²) for 1.5-2 h.

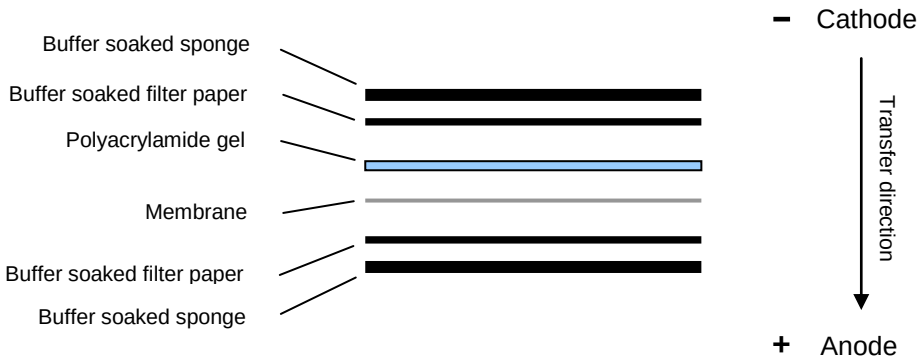

Figure 3: Assembly of the Wet-Blot-System

After transferring proteins onto the PVDF membrane, this was briefly washed with TBS/T (Tris-Buffered Saline and Tween 20). Then the membrane was blocked with 5 % milk powder solution for 1 h at RT in order to prevent unspecific interactions between the membrane and the antibody used in subsequent steps. Afterwards, the membrane was incubated overnight with an adequate dilution in 5 % milk powder solution of the primary antibody (Table 7) at 4°C. On the next day, the membrane was rinsed three times in TBS/T for 10 min each. A dilution of the secondary antibody in 5 % milk powder solution (Table 8) was then applied for another hour at RT. At the end of the incubation time, the membrane was rinsed three times in TBS/T followed by three times in TBS for 10 min each. Secondary antibodies used in this study were conjugated with horseradish peroxidase (HRP) and therefore allowed a chemiluminescent detection after incubation with ECL solution. This was prepared freshly by mixing Reagent A and B in a ratio of 1:1 according to the manufacturer's instructions. Following an incubation of 5 min, the membrane was analyzed by using the ChemiDoc System (Bio-Rad).

For further protein analysis, the ECL solution was washed off the membrane with TBS and the membrane was incubated in stripping buffer for 1 h at RT. The membrane was then briefly rinsed in TBS/T. After 1 h blocking in 5 % milk powder solution, overnight incubation at 4°C with the new antibody followed. Subsequent steps were the same as described above.

Acquired images were further analyzed for protein quantification via ImageJ. For this, each lane and the corresponding, unspecific background was marked by the rectangle tool. The program then calculated the signal intensity based on the area

and the pixel density. Relative values were determined by subtracting the background from the lane of interest, followed by normalization to the loading control.

4.2.3 Flow cytometry

Flow cytometry was performed by fluorescence activated cell sorting (FACS). This technique allows detection and sorting of pre-labeled cells.

4.2.3.1 Sample preparation

For cell sorting, cells were trypsinized, filtered through a 40 µm filter and counted. For each sample, $1x10^6$ cells were resuspended in 100 µl FACS buffer. Cells were double stained with CD44 and CD24 antibodies (Table 7) for 45 min on ice, washed with PBS and resuspended in FACS buffer ($1x10^7$ cells/ml). Prior to sorting, cells were filtered through a 35 µm strainer into 5 ml round-bottom FACS tubes and 7AAD (Table 7) was added to distinguish between dead and alive cells. Cells without staining, singly stained for CD44, CD24 and 7AAD were used as a control.
Cells sorted for GFP were handled as described above, without antibody staining. Cells without an incorporated GFP plasmid served as a control.

4.2.3.2 Cell sorting

GFP-positive or CD44 and CD24 stained HMLE-Twist1-ER cells were sorted on a BD FACSAriaIIIu using the 70 µm nozzle. FITC fluorescence of CD24 and GFP were analyzed with the 488 nm laser and detected by the 530/30 nm filter, while APC fluorescence of CD44 was analyzed with the 633 nm laser and detected by the 660/20 nm filter. 7AAD was excited with the 488 nm laser and detected by the 695/40 nm filter. Cell doublets and debris were excluded by using forward and side scatter, followed by discrimination of live cells by absence of 7AAD fluorescence. Unstained and single-antibody stained controls served as references to draw positive and negatives gates. To obtain highly purified populations according to set gates, the sort mode “4-way purity” was used. The population $CD44^+/CD24^{high}$ or GFP-positive cells were sorted into a sorting tube containing Mammary Epithelial Cell Growth Medium. Sorted populations were plated into 6-well plates and further expanded.

4.2.3.3 Cell surface marker analysis

For cell surface marker analysis, cells were trypsinized, filtered through a 40 µm filter and counted. For each condition, $2x10^5$cells were resuspended in 100 µl FACS buffer. Cells were double-stained with CD44 and CD24 antibodies (Table 7) for 45 min on ice, washed with PBS and resuspended in 500 µl FACS buffer. Prior to analysis, cells were filtered through a 35 µm strainer into 5 ml round-bottom FACS tubes and 7AAD (Table 7) was added to distinguish between dead and live cells. Cells without staining, singly stained for CD44, CD24 and 7AAD were used as a control. Cells were analyzed on the BD FACSAriaIIIu instrument using the same settings as described in *section 4.2.3.2*.

4.2.4 Immunostaining and histological staining

Immunostaining techniques use labeled antibodies for visualization of specific proteins in experimental samples. If the antibody is tagged with a fluorescent dye, this assay is called immunofluorescence. Direct (primary) immunofluorescence refers to an already fluorescently labeled primary antibody, whereas indirect (secondary) immunofluorescence requires a secondary antibody tagged with a fluorescent dye that recognizes the primary antibody. In this study, primary and secondary immunofluorescence techniques were used for cells either grown in 2D (on coverslips) or in 3D collagen gels. Samples were kept in a humidity chamber for all incubation steps.

Histological staining methods are commonly used for visualization of cell populations, nuclei or other cellular compartments in tissues or structures that have been removed from their biological context. In this study, the natural dye, carmine, was employed for the staining of cellular structures growing in 3D collagen gels. Additionally, the Hemacolor Rapid staining Set (Merck) was used to stain cells cultured in 2D.

4.2.4.1 Immunofluorescence of cells grown in 2D

For indirect immunofluorescence, cells were seeded on Poly-D-Lysine coated coverslips and cultured until they reached 80 % confluency. Coverslips were then washed with PBS and cells were fixed with 4 % PFA/PBS for 10-15 min at RT. After washing 3 times with PBS, cells were permeabilized with 0.2 % Triton-X-100/PBS for

2 min, washed 3 times with PBS and then blocked with 10 % NGS/0.1 %BSA/PBS for 1h at RT. Slides were again washed 3 times with PBS, followed by incubation overnight at 4°C with primary antibodies (Table 7) diluted in 0.1 %BSA/PBS. The following day, coverslips were washed with PBS and incubated with secondary antibodies (Table 8) diluted in 0.1 % BSA/PBS for 2-3h at RT protected from light. Proceeded by a further washing step with PBS, coverslips were briefly incubated with DAPI/PBS solution (167 ng/ml) for staining of cell nuclei. Afterwards, the coverslips were washed with MilliQ water and mounted with AQUA-POLY/MOUNT mounting medium on slides. Slides were stored at -20°C. Images were acquired on an Axioplan 2 imaging light/fluorescence microscope using a 20x objective and processed with Axiovision Rel 4.7 and Adobe Photoshop C55 software.

4.2.4.2 Immunofluorescence of 3D collagen gels

All washing steps, as well as the fixation, permeabilization and quenching of 3D collagen gels were performed using an orbital shaker.

Cells grown in 3D collagen gels were washed with PBS for 10 min, fixed with 4 % PFA/PBS for 15 min and then washed again with PBS for 10 min. PFA was quenched with 0.15 M Glycine for 10 min, followed by a washing step with PBS for 10 min. Then, cells were permeabilized with 0.2 % Triton-X-100/PBS for 10 min and washed with PBS for 10 min. Cells were blocked with 10 % NGS/0.1 %BSA/PBS overnight at 4 °C. The next day, cells were washed with PBS for 10 min and then incubated with primary antibodies (Table 7) diluted in 0.1 % BSA/PBS at 4 °C overnight. Next, cells were washed with PBS three times for 10 min and incubated with secondary antibodies (Table 8) diluted in 0.1 % BSA/PBS for 2-3h at RT, followed by two further washing steps with PBS for 10 min each. Cell nuclei were stained with DAPI/PBS solution (167 ng/ml) for 2 min. Then, cells were washed with PBS three times for 10 min and with MilliQ water two times for 5 min. Collagen gels were mounted with AQUAPOLY/MOUNT mounting medium, dried overnight, sealed, and stored at -20 °C. Samples were imaged on a FV1000 inverted confocal laser scanning microscope by acquisition of Z-stacks in 2 µm intervals. Z-stacks were collapsed with the FV-10-ASW 1.7 Viewer and images were processed with the Adobe Photoshop C55 software.

4.2.4.3 Carmine staining of 3D collagen gels

Carmine-aluminium staining solution was prepared by boiling 1 g Carmine and 2.5 g aluminum potassium sulfate in 500 ml distilled water for 20 min. After reaching lukewarm temperature, one crystal of thymol was added for preservation and the solution was sterile filtered. 3D collagen gels were fixed with 4 % PFA/PBS, as described in *section 4.2.4.2*, and were incubated in Carmine solution on a shaker overnight at RT. For structure quantification, gels were imaged on a Leica DM IL LED microscope with a HiPlan 10x/0.22 PH1 objective. Whole mount pictures were taken with a SteREO Lumar. V12 microscope with a NeoLumar S 0.8x objective, at 20-fold magnification.

4.2.4.4 Staining with the Hemacolor Rapid staining Set

Cells were fixed for 30 sec with the methanol-containing Fixing Solution. Afterwards, cells were incubated for 2 min with Staining Solution 1 (for visualization of the cytoplasm), followed by 2 min incubation with Staining Solution 2 (for visualization of nuclei). Cells were briefly washed with the incorporated buffer solution and wells were air-dried overnight.

4.2.5 Molecular biology methods

Molecular biology methods refer to all techniques used for DNA/RNA handling and analysis, including nucleic acid amplification, transient transfection and lentiviral transduction.

4.2.5.1 Gene Expression Analysis

4.2.5.1.1 RNA isolation and reverse transcription

For RNA extraction, cells were grown on either 10 cm cell culture dishes or 6-well plates until they reached 80 % confluency. Cells were then washed with PBS and lysed with either RLT/β-mercaptoethanol solution (for mRNA only) or Qiazol reagent (for total RNA). Cell lysates were then homogenized by 2 min centrifugation at

14.000 g in QIAshredder columns (Qiagen). Subsequent steps for RNA isolation were applied using the RNeasy Mini Kit (for mRNA only) or the miRNeasy Mini Kit (for total RNA) corresponding to the manufacturer's instructions. An additional DNA digestion step was performed using the RNase-Free DNase Set (Qiagen) according to manufacturer's instructions. Isolated RNA was stored at -80°C.
For the reverse transcription of mRNA the EasyScriptPlus cDNA Synthesis Kit (Applied Biological Materials) was used according to manufacturer's instructions. miRNA was reverse transcribed using the miScript RT Kit (Qiagen) according to manufacturer's instructions. cDNA, as well as transcribed miRNA was stored at -20°C.

4.2.5.1.2 Real-Time Polymerase Chain Reaction (RT-PCR)

Real-Time quantitative PCR of cDNA was performed using the Power SYBR® Green PCR Master Mix (Applied Biosystems) for sample preparation. The exact mixture for each sample is listed in *Table 17*. Samples were run on a QuantStudio 12K Flex qPCR System according to the cycling program illustrated in *Table 18*. RPL32, a housekeeping gene, was used as loading control and each primer was run in a water control. All primer sequences are mentioned in *Table 4*.

Table 17: Reaction mixture for RT-PCR amplification

Component	10 µl Reaction
Forward Primer (20 µM)	0.25 µl
Reverse Primer (20 µM)	0.25 µl
Power SYBR® Green PCR Master Mix	5 µl
RT-PCR grade water	2.5 µl
cDNA	100 ng

Table 18: Cycling parameters for RT-PCR

Step	Cycles	Duration	Temperature
Initial activation	1	10 min	95°C
Denaturation	40	15 sec	95°C
Annealing		30 sec	60° (T_m of primers)
Extension		16 sec	72°C

For amplification of transcribed miRNA, the miScript Primer Assays (HS-RNU6-2_11, HS-miR-141_1, HS-miR-200a_1, HS-miR-200b_3, HS-miR200c_1) together with the miScript SYBR Green PCR Kit (Qiagen) were used according to manufacturer's instructions. RNU6-2 served as internal control.

Data were analyzed using the ΔC_T method to present data as fold change expression compared to internal control (RPL32 or RNU6-2). The threshold cycle Ct is defined as the PCR cycle at which the fluorescent signal (here SYBR Green) crosses an arbitrarily set threshold that is slightly above background. First, the expression of the gene of interest is normalized to the expression of the housekeeping gene by subtracting the C_T value of the gene of interest from the Ct value of the housekeeping gene ($\Delta C_T = C_T$(RPL32 or RNU6-2)-C_T (gene of interest)). Then, fold expression of the gene of interest compared to the housekeeping gene expression was calculated by the formula $2^{\Delta C_T}$. In this way, it is possible to compare the expression levels of different genes of interest relative to the housekeeping gene (Schmittgen and Livak, 2008).

4.2.5.2 Chromatin Immunoprecipitation Assay (ChIP)

ChIP analysis is a technique used to detect the interactions of proteins and DNA sequences. The principle of this method consists in the crosslinking of proteins bound to a specific DNA sequence, followed by fragmentation of the chromatin and antibody-based retrieval of the protein-DNA complex. Subsequently, the retrieved DNA sequence is amplified by PCR. In the present study, ChIP analysis was used to determine the binding of the EMT-TF Twist1 to the ZEB1 promoter region.

First, media was removed from adherent growing HMLE-Twist1-ER cells. For crosslinking, 8 ml of 1 % formaldehyde (freshly prepared in PBS by diluting 37 % formaldehyde) was added to each 10 cm cell culture plate, followed by 20 min incubation at room temperature. Next, formaldehyde was quenched by addition of 125 mM glycine and 5 min incubation on a slowly rotating shaker. Cells were then washed twice with ice-cold PBS and plates were kept on ice. Cells were scraped and collected in 1 ml ice-cold PBS and frozen at -20°C. Subsequent steps were performed in collaboration with the Steven Johnsen Laboratory at the University of Göttingen, Germany and according to a previously published protocol (Nagarajan et al., 2014). Briefly, nuclei were isolated and sonicated. Next, chromatin extracts were purified by centrifugation, diluted, coupled to sepharose 4B beads and used for immune-precipitation with ERα antibody or IgG isotype control antibody (Table 7). The ChIP immune complexes were pulled down using blocked protein A sepharose beads and washed. Following protein digestion, DNA was purified by the phenol-chloroform-isoamyl alcohol extraction method and precipitated. The DNA was dissolved in nuclease free water and analyzed by RT-PCR with specific primers (Table 5). RT-PCR reaction was performed as previously described (Prenzel et al., 2011).

4.2.5.3 Plasmid amplification methods

4.2.5.3.1 Bacterial culture

For bacterial culture, 25 g of Luria Broth Base were dissolved in 1 l MilliQ water, constituting the initial microbiological culture media called LB medium. A sufficient amount of LB medium was supplemented with Bacto Agar, a solidifying agent, at a concentration of 15g/l. This was used for bacterial culture plates. Both media were autoclaved. After reaching lukewarm temperature, antibiotic was added to the latter media according to plasmid resistance gene (here: 100 µl/ml ampicillin). Media was then poured into cell culture plates (100x20 mm) under a sterile work bench. Plates were allowed to cool down completely for 2-3 h and were stored at 4°C until further notice. This procedure allows selection of positive clones that have incorporated the antibiotic resistant plasmid of interest.

4.2.5.3.2 Transformation

DNA-plasmids were cloned by transformation into XL10-Gold Ultracompetent Cells from Agilent Technologies according to manufacturer's instructions. First, 0.2-0.5 µl of DNA was added into a tube of XL10-Gold Ultracompetent Cells and this was gently mixed. The vials were incubated on ice for 30 min and then the cells were heat-shocked for 45 seconds at 42°C without shaking. The vials were then placed on ice for 2 min. Afterwards, 50 µl LB medium containing antibiotics was added to each tube and gently mixed. The bacterial suspension was seeded on a pre-warmed selective plate and incubated overnight at 37°C.

4.2.5.3.3 Plasmid preparation

Plasmid isolation from bacteria was done by using the Plasmid Midi Kit (Qiagen) according to manufacturer's instructions. Briefly, a colony was picked from a selective plate and used to inoculate 3 ml LB medium containing antibiotics at the concentration mentioned above (see *section 4.2.5.3.1*). Alternativley, when glycerol stocks of bacteria containing the plasmid of interest (e.g. shRNAs targeting TGFBRI) were purchased, 3 ml LB medium were inoculated with 0.5 µl glycerol stock solution. After an initial incubation of 6-8 h at 37°C and 300 rpm, the culture was transferred to a conical flask (not sealed) containing 200 ml of LB medium with antibiotics and incubated for another 16 h at 37°C and 300 rpm. Bacterial cells were then harvested by centrifugation at 6000 g for 15 min at 4°C. The bacterial pellet was resuspended in buffer, followed by cell lysis and precipitation of cell components. After centrifugation, the DNA containing supernatant was allowed to drain through an anion-exchange column. This technique allowed DNA to bind to the column by ion exchange. DNA was then washed, eluted from the column and precipitated. The pellet was washed with ethanol (70 %) and allowed to air-dry. Finally, the DNA was redissolved in a suitable volume of molecular grade water, followed by concentration determination with NanoDrop® ND 1000 Spectrophotometer at 260 nm.

4.2.5.4 Transfection for reporter assays

For measurements of the transcriptional activity of gene regulatory factors, cells were transfected with plasmids containing the promoter of target genes coupled to a luciferase gene. In this way, when the transcription factor is active and binds to the promoter of its target gene this can be measured via the luciferase activity. For this purpose, HEK293T or HMLE-Twist1-ER cells were plated in triplicates at a density of 10,000 cells per well in a 96-well plate 24 h prior to transfection. Next, transfection mixes were prepared as stated in *Table 19* and incubated for 15 min at RT. Cells were transfected with a combination of the Firefly reporter gene construct (900 ng/reaction) and SV-40 Renilla (100 ng/reaction) as a control. Additionally, cells were transfected with either a TGFβ or a Wnt3a containing vector as a positive control for the reporter activity. 10 µl of each transfection mix were pipetted directly into the media of each cell containing well and the plate was briefly shaken before being returned to the incubator.

Table 19: Composition of the transfection mix

Component	100 µl Reaction
DNA	1 µg
X-tremeGENE HP DNA Transfection Reagent	3 µl
Medium w/o supplements	Add to 100 µl

The following day, media was changed and fresh media containing sm-inhibitors was added to the transfected cells. After another 24 h, cells were lysed using the Dual-Luciferase® Reporter Assay System from Promega (according to the manufacturer's instructions) and the luciferase activity was measured via a Luminometer Centro XS³ LB 960. For data analysis, values of the Firefly reporter gene were normalized to the SV-40 Renilla activity for each sample.

4.2.5.5 Viral transduction

All handling of infectious viral material during this experiment was in agreement with the recommended guidelines for working with BSL-2 safety class.

In this study, HMLE-Twist1-ER and A549 cells were lentivirally transduced with several shRNA constructs targeting TGFBRI with the purpose of silencing this gene. Additionally, A549 cells were retrovirally transduced with the Twist1-ER construct to obtain inducible Twist1-expressing A549 cells.

4.2.5.5.1 Transfection of the producer cells HEK293T

Transfection refers to the introduction of foreign naked DNA into eukaryotic cells. For this procedure, the pWZL Blast Twist1-ER plasmid or shRNA constructs targeting the TGFBRI were packaged into pseudoviral particles using the envelope protein encoding pCMV-VSV-G plasmid and pCMV-dR8.2 dvpr or pUMVC packaging plasmids for lentiviral or retroviral transduction, respectively. To improve gene delivery into the cells, the polymeric reagent PEI was used. Due to its positive charge, PEI encircles DNA molecules and precipitates them onto the anionic cell surface, where they are easily endocytosed (Boussif et al., 1995). HEK293T cells were used for viral packaging, having the characteristics of a highly transfectable cell line. 18-24 h prior to transfection, $2.5x10^6$ HEK293T cells were seeded in a 10 cm cell culture dish. Next, the expression vector was mixed with the packaging and envelope vectors, and the transfection reagent as listed in *Table 20*.

Table 20: Composition of the transfection mix

Component	500 µl Reaction
Expression vector	5 µg
pCMV-dR8.2 dvpr OR pUMVC	4.5 µg
pCMV-VSV-G	0.5 µg
PEI	15 µl
Medium w/o supplements	Add to 500 µl

The transfection mix was incubated at RT for 15 min. Finally, the mixture was evenly distributed to the cell culture dish and this was returned to the incubator. Media was replaced approx. 16 h after transfection with the media of the target cells.
At 48 and 72 h after transfection, media was collected from the cells and filtered through a PVDF filter pore, size 0.45 uM, to eliminate cell debris. The viral supernatant was either stored at -80°C until ready for use or supplemented with protamine sulfate (10 µg/ml) and added to the target cells.

4.2.5.5.2 Lentiviral and retroviral transduction of target cells

Lentiviral or retroviral transduction describes the infection of eukaryotic cells by lentiviruses or retroviruses, respectively. Usually, these viruses contain a DNA sequence of interest that is then inserted into the genome of the target cells at a random position.
On the day prior to transduction, $1.5x10^6$ target cells (HMLE-Twist1-ER and A549) were seeded in a 10 cm cell culture dish. Target cell density is crucial for retroviral transduction, since retroviruses can integrate carrying vectors only into the genome of actively dividing cells (Miller et al., 1990). After 24 h media was replaced with 10 ml of the viral supernatant described in *section 4.2.5.5.1*. In order to avoid downregulation of the cell surface receptor for viral particles, fresh media was added 6-8 h after the first transduction round. On the following day, target cells were transduced a second time to maximize DNA transfer. After another 48 h, media was replaced and puromycin (for shRNA constructs) or blasticidin (for the Twist1-ER construct) was added for the selection of positively transduced cells. At this point cells were stably expressing the gene of interest. This was monitored by fluorescence microscopy, where successfully transduced cells appeared in a fluorescent green color.
For HMLE-Twist1-ER cells transduced with shRNAs against TGFBRI, selection via puromycin was not possible because they already had a puromycin-resistance gene incorporated. Since the expression vector also contained the GFP gene linked to the shRNA sequence, this allowed flow cytometry sorting of positive transduced cells 72 h after the last transduction round (see *section 4.2.3*).

4.2.6 Statistical analysis

Data are presented as mean ± standard deviation (SD). A Student's t-test was used to compare two groups (two-tailed, unpaired), unless stated otherwise. *$p<0.05$ was considered significant.

5. Results

5.1 Inhibition of developmental pathways in human breast cancer cell lines

5.1.1 TNBC and luminal breast cancer cell lines delineate differences in clonogenic growth potential

This study aimed to find candidate compounds which specifically inhibit EMT features in TNBC. For this purpose, I utilized the TNBC cell line MDA-MD-231, originally derived from a pleural effusion (Brinkley et al., 1980). MDA-MB-231 cells display an invasive phenotype and have the ability to self-renew (Kenny et al., 2007; Fillmore and Kuperwasser, 2008). Together with an increased tumor initiation capacity and resistance to chemotherapy, the characteristics of this cell line indicate aggressive growth and high tumorigenic potential, thereby confirming its suitability as a model for the development of new treatment strategies against TNBC (Fillmore and Kuperwasser, 2008). Moreover, MDA-MB-231 cells have been shown to cluster with the Claudin-low gene signature, thus exhibiting several EMT traits (Prat et al., 2010). For example, MDA-MB-231 cells display a front-to-back polarity characteristic of mesenchymal cells (Fig. 4A) and express N-cadherin, ZEB2 and Slug, while having low E-cadherin expression, as assessed by RT-PCR (Fig. 4B). In order to distinguish between drug effects that are specific due to inhibition of EMT features and those that target other cellular processes not restricted to TNBC, I chose to include in this study the luminal, epithelial cell line MCF7-Ras. MCF7-Ras cells were created by transfection of the v-rasH onc gene into the ER positive MCF7 cells, thus overcoming estradiol dependency for cell growth (Kasid et al., 1985). Although MCF7-Ras have been shown to be tumorigenic, they are able to initiate tumor formation at much lower rates compared to MDA-MB-231 cells (Scheel and Weinberg, unpublished). In line with their epithelial, cobble-stone-like morphology (Fig 4A), MCF7-Ras cells express high levels of E-cadherin and have 5 to 1000-fold lower N-cadherin, ZEB1, ZEB2 and Slug transcript levels compared to MDA-MB-231 cells (Fig. 4B).

To confirm the differences in tumorigenic potential of MDA-MB-231 and MCF7-Ras cells, their abilities to form mammospheres were tested. The mammosphere assay is widely used for identification and culturing of self-renewing undifferentiated mammary

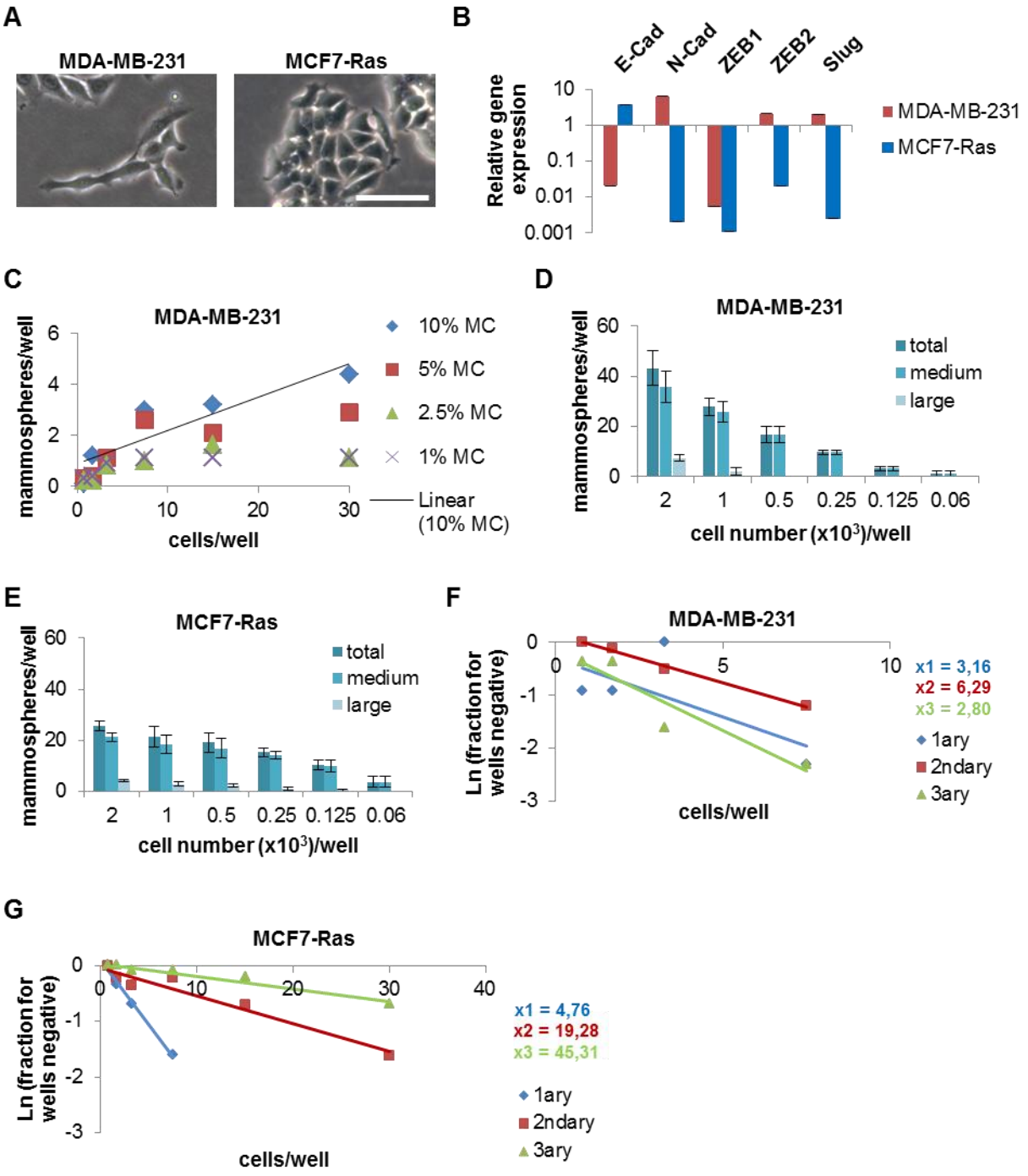

Figure 4: Breast cancer cell lines and their behavior in the mammosphere assay.
A. Brightfield pictures of MDA-MB-231 and MCF7-Ras cells grown under adherent conditions. MDA-MB-231 cells display a mesenchymal phenotype with an elongated cell body and front-to-back polarity. MCF7-Ras cells build epithelial islets with cobblestone-like morphology. Scale bar: 100 µm. **B.** RT-PCR analysis of E-cadherin (E-cad), N-cadherin (N-cad), ZEB1, ZEB2 and Slug in MDA-MB-231 and MCF7-Ras cells. **C.** Titration of methylcellulose concentration in the mammosphere media; MC, methylcellulose. **D.** and **E.** Titration of cell density of MDA-MB-231 and MCF7-Ras cells plated into the mammosphere assay and quantification of resulting medium, large and total amount of mammospheres. **F.** and **G.** Limiting dilution analysis of MDA-MB-231 and MCF7-Ras over two rounds of serial passaging. X-values next to the diagram indicate sphere forming efficiency (e.g.: x=2 means that every second cell generated a mammosphere). n=10.

epithelial cells and tumor-initiating cells (TICs) of the mammary gland *in vitro* (Dontu et al., 2003; Ponti et al., 2005; Fillmore and Kuperwasser, 2008). Cells with properties of stem cells have been shown to survive in anchorage-independence and build clonal, 3D outgrowths, referred to as mammospheres (Dontu et al., 2003). To increase viscosity and thus reduce the risk of cell clumping (which would otherwise temper with clonality), methylcellulose was added to the originally described mammosphere medium. First, the methylcellulose concentration in the mammosphere medium was titrated to determine the minimal amount of methylcellulose required to impede cell clumping. For this, MDA-MB-231 cells were plated into the mammosphere assay at densities ranging from 0.8 to 30 cells per 96-well. Additionally methylcellulose concentration was varied from 1 % to 10 % for each cell density (Fig. 4C). Ten days later, the number of mammospheres per well was counted. When using low concentrations of methylcellulose (1 % - 2.5 %), the number of mammospheres merely increased with higher amounts of plated cells (Fig. 4C), suggesting enhanced cell-cell interactions and clumping due to a rather aqueous media. Indeed, augmenting the methylcellulose concentration to 10 % resulted in a linear correlation between the number of seeded cells and the amount of generated mammospheres (Fig. 4C), thereby indicating clonal growth. For further experiments mammosphere media was therefore supplemented with 10 % methylcellulose.

I next analyzed another aspect that might interfere with the clonality of the mammosphere assay, which is cell density. I postulated that plating high cell densities might facilitate clumping. To test this hypothesis, 60 to 2000 cells (MDA-MB-231 and MCF7-Ras) were seeded per 96-well into the mammosphere assay and counted 8 days later. The size of the mammospheres was divided into medium and large, assuming that large mammospheres most probably derive from cell clumping. MDA-MB-231 cells, as well as MCF7-Ras cells formed higher amounts of large mammospheres with increasing numbers of plated cells (Fig. 4D and 4E), indicating that seeding high cell densities results in aggregations. The density at which large mammospheres could not be detected anymore was defined as suitable for the assessment of clonal growth. For MDA-MB-231 cells, this threshold was reached at a cell density of 500 cells/well. However, MCF7-Ras cells stopped generating large mammospheres at a seeding density of around 100 cells/well. To facilitate

comparable culture conditions for all cell lines, a density of 100 cells/well was used for further experiments.

It was previously reported that serial passaging of cells in the mammosphere assay enriches for multipotent progenitors (Dontu et al., 2003). To investigate whether MDA-MB-231 and MCF7-Ras cells have different abilities of generating TICs in long-term cultures, cells from both cell lines were passaged twice. Additionally, a limiting dilution approach was used for a precise quantification of sphere forming efficiency (SFE), resembling serial transplantation experiments with tumor initiating cells performed *in vivo* (Rota et al., 2012). To this end, MDA-MB-231 and MCF7-Ras cells were seeded into densities varying from 0.8 to 30 cells per 96-well. After 7 days, the number of wells negative for sphere formation was counted and spheres were dissociated by trypsinization and reseeded using the same density series as before. The same protocol was employed for the generation of later passages. Even though MDA-MB-231 and MCF7-Ras cells displayed comparable SFEs during primary sphere formation (every 3rd-5th cell generated a sphere), the SFE of MCF7-Ras cells decreased dramatically with each passage (Fig. 4F and 4G). In contrast MDA-MB-231 cells maintained similar SFEs over 3 passages, thus every third to sixth cell being able to form a mammosphere (Fig. 4F).

These results suggest that cells with an increased tumorigenic potential, like MDA-MB-231 cells, have a long-term ability to give rise to TICs, while non-invasive MCF7-Ras cells loose this capacity with time. In conclusion, the mammosphere assay may help distinguish between different levels of cell line tumorigenicity *in vitro* only when using serial passaging. Moreover, these data corroborated the choice of employing MDA-MB-231 cells as a model for aggressive TNBC and using MCF7-Ras cells as an epithelial and less tumorigenic control cell line.

5.1.2 Titration of small-molecule inhibitors targeting developmental EMT signaling pathways

The association of TNBC with an EMT gene expression signature provided new possibilities into targeted therapies against this disease (Prat et al., 2010). EMT is exogenously triggered by growth factors and signaling molecules which bind to their membranous receptors and propagate the signal inside the cell (Lamouille et al., 2014). Since TGFβ and Wnt signaling have been described as main inducers of the

EMT program (Scheel et al., 2011; Garcia-Castro, 2002; Brabletz, 2001), I tested whether inhibitors of both pathways can impair EMT features in the TNBC cell line MDA-MB-231 and thereby reduce its tumorigenicity. For blocking both canonical and non-canonical TGFβ signaling, I used the TGFRI inhibitor A83-01, described to be more potent than other small-molecule inhibitors of the same class (Tojo et al., 2005; Vogt et al., 2011). A83-01 binds to the ATP-binding pocket of the intracellular kinase domain of the TGFRI and thus inhibits recruitment and activation by phosphorylation of the downstream effectors Smad2 and Smad3 (Tojo et al., 2005). Canonical and non-canonical Wnt signaling was blocked by using the inhibitor of Wnt production 2 (IWP-2). IWP-2 targets Porcn, a member of the membrane-bound O-acyltransferase (MBOAT) family, which palmitoylates Wnt ligands and thus completes a necessary step for their secretion (Chen et al., 2009). XAV939 blocks tankyrase activity, thereby stabilizing axin and antagonizing canonical Wnt signaling (Huang et al., 2009). Non-canonical Wnt, as well as non-canonical TGFβ signaling activate JNK, which can be inhibited by the small-molecule SP600125 by competitive binding to the ATP-binding pocket (Moustakas and Heldin, 2005; Kühl, 2002; Weston and Davis, 2002).

To determine the optimal drug concentration, two independent parameters were taken into consideration, general cytotoxicity and efficient inhibition of the targeted pathways. As this study aimed to find compounds that specifically target EMT, the employed dosage should not display unspecific, cytotoxic effects, here measured by the impact on cell proliferation. For this, the concentration of small-molecule inhibitors was titrated by daily treatment of MDA-MB-231 and MCF7-Ras cells, followed by assessment of cell growth via the WST-1 assay. In the current analysis, A83-01 did not impair proliferation of MDA-MB-231 cells at any of the employed concentrations ranging from 0.1 to 3 µM compared to the untreated control (Fig. 5A, i). However, treatment with 3 µM A83-01 for 4 days slightly decreased cell growth of MCF7-Ras compared to the control (Fig. 5A, ii). Thus, the maximum A83-01 concentration that was registered as not cytotoxic was 1 µM. Based on the same principle, the highest non-cytotoxic dosage was established for all employed inhibitors. This resulted in 1 µM for IWP-2, 3 µM for XAV939 and 200 nM for SP600125 (Fig. 5B-D).

A second parameter for the assessment of the optimal drug concentration refers to the minimal dose, which can still efficiently block the targeted pathway. This prerequisite was assured by analysis of the transcriptional activity of downstream

A

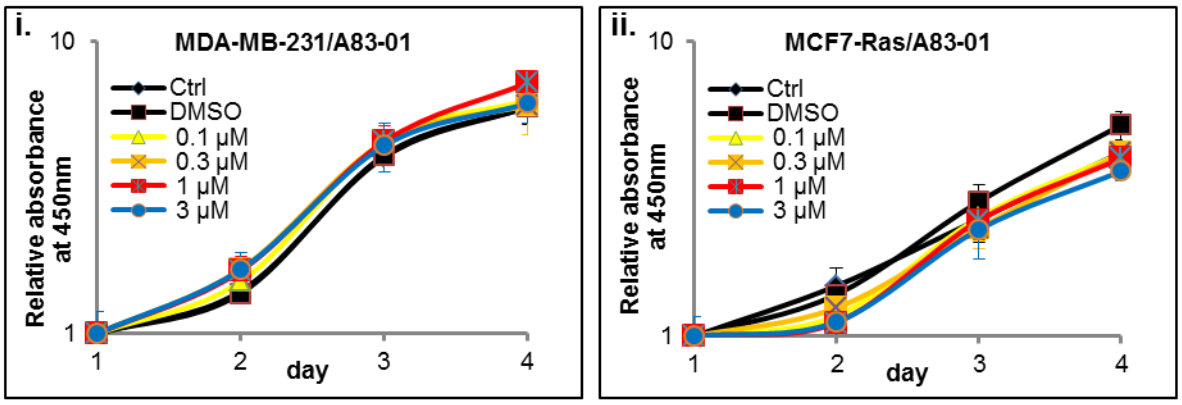
i.
MDA-MB-231/A83-01
Relative absorbance at 450nm
10
1
1
2
3
4
day
Ctrl
DMSO
0.1 µM
0.3 µM
1 µM
3 µM
ii.
MCF7-Ras/A83-01
Relative absorbance at 450nm
10
1
1
2
3
4
day
Ctrl
DMSO
0.1 µM
0.3 µM
1 µM
3 µM

B

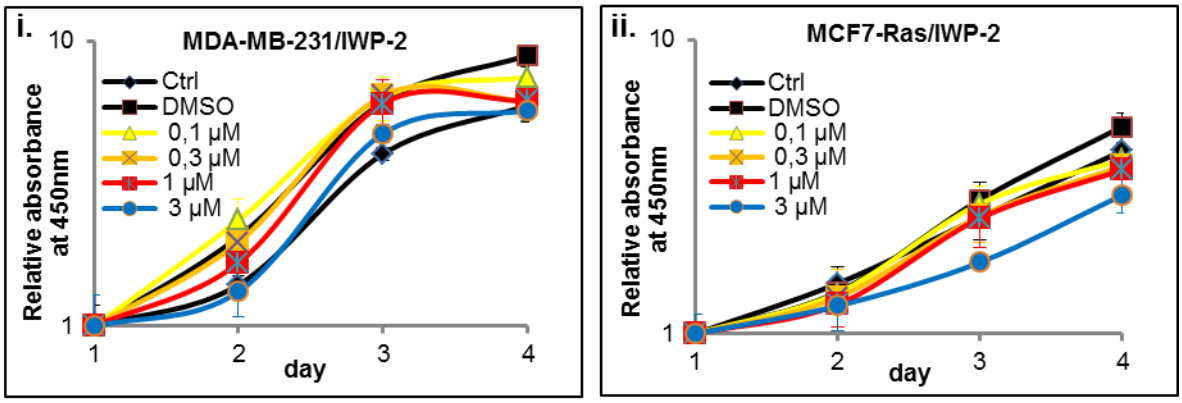
i.
MDA-MB-231/IWP-2
Relative absorbance at 450nm
10
1
1
2
3
4
day
Ctrl
DMSO
0,1 µM
0,3 µM
1 µM
3 µM
ii.
MCF7-Ras/IWP-2
Relative absorbance at 450nm
10
1
1
2
3
4
day
Ctrl
DMSO
0,1 µM
0,3 µM
1 µM
3 µM

C

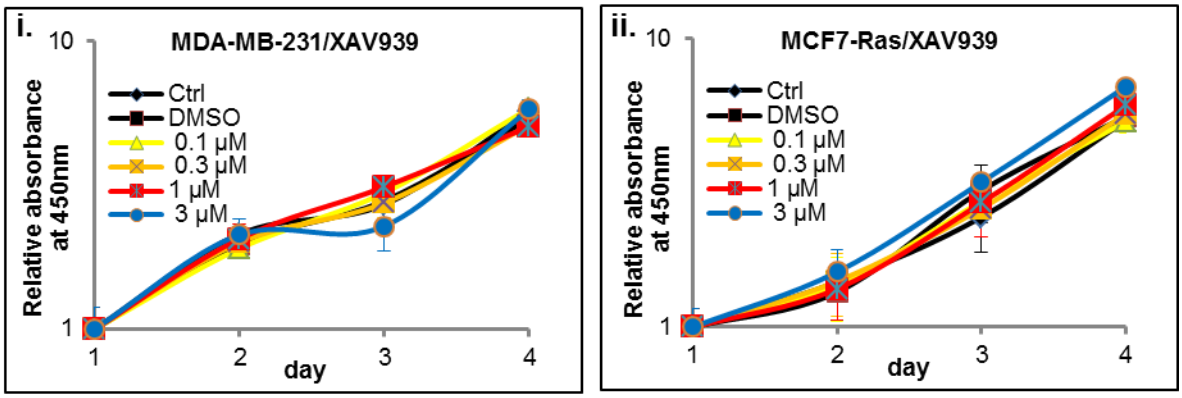
i.
MDA-MB-231/XAV939
Relative absorbance at 450nm
10
1
1
2
3
4
day
Ctrl
DMSO
0.1 µM
0.3 µM
1 µM
3 µM
ii.
MCF7-Ras/XAV939
Relative absorbance at 450nm
10
1
1
2
3
4
day
Ctrl
DMSO
0.1 µM
0.3 µM
1 µM
3 µM

D

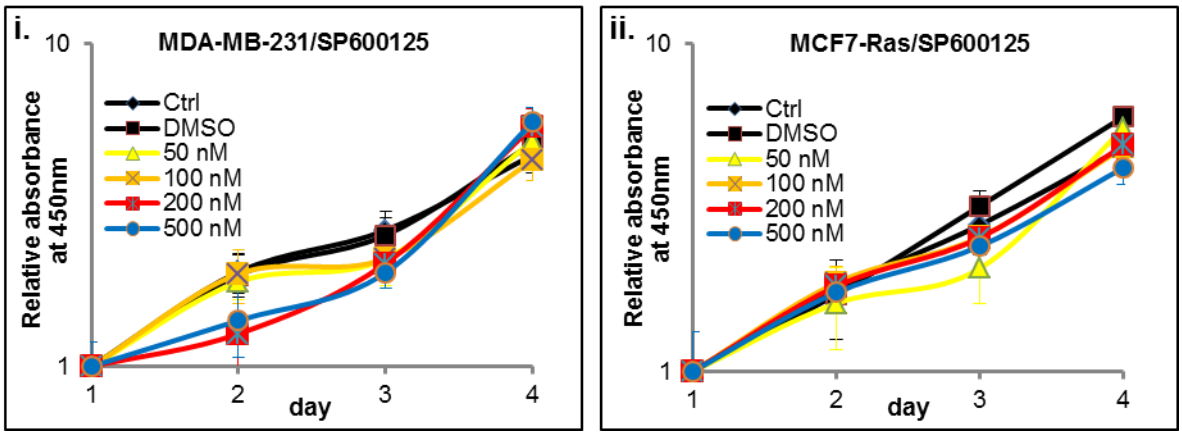
i.
MDA-MB-231/SP600125
Relative absorbance at 450nm
10
1
1
2
3
4
day
Ctrl
DMSO
50 nM
100 nM
200 nM
500 nM
ii.
MCF7-Ras/SP600125
Relative absorbance at 450nm
10
1
1
2
3
4
day
Ctrl
DMSO
50 nM
100 nM
200 nM
500 nM

Figure 5: Titration of small-molecule inhibitors via measurement of cell proliferation.
Impact on cell growth of A83-01 (**A**), IWP-2 (**B**), XAV939 (**C**) and SP600125 (**D**) in the cell lines MDA-MB-231 (**i**) and MCF7-Ras (**ii**) treated daily, over a period of 4 days. Treatment with the solvent DMSO and untreated cells (Ctrl) served as a control. n=6.

effectors via luciferase reporter assays. The minimal effective dosage of A83-01 was titrated by determining activity of the Smad-binding Element (SBE)-reporter (Zawel et al., 1998). For this, HEK293T cells were transfected with luciferase and SBE reporters, and a TGFβ expressing plasmid. Following 48 hours of treatment with different concentrations of A83-01, reporter activity was measured. As a positive control, overexpression of TGFβ enhanced SBE reporter activity 5-fold compared to the negative control lacking the TGFβ plasmid (Fig. 6A). Additional treatment with A83-01 (0.1 – 1 µM) showed a dose-dependent suppression of the reporter activity despite TGFβ overexpression (Fig. 6A). Comparing activity levels in the cells which overexpressed TGFβ and were treated with A83-01 to the ones that only received treatment with the inhibitor revealed that used in concentrations below 1 µM, A83-01 was able to significantly reduce, but not completely abrogate exogenously-triggered TGFβ signaling (Fig. 6A). Therefore, the minimal effective dosage for A83-01 was 1 µM. Since this dosage did not display cytotoxic effects (Fig. 5A), it was employed for all further experiments. To investigate whether 1 µM A83-01 is also sufficient to block TGFβ signaling in the target cell line MDA-MB-231, SBE reporter activity was measured in these cells. Even though MDA-MB-231 cells displayed a weaker activation of the SBE reporter in response to TGFβ than HEK293T cells (Fig. 6A and 6B), this was efficiently suppressed by treatment with 1 µM A83-01 (Fig. 6B). Notably, MDA-MB-231 cells overexpressing TGFβ and treated with A83-01 showed comparable activity to cells which only received inhibitor treatment (Fig. 6B). Similar to A83-01, the Wnt inhibitors IWP-2 and XAV939 were titrated in HEK293T cells. For this, a reporter containing TCF/LEF binding sites was used (Veeman et al., 2003). To activate Wnt signaling, cells were treated with an ATP-competitive inhibitor for GSK-3α/β, BIO (Meijer et al., 2003), or the canonical Wnt ligand Wnt3A was transiently overexpressed. Cells treated with IWP-2 and BIO showed significantly less reporter activity compared to cells treated only with BIO (Fig. 6C). Of note, increasing IWP-2 concentration from 1 to 10 µM did not result in less reporter activity, indicating that 1 µM IWP-1 are sufficient to efficiently block Wnt signaling (Fig. 6C). Similar to IWP-2, XAV939 was also able to potently inhibit Wnt signaling. Canonical Wnt signaling

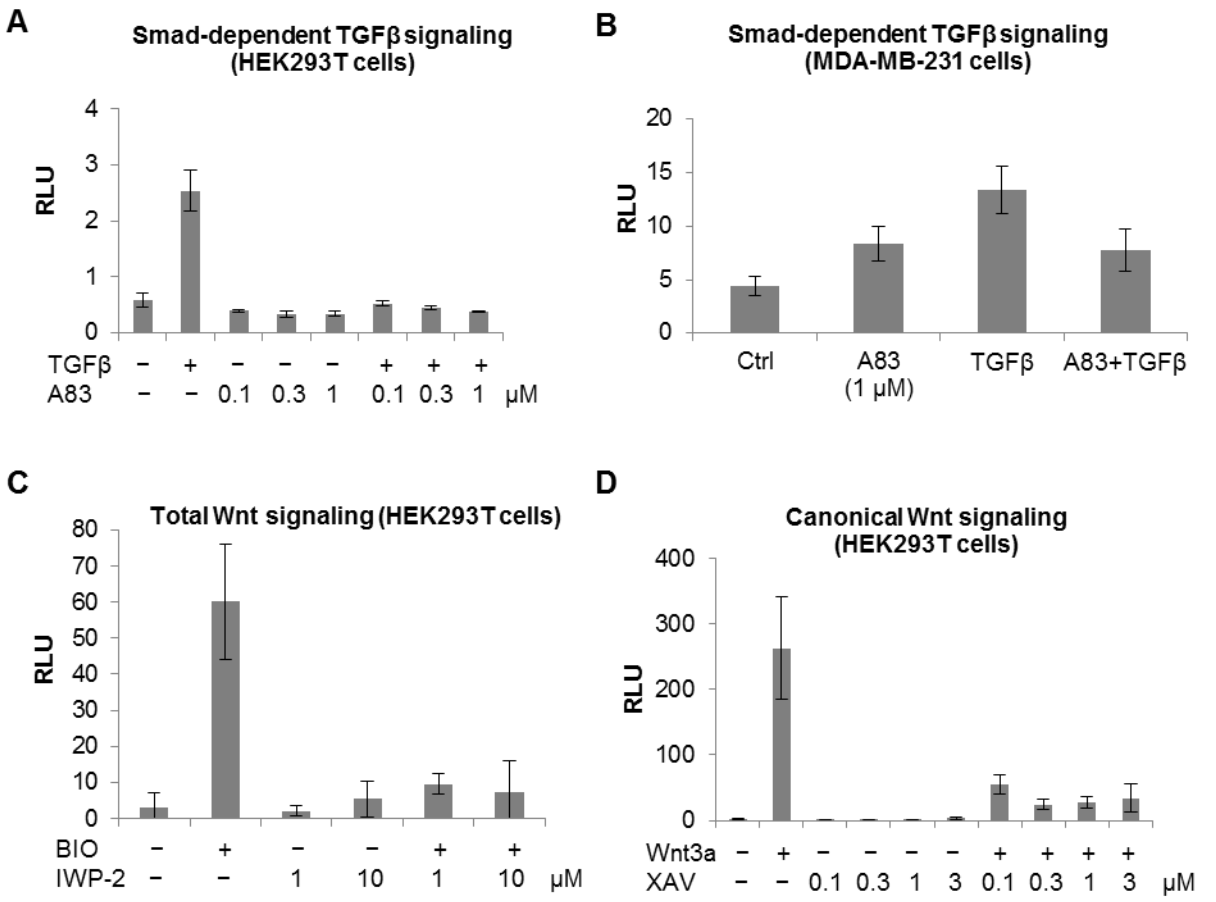

Figure 6: Titration of small-molecule inhibitors via reporter assay.
A. SBE reporter activity in HEK293T cells overexpressing TGFβ and/or treated with A83-01 (A83) for 24 h as indicated. n=6. **B.** SBE reporter activity in MDA-MB-231 cells overexpressing TGFβ and/or treated with 1 μM A83-01 (A83) for 24 h. Control (Ctrl) = untreated. n=6. **C.** TCF/LEF reporter activity in HEK293T cells treated with BIO (250 nM) and/or IWP-2 for 24 h at the indicated concentrations. n=6. **D.** TCF/LEF reporter activity in HEK293T cells overexpressing Wnt3A and/or treated with XAV939 (XAV) for 24 h as indicated. RLU, relative light units. n=6.

induced by Wnt3a was abrogated by concomitant treatment with XAV939 in HEK293T cells (Fig. 6D). A dose-dependent effect was observed when increasing the XAV939 concentration from 0.1 to 0.3 μM, but not with respect to higher concentrations, indicating a maximum response already at 0.3 μM. However, the original publication, in which the discovery of XAV939 is described, shows that 1 μM XAV939 is required for blocking β-catenin-dependent Wnt signaling (Huang et al., 2009). Since 1 μM XAV939 did not show any cytotoxic effects (Fig. 5C), this concentration was employed for further experiments. Unfortunately it was not possible to analyze JNK activity via reporter assay. Therefore, it was investigated in the available literature whether the assessed highest non-cytotoxic concentration of SP600125 (200 nM; Fig. 5D) would suffice to block JNK activity.

Indeed, it was reported before that 200 nM SP600125 or more efficiently inhibited JNK activity (Ohba et al., 2009).

Taken together, the minimal effective concentration that did not show general cytotoxic effects was assessed for each compound and employed for further experiments.

5.1.3 Inhibition of EMT developmental pathways does not impact mammosphere formation

As described in *section 5.1.1.*, MDA-MB-231 cells display enhanced clonogenic growth potential in the mammosphere assay, which is associated with tumor initiating capacity. Having established the optimal dosage of each inhibitor, I next investigated whether inhibition of EMT developmental pathways reduces mammosphere forming ability. To this end, MDA-MB-231 cells were cultivated in the mammosphere assay for 8 days and treated with A83-01 alone or in combination with IWP-2. By comparing the number of spheres formed in the untreated control versus those in the inhibitor-treated samples, no significant differences could be observed (Fig. 7). More precisely, treatment with A83-01 or IWP-2 over 2 passages did not reduce mammosphere forming ability of MDA-MB-231 cells (Fig. 7). Moreover, combined treatment with both A83-01 and IWP-2 did not impede clonogenic growth either, suggesting that the TGFβ and Wnt signaling pathways are not required for maintenance of tumor initiating properties (Fig. 7).

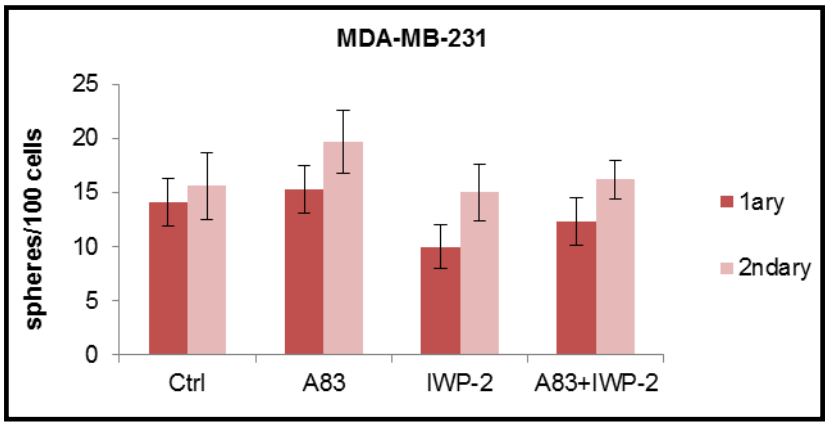

Figure 7: Inhibition of TGFβ and Wnt signaling does not impair mammosphere formation.
MDA-MB-231 cells were plated in the mammosphere assay and passaged once after 8 days. Cells were treated with A83-01 (A83) and/or IWP-2 every second day. Control (Ctrl) = untreated. n=10.

5.1.4 Inhibition of EMT developmental pathways partially suppresses cell motility

Besides clonogenic growth, aggressive tumor cells also display migratory and invasive abilities. EMT has been shown to promote invasiveness by enabling dissolution of cell-cell contacts (Scheel and Weinberg, 2012) and inducing cytoskeleton rearrangements resulting in invading protrusions, such as filopodia (Eckert et al., 2011). I therefore investigated whether inhibition of EMT developmental pathways might attenuate migration in TNBC. For this, MDA-MB-231 and MCF7-Ras cells were seeded onto porous membranes and treated with small-molecule inhibitors for 24 hours. Afterwards the number of singly migrated cells was counted. Migration ability was significantly less pronounced in MCF7-Ras cells compared to MDA-MB-231 cells, thus correlating with their non-invasive phenotype (Fig. 8A and 8B). When treated with A83-01 both cell lines displayed reduced migratory capacity compared to the untreated control. More precisely, the number of migrated cells treated with A83-01 was decimated by half compared to the control (Fig. 8B), suggesting that single-cell migration partially depends on TGFβ signaling. Due to the low cell motility of MCF7-Ras cells, other compounds were only tested in MDA-MB-231 cells. For example, in contrast to the DMSO-treated control, treatment with IWP-2 was observed to decrease single-cell migration in MDA-MB-231 cells to levels comparable to A83-01 treatment (Fig.8C). Interestingly, combining A83-01 and IWP-2 resulted in 50 % stronger reduction of migrated cells compared to treatment with a singular inhibitor (Fig. 8C). These data indicated that TGFβ and Wnt signaling might cooperate to facilitate migration of mesenchymal TNBC cells. Inhibition of canonical Wnt signaling by treatment with XAV939 also decreased the number of migrating cells by half compared to the DMSO-treated control (Fig. 8D). However, addition of A83-01 did not result in enhanced inhibition of migration compared to XAV939 treatment alone (Fig. 8D). The observation that the combination of A83-01 and IWP-2, but not that of A83-01 and XAV939 suppressed migration to levels beyond the effects of singular inhibitors, suggested that non-canonical Wnt (rather than canonical) and TGFβ signaling complement each other in facilitating cell migration. Nevertheless, inhibition of JNK-dependent non-canonical Wnt signaling did not synergize with TGFβ inhibition in reducing the number of migrating cells (Fig. 8E). One possible explanation is that the effects seen with IWP-2 are due to blocking other non-canonical Wnt pathways than JNK, such as Rho kinase signaling (Habas

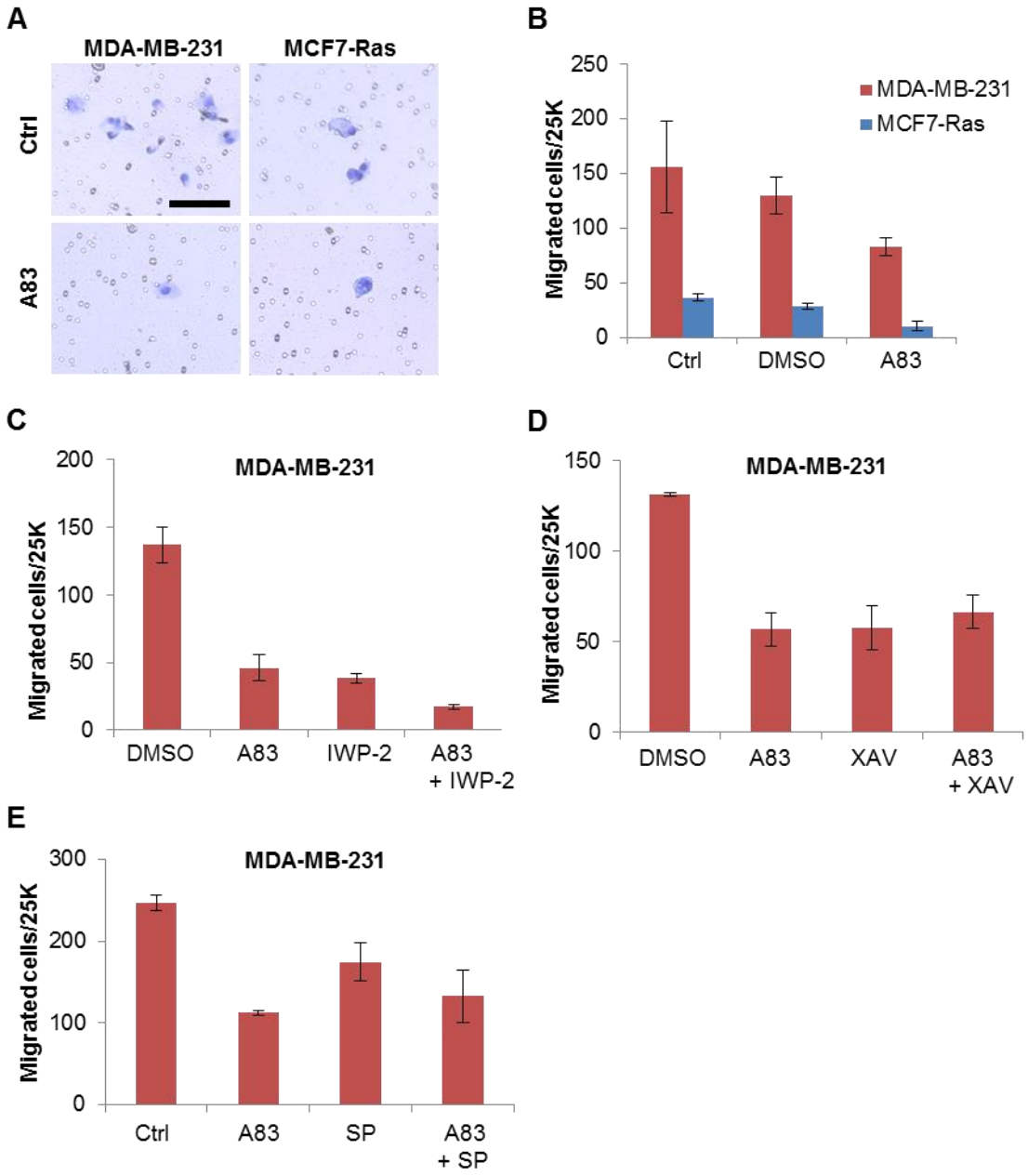

Figure 8: Inhibition of TGFβ and Wnt signaling partially suppresses single-cell migration.
A. Representative brightfield images of migrated MDA-MB-231 and MCF7-Ras cells treated with or w/o A83-01 (A83) for 24 h. Control (Ctrl) = untreated. Scale bar: 100 µm. **B.** Quantification of cells decribed in (A). DMSO treatment served as a solvent control. n=3. **C-E.** Quantification of single-cell migration in MDA-MB-231 cells treated with A83-01 (A83), IWP-2, XAV939 (XAV), SP600125 (SP) or combinations hereof for 24 h. Control (Ctrl) = untreated. n=3.

and Dawid, 2005). In conclusion, these results indicate that both TGFβ and Wnt signaling contribute to cell motility in TNBC, but single or combined inhibition of these pathways is not sufficient to completely abrogate single-cell migration.

Because tumor cells not only have to migrate, but also have to invade surrounding tissue to accomplish the first steps of the metastatic cascade (Scheel and Weinberg,

2012), I set out to investigate if inhibition of EMT developmental pathways impacts cell invasion. For this, MDA-MB-231 cells were seeded into floating 3-dimensional (3D) collagen gels and treated with small-molecule inhibitors for 7 days. Untreated MDA-MB-231 cells spread throughout the gel as singly invading cells (Fig. 9A and 9B). Whereas treatment with Wnt-C59 (an analogue compound to IWP-2), did not impact cell morphology (Fig. 9A), incubation with A83-01 resulted in the generation of cell clusters, which were positive for the epithelial marker E-cadherin (Fig. 9B). However, these structures displayed an invasive phenotype, building membrane protrusions at the edges (Fig. 9B, magnified window). In conclusion, it was observed that treatment with A83-01 inhibited single-cell dispersion, but concomitantly promoted collective invasion of MDA-MB-231 cells. The clinical relevance of this switch still remains to be investigated, as it has been shown before that cells can

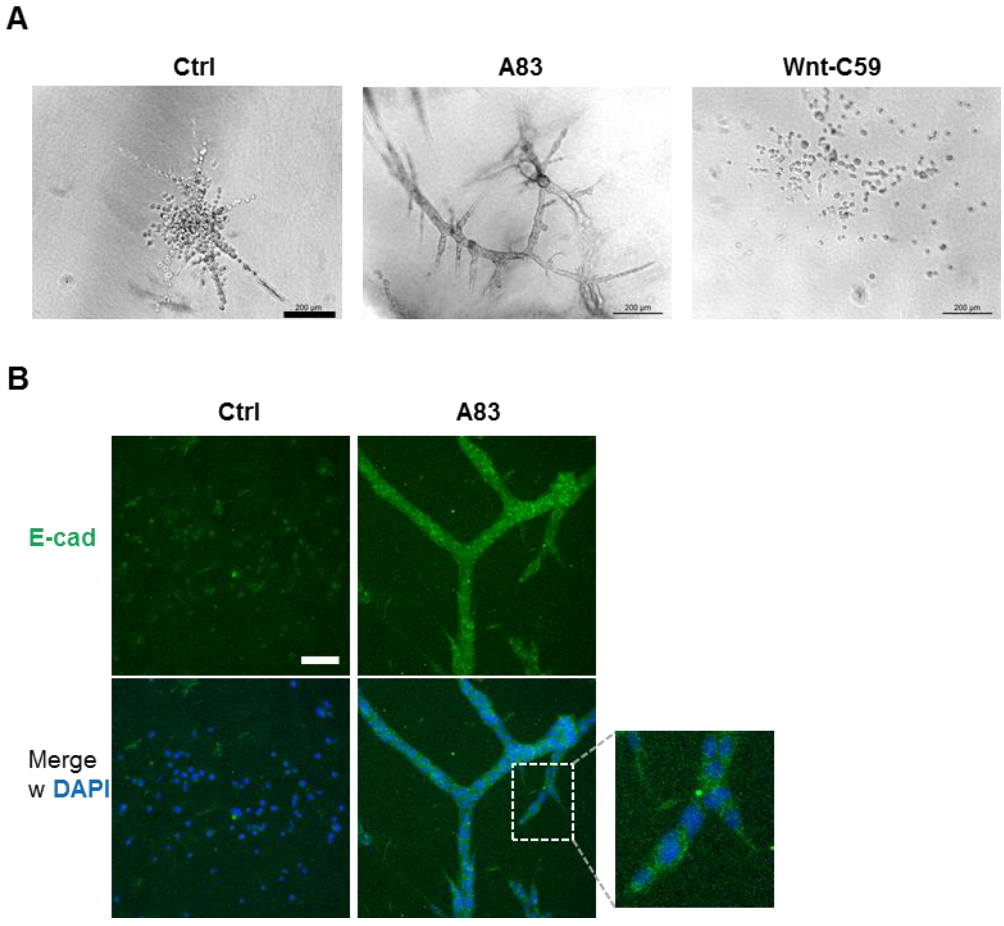

Figure 9: Inhibition of TGFβ signaling switches cells from single-cell to collective invasion.
A. Brightfield images of MDA-MB-231 cells treated every second day with A83-01 (A83) or Wnt-C59 in 3D collagen gels for 7 days. Control (Ctrl) = untreated. Scale bar: 200 µm. **B.** Immunofluorescence staining for E-cadherin (E-cad) of MDA-MB-231 cells cultured in 3D collagen gels and treated with or without A83-01 (A83) for 7 days every second day. Control (Ctrl) = untreated. Nuclei were stained with DAPI. Scale bar: 100 µm.

disseminate although preserving an epithelial identity, a mechanism that might also be employed by metastatic tumor cells (Shamir et al., 2014).

5.1.5 TGFβ signaling is not required for EMT maintenance in MDA-MB-231 cells

Because inhibition of TGFβ and/or Wnt signaling did not impair mammosphere forming ability and only partially suppressed single-cell migration, I set out to investigate whether these pathways are required for EMT maintenance in MDA-MB-231 cells. Since TGFβ is the main EMT inducer and was the only pathway also required for single-cell invasion, epithelial and mesenchymal markers were assessed by RT-PCR in cells treated with or without A83-01. To determine if the requirement of TGFβ signaling for EMT maintenance depends on 2D or 3D growth conditions, cells growing under adherent conditions, in the mammosphere assay and in 3D collagen gels were analyzed. Even though MDA-MB-231 cells were chronically treated with A83-01 (8 days in 3D collagen gels and 15 days in 2D and mammosphere assay), expression of the mesenchymal markers N-cadherin and vimentin did not change compared to the untreated control in any of the analyzed culturing conditions (Fig. 10). Additionally, treatment with A83-01 did not enhance E-cadherin expression levels of cells grown in 3D collagen gels, which contrasted the results obtained by immunofluorescence staining (Fig. 10 and Fig. 9B). It is therefore more likely that in this context E-cadherin is regulated on a post-translational level. Indeed, it has been

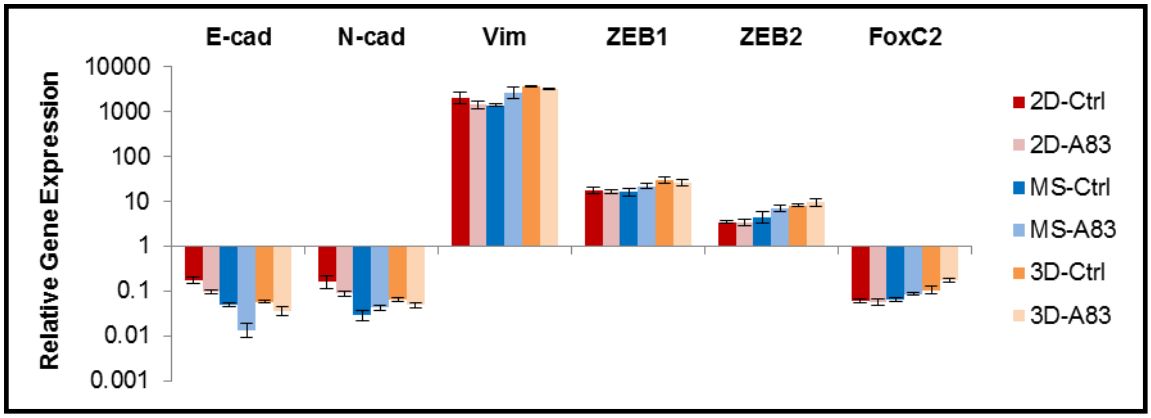

Figure 10: TGFβ signaling is not required for the maintenance of the EMT transcriptional profile.
RT-PCR analysis of E-cadherin (E-cad), N-cadherin (N-cad), vimentin (Vim), ZEB1, ZEB2 and FoxC2 expression in MDA-MB-231 cells cultured as indicated and treated with A83-01 (A83) every second day for either 8 days in 3D collagen gels or 15 days in 2D and the mammosphere assay (MS). Control (Ctrl) = untreated. n=3.

reported before that E-cadherin can be delocalized from the cell membrane into the cytoplasm during EMT and that E-cadherin protein levels can be balanced by proteasomal degradation (Khew-Goodall and Wadham, 2005). Moreover, treatment with A83-01 did not impact the expression of EMT-TFs, such as ZEB1, ZEB2 or FoxC2, suggesting that inhibition of TGFβ signaling is not sufficient to abrogate EMT maintenance (Fig. 10).

Taken together, inhibition of several developmental pathways involved in EMT induction did not impair EMT traits in the TNBC cell line MDA-MB-231, indicating that the signaling mechanisms required for EMT induction differ from the ones regulating EMT maintenance.

5.2 Inhibition of developmental pathways during EMT induction

To better understand why TGFβ and Wnt signaling are not crucial for the maintenance of the mesenchymal phenotype it was necessary to investigate previous steps during the epithelial-mesenchymal transdifferentiation process. Therefore, I examined to which extent these pathways are required for EMT induction and through which potential mechanisms they orchestrate the mesenchymal transdifferentiation program. To this end, I utilized immortalized human mammary cells (HMLE) (Elenbaas et al., 2001), retrovirally transduced with the Twist1 gene and coupled to a mutated ER ligand binding domain (Casas et al., 2011). To prevent selection of a pre-existing mesenchymal population (Scheel et al., 2011), bulk HMLE-Twist1-ER cells were sorted according to the surface markers CD24^{high} and CD44^{+} (Fig. 11; Schmidt et al., 2015).

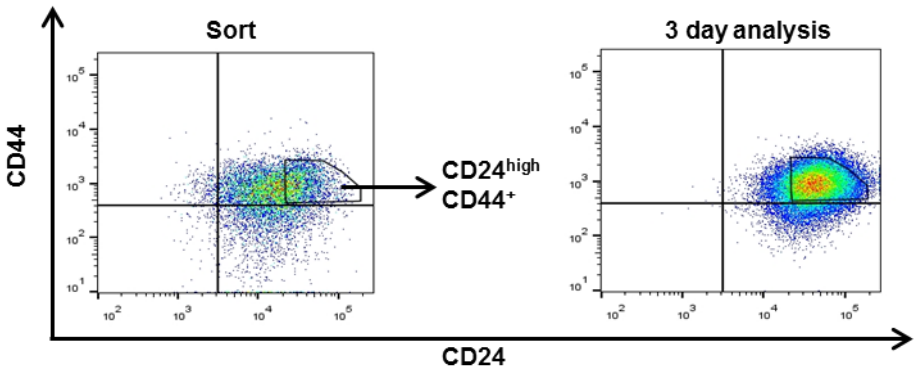

Figure 11: FACS analysis of HMLE-Twist1-ER cells.
Cells were sorted for the cell surface markers CD24^{high} and CD44^{+}. 3 days after sorting, cells were re-analyzed.

5.2.1 Twist1 requires autocrine TGFβ signaling for EMT induction

Upon treatment with 4-hydroxytamoxifen (TAM), the Twist1-ER construct translocates into the nucleus and binds to EMT target genes (Casas et al., 2011). As previously described (Schmidt et al., 2015), after a period of 14-16 days of TAM-treatment, HMLE-Twist1-ER cells transdifferentiated from an epithelial to a mesenchymal state (Fig. 12A). As shown by immunofluorescence, EMT manifested as dissolution of adherens junctions, marked by loss of membranous E-cadherin and upregulation of mesenchymal intermediary filament vimentin (Fig. 12A; Savagner, 2010). HMLE-Twist1-ER cells treated with both TAM and XAV939 or SP600125 acquired a mesenchymal phenotype, lost E-cadherin expression and stained positive for vimentin (Fig. 12A). This indicates that Twist1 can induce EMT independently of canonical Wnt and JNK signaling. By contrast, cells treated with TAM in combination with A83-01 retained membranous E-cadherin expression and failed to upregulate vimentin and the EMT-TF ZEB1 compared to cells treated with TAM alone (Fig. 14B). Protein and mRNA expression analysis of a broad panel of EMT markers and regulators by immunoblot and RT-PCR, respectively, showed that Twist1-mediated upregulation of mesenchymal markers such as N-Cadherin, vimentin and fibronectin was completely suppressed by simultaneous inhibition of TGFβ signaling (Fig. 12C and 12D). In fact, treatment with A83-01 repressed mRNA levels of several mesenchymal markers below untreated control cells (Fig. 12C). Moreover, whereas E-cadherin mRNA levels were repressed in TAM-treated cells, concomitant addition of A83-01 prevented E-cadherin downregulation (Fig 12C). At the same time, upregulation of EMT-TFs Slug and ZEB1 in TAM-treated cells was attenuated by simultaneous treatment with A83-01 (Fig. 12C and 12D). Importantly, both Slug and ZEB1 are direct downstream effectors of Twist1 (Casas et al., 2011, Dave et al., 2011), and repress E-cadherin transcription directly (Eger et al., 2005; Alves et al., 2009). Moreover, upregulation of Wnt5a, another Twist1 target gene (Shi et al., 2014), was also inhibited by A83-01. Since inhibition of TGFRI-kinase domain by A83-01 impaired mesenchymal transdifferentiation, it was most likely that HMLE-Twist1-ER cells display autocrine TGFβ signaling required for EMT, as described previously (Scheel et al., 2011). In support of this hypothesis, faint, but robust phosphorylated Smad2/3 was detected by immunoblot in the untreated HMLE-Twist1-ER cells, which was blocked by treatment with A83-01 (Fig. 12E).

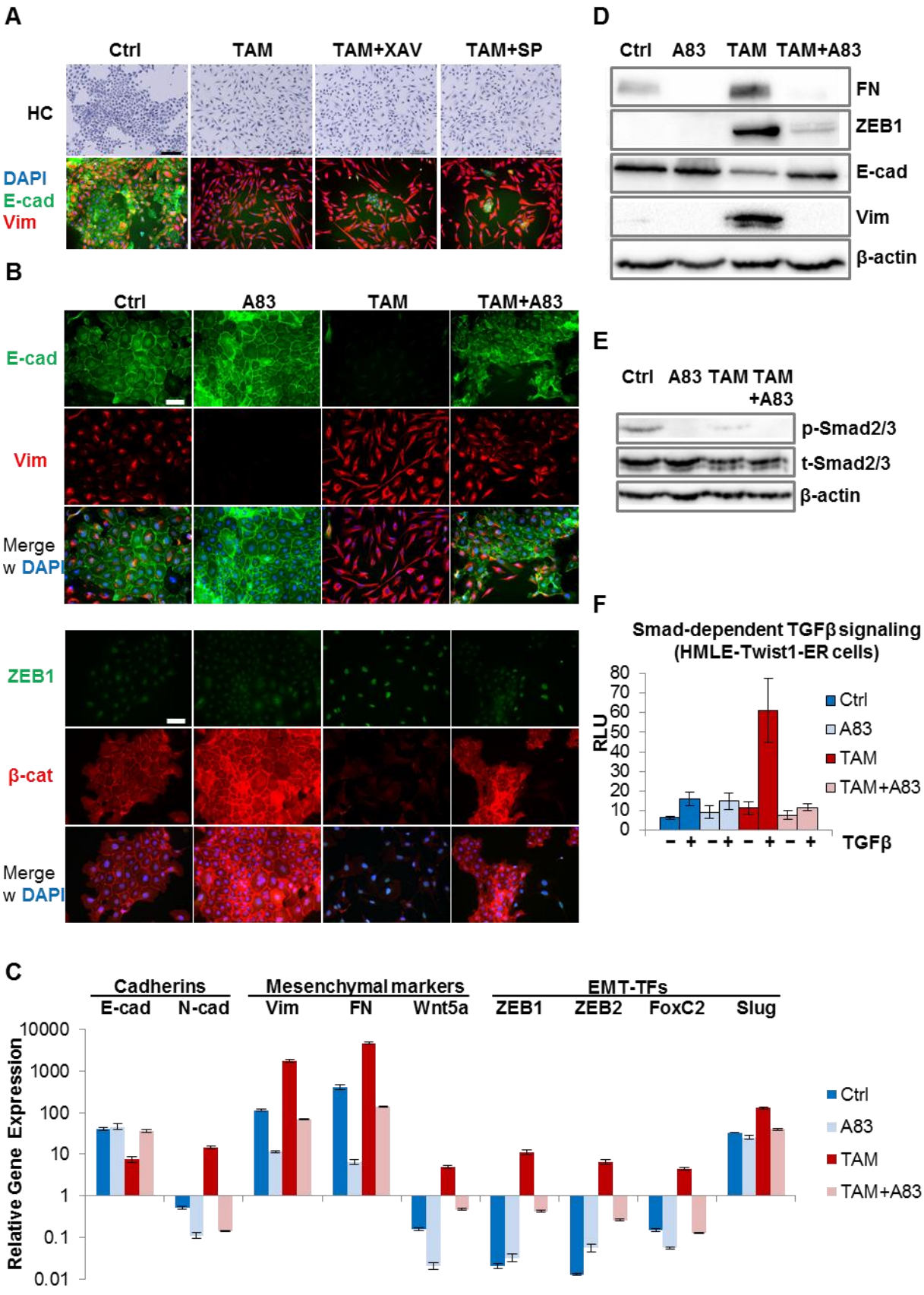
A
Ctrl
TAM
TAM+XAV
TAM+SP
HC
DAPI
E-cad
Vim
B
Ctrl
A83
TAM
TAM+A83
E-cad
Vim
Merge w DAPI
ZEB1
β-cat
Merge w DAPI
D
Ctrl A83 TAM TAM+A83
FN
ZEB1
E-cad
Vim
β-actin
E
Ctrl A83 TAM TAM +A83
p-Smad2/3
t-Smad2/3
β-actin
F
Smad-dependent TGFβ signaling
(HMLE-Twist1-ER cells)
RLU
80
70
60
50
40
30
20
10
0
Ctrl
A83
TAM
TAM+A83
– + – + – + – +
TGFβ
C
Cadherins
Mesenchymal markers
EMT-TFs
E-cad
N-cad
Vim
FN
Wnt5a
ZEB1
ZEB2
FoxC2
Slug
Relative Gene Expression
10000
1000
100
10
1
0.1
0.01
Ctrl
A83
TAM
TAM+A83

Figure 12: Inhibition of endogenous TGFβ signaling blocks Twist1-induced EMT.
A. Hemacolor (HC) and immunofluorescence staining (E-cadherin: E-cad, vimentin: Vim and DAPI for visualization of nuclei) of HMLE-Twist1-ER cells treated with 4-hydroxytamoxifen (TAM) alone or in combination with the canonical Wnt inhibitor XAV939 (XAV) or with the JNK inhibitor SP600125 (SP) for 16 days every second day. Control (Ctrl) = untreated. Scale bar: 200 µm. **B.** Immunofluorescence staining at 16 days post induction (dpi) of HMLE-Twist1-ER cells treated every second day with the TGFRI inhibitor A83-01 (A83), 4-hydroxytamoxifen (TAM) or the combination of the latter two compounds. Control (Ctrl) = untreated. Cells were stained with antibodies against E-cadherin (E-cad), vimentin (Vim), ZEB1 and β-catenin (β-cat). Nuclei were stained with DAPI. Scale bar: 100 µm. **C.** RT-PCR analysis of E-cadherin (E-cad), N-cadherin (N-cad), vimentin (Vim), fibronectin (FN), Wnt5a, ZEB1, ZEB2, FoxC2 and Slug mRNA expression in HMLE-Twist1-ER cells treated as in (B). n=3. **D.** Western blot analysis of fibronectin (FN), ZEB1, E-cadherin (E-cad) and vimentin (Vim) in HMLE-Twist1-ER cells treated as in (B). **E.** Western blot analysis of phosphorylated (p-) and total (t-) Smad2/3 in HMLE-Twist1-ER cells treated as in (B). **F.** SBE reporter assay of HMLE-Twist1-ER cells treated as in (B) and additionally incubated with TGFβ (2 ng/ml) for 24 h prior to analysis. n=6.

Interestingly, TAM-treated cells displayed less Smad 2/3 phosphorylation compared to control cells, suggesting a negative feedback. However, in response to exogenous TGFβ-treatment, cells that have undergone Twist1-induced EMT showed a 6-fold increase in SBE reporter activity, compared to a 2.5-fold increase in control cells (Fig. 12F). This indicated that Twist1-activation results in enhanced sensitivity to TGFβ.
Together, these results suggested that TGFRI-Smad2/3 signaling is required for both Twist1-induced upregulation of mesenchymal markers as well as downstream effectors.
To validate that the effects observed on Twist1-induced EMT are specifically due to inhibition of TGFRI-kinase domain, shRNA-mediated knockdown of TGFBRI was performed. Since expression of TGFBRI measured by RT-PCR in HMLE-Twist1-ER cells was rather low (Ct value = 28-29; Fig. 13A), I have searched for another cell line with higher TGFBRI levels, more appropriate for the validation of potent shRNAs. For this, candidate cell lines which have shown a strong TGFβ responsiveness in the past were considered, such as the lung carcinoma derived A549 cells (Kim et al., 1989), MDA-MB-231 cells (Bouquet et al., 2011) and HEK293T cells (Fig. 6A). Indeed, these cell lines displayed significantly higher TGFBRI mRNA levels compared to HMLE-Twist1-ER cells (Fig. 13A). More precisely, MDA-MB-231 and A549 cells showed the highest TGFBRI expression levels amongst all cell lines (Fig. 13A). Unlike MDA-MB-231 cells, A549 cells have an epithelial phenotype (Giard et al., 1973), thus resembling HMLE-Twist1-ER cells. Therefore, shRNA-mediated knockdown of the TGFBRI was performed in A549 cells. From 6 tested shRNAs, two of them (shRNA 3 and 4) reduced TGFBRI expression by 91-92 % compared to the

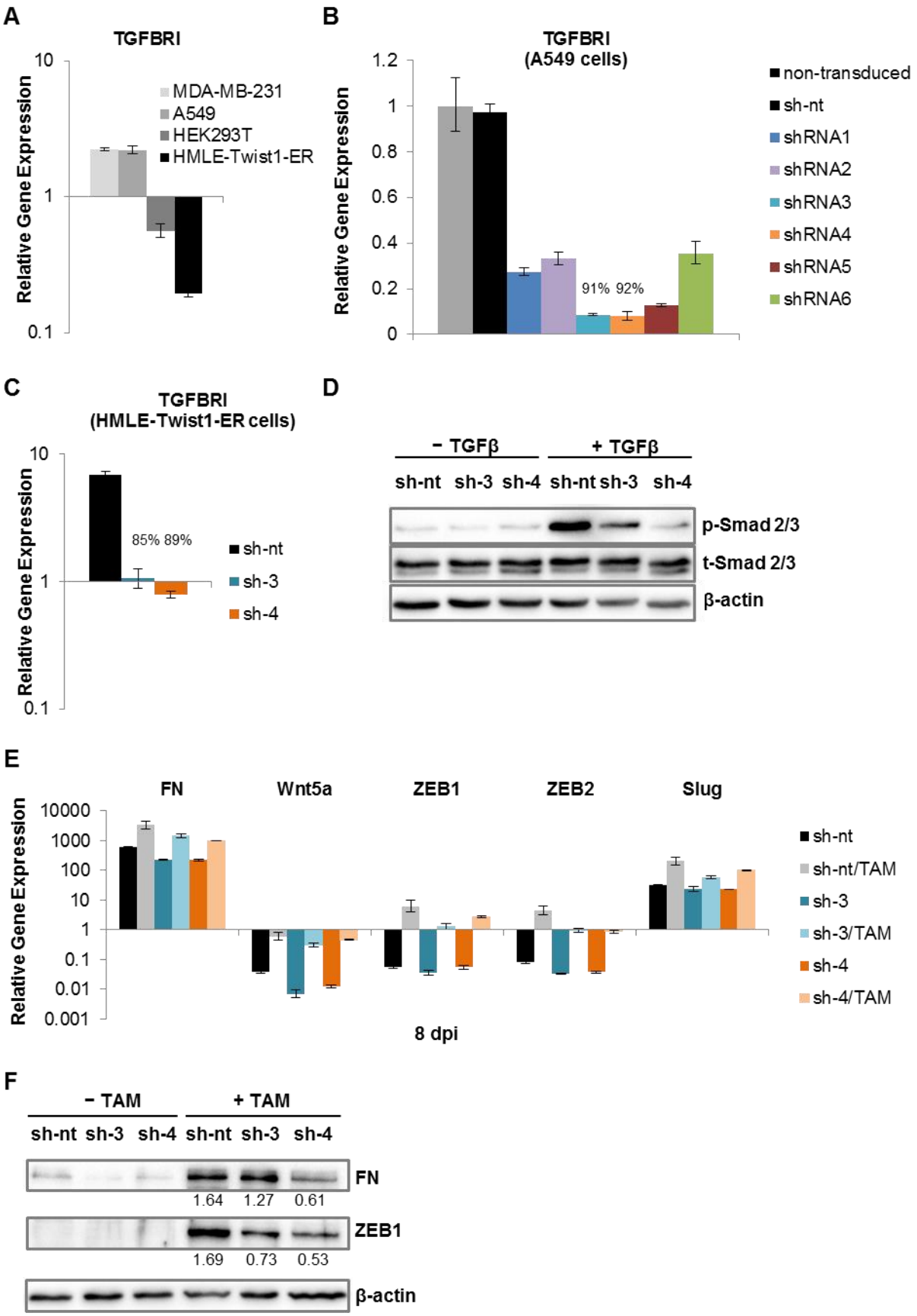
A
TGFBRI
Relative Gene Expression
10
1
0.1
MDA-MB-231
A549
HEK293T
HMLE-Twist1-ER
B
TGFBRI
(A549 cells)
Relative Gene Expression
1.2
1
0.8
0.6
0.4
0.2
0
91% 92%
non-transduced
sh-nt
shRNA1
shRNA2
shRNA3
shRNA4
shRNA5
shRNA6
C
TGFBRI
(HMLE-Twist1-ER cells)
Relative Gene Expression
10
1
0.1
85% 89%
sh-nt
sh-3
sh-4
D
− TGFβ
+ TGFβ
sh-nt sh-3 sh-4 sh-nt sh-3 sh-4
p-Smad 2/3
t-Smad 2/3
β-actin
E
FN
Wnt5a
ZEB1
ZEB2
Slug
Relative Gene Expression
10000
1000
100
10
1
0.1
0.01
0.001
8 dpi
sh-nt
sh-nt/TAM
sh-3
sh-3/TAM
sh-4
sh-4/TAM
F
− TAM
+ TAM
sh-nt sh-3 sh-4 sh-nt sh-3 sh-4
FN
1.64 1.27 0.61
ZEB1
1.69 0.73 0.53
β-actin

Figure 13: Knockdown of TGFBRI recapitulates the effects observed with A83-01.
A. RT-PCR analysis of endogenous TGFBRI expression in MDA-MB-231, A549, HEK293T and HMLE-Twist1-ER cells. n=3. **B.** RT-PCR analysis of endogenous TGFBRI expression in A549 cells transduced with shRNAs against the TGFBRI or with a non-targeting control (sh-nt). n=3. **C.** Validation of the shRNA-mediated TGFBRI knock-down in HMLE-Twist1-ER cells on a transcriptional level via RT-PCR. n=3. **D.** Western blot analysis of phosphorylated (p-) and total (t-) Smad2/3 in HMLE-Twist1-ER cells transduced with a non-targeting control (sh-nt) or sh-RNA targeting the TGFBRI (sh-3 or sh-4). Cells were treated with 2 ng/ml recombinant TGFβ for 45 min before lysis. **E.** RT-PCR analysis of Fibronectin (FN), Wnt5a, Slug, ZEB1 and ZEB2 mRNA expression in HMLE-Twist1-ER cells harboring shRNAs against TGFBRI (sh-3 or sh-4) or a non-targeting control (sh-nt) and treated every second day with 4-hydroxytamoxifen (TAM) for 8 days. n=3. **F.** Western blot analysis of fibronectin (FN) and ZEB1 protein expression in HMLE-Twist1-ER cells described in (E). Protein levels were quantified relatively to β-actin.

non-targeting shRNA (Fig. 13B). These two shRNAs were then used for the TGFBRI knockdown in HMLE-Twist1-ER cells. Transduction of HMLE-Twist1-ER cells with shRNA 3 and 4 impaired TGFBRI expression by 85-89 % compared to cells harboring a non-targeting shRNA (Fig. 13C). Additionally, cells harboring shRNAs against TGFBRI showed significantly less Smad2/3 phosphorylation upon TGFβ treatment (Fig. 13D). When Twist1 was activated by treatment with TAM for 8 days, the induction of mesenchymal markers such as fibronectin and Wnt5a, as well as downstream effectors of Twist1, ZEB1 and Slug, was significantly reduced in cells where TGFBRI was knocked down compared to cells transduced with a non-targeting shRNA (Fig. 13E and 13F).

Nevertheless, shRNA-mediated knockdown of TGFBRI blocked Twist1-induced upregulation of EMT markers and effectors to a lesser extent than A83-01 (Fig. 12C and Fig. 13E). Since A83-01, as an ATP-competitive inhibitor, may block the active domain of other kinases, I set out to determine whether A83-01 might exert its effects partly through inhibition of additional kinases (Vogt et al., 2011). For example, receptor-interacting serine/threonine-protein kinase 2 (RIPK2) was shown to have high affinity to A83-01 (Vogt et al., 2011). However, its downstream target, p65 (Zhang et al., 2010; Meylan and Tschopp, 2005), was strongly phosphorylated upon Twist1-induction, but not inhibited by concomitant treatment with A83-01 (Fig. 14A). Another kinase targeted by A83-01 is VEGFR (Vogt et al., 2011). Therefore, I tested whether concomitant treatment of HMLE-Twist1-ER cells with TAM and the VEGFR inhibitor Axitinib would mimic the effects of A83-01. However, cells treated with both TAM and Axitinib displayed similar mRNA levels for several EMT markers (vimentin, fibronectin and Wnt5a) as cells treated with TAM alone (Fig. 14B). Furthermore,

Axitinib did not impair Twist1-mediated transcriptional induction of other EMT-TFs, such as ZEB1, ZEB2 and Slug (Fig. 14B).

Together, these results suggested that Twist1 requires Smad-dependent TGFβ signaling to induce a complete EMT and that the effects of A83-01 on EMT induction by Twist1 were specifically due to inhibition of TGFR1-kinase domain.

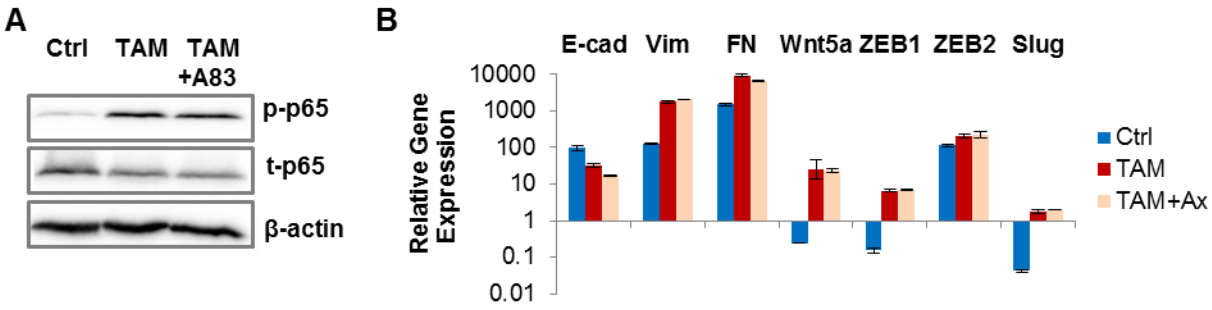

Figure 14: A83-01 does not target RIPK2 or VEGFR.

A. Western blot analysis of phosphorylated (p-) and total (t-) p65 in HMLE-Twist1-ER cells treated every second day with 4-hydroxytamoxifen (TAM) or TAM and A83-01 (A83) for 16 days. Control (Ctrl) = untreated. **B.** RT-PCR analysis of E-cadherin (E-cad), vimentin (Vim), fibronectin (FN), ZEB1, ZEB2 and Slug mRNA expression in HMLE-Twist1-ER cells treated every second day with 4-hydroxytamoxifen (TAM) or TAM in combination with the VEGFR inhibitor Axitinib (Ax) for 16 days. Control (Ctrl) = untreated. n=3.

5.2.2 TGFβ synergizes with Twist1 at early time points of EMT induction

Because endogenous Smad2/3-phosphorylation was robustly detectable in both control, and TAM-treated cells, but the signal was weak (Fig. 12E), I set out to determine whether adding exogenous TGFβ would accelerate induction of EMT. Indeed, cells treated with both TAM and TGFβ had undergone EMT already after 8 days, as assessed by immunofluorescence staing (Fig. 15A). This manifested as a complete loss of membranous E-cadherin expression and acquisition of a spindle-like shape with an even distribution of vimentin throughout the cell body (Fig. 15B, left panel). In contrast, cells treated with TAM and A83-01 displayed an epithelial phenotype, building condensed cell clusters with pronounced membranous E-cadherin expression (Fig. 15A, left panel). Of note, cells treated with TAM or TGFβ alone had only undergone a partial EMT at that time, where part of the cells detached from epithelial colonies and upregulated vimentin expression, while others still built epithelial cell clusters with retained E-cadherin and β-catenin membranous

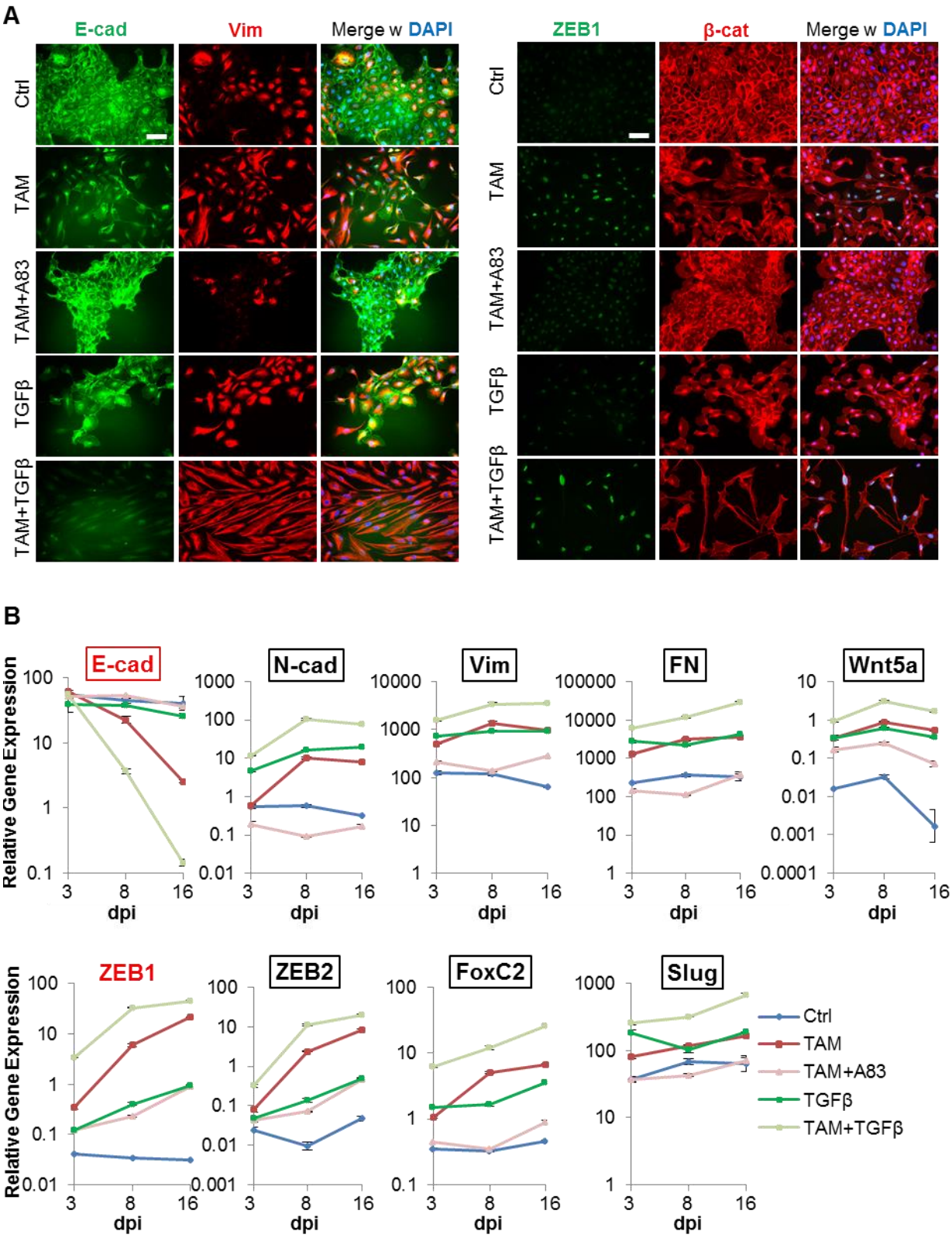

Figure 15: Twist1 and TGFβ cooperate to induce EMT in HMLE-Twist1-ER cells.
A. Immunofluorescence staining of HMLE-Twist1-ER cells treated every second day with 4-hydroxytamoxifen (TAM), A83-01 (A83), TGFβ or combinations hereof for 8 days. Cells were stained with antibodies against E-cadherin (E-cad), vimentin (Vim), ZEB1 and β-catenin (β-cat). Nuclei were stained with DAPI. Scale bar: 100 µm. Control (Ctrl) = untreated. **B.** RT-PCR analysis of E-cadherin (E-cad), N-cadherin (N-cad), vimentin (Vim), fibronectin (FN), Wnt5a, ZEB1, ZEB2, FoxC2 and Slug mRNA expression at 3, 8 and 16 days post induction (dpi) in HMLE-Twist1-ER cells treated as in (A). Control (Ctrl) = untreated, n=3.

expression (Fig. 15A). Importantly, whereas mesenchymal cells which have lost β-catenin upon TAM-treatment displayed nuclear localization of ZEB1, cells treated with TGFβ failed to induce ZEB1 nuclear expression (Fig. 15A, right panel). This indicates that treatment with TGFβ contributes to the dissolution of adherence junctions, but cannot induce EMT effectors, such as ZEB1 on its own.

Consistent with these findings, RT-PCR analysis revealed that exogenous TGFβ accelerates Twist1-induced EMT by boosting the mesenchymal transcriptional program. Thus, cells treated with both TAM and TGFβ upregulated a series of mesenchymal markers (N-cadherin, vimentin, fibronectin, Wnt5a) and effectors (ZEB1, ZEB2, FoxC2, Slug) beyond the transcriptional levels assessed in TAM-treated cells (Fig. 15B). Corroborating the immunofluorescence analysis, combined treatment with TAM and TGFβ for 8 days resulted in a significant reduction of E-cadherin expression. Notably, cells treated with TAM and TGFβ for 8 days displayed similar transcript levels of E-cadherin and its repressor ZEB1 as TAM-treated cells at 16 days post induction (dpi). This once again demonstrated that addition of TGFβ accelerates Twist1-induced EMT by potentiating transcription of EMT markers and effectors.

Based on previous reports showing that TGFβ is sufficient for EMT induction (Miettinen et al., 1994; Piek et al., 1999; Valcourt et al., 2005), it was investigated whether cells treated with TGFβ undergo EMT as efficiently as TAM-treated cells over a period of 16 days. Treatment with TGFβ alone was able to induce gene expression of mesenchymal markers such as vimentin and fibronectin as efficiently as activation of Twist1 by TAM did (Fig. 15B). Indeed, this is consistent with previous reports showing that fibronectin is a direct TGFβ target gene, mainly produced by mesenchymal cells and exocytosed into the extracellular matrix (Hocevar et al., 1999). However, cells treated with TGFβ showed lower levels of ZEB1 and failed to downregulate E-cadherin expression, compared to TAM-treated cells (Fig. 15B). Additionally, transcript levels of the EMT-TFs ZEB2 and FoxC2 were 10 to 100-fold lower in cells treated with TGFβ compared to TAM-treated cells (Fig. 15B). This suggested that TGFβ is a poorer EMT inducer than Twist1 in HMLE-Twist1-ER cells. Moreover, these results show not only that Twist1 requires TGFβ for a complete EMT induction, but that addition of exogenous TGFβ supports the transcriptional activation of Twist1 effectors.

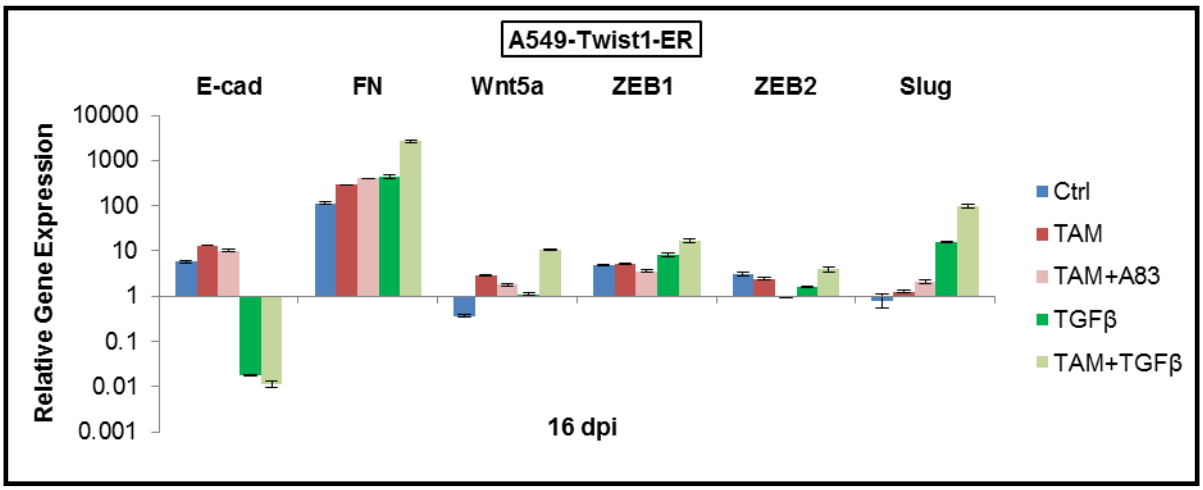

Figure 16: Twist1 and TGFβ cooperate to induce EMT in A549-Twist1-ER cells.
A. RT-PCR analysis of E-cadherin (E-cad), fibronectin (FN), Wnt5a, ZEB1, ZEB2, and Slug mRNA expression at 16 dpi in A549-Twist1-ER cells treated every second day with 4-hydroxytamoxifen (TAM), A83-01 (A83), TGFβ or combinations hereof. Control (Ctrl) = untreated. n=3.

EMT is thought to contribute to cancer initiation and progression in many different tissues (Thiery et al., 2009). Therefore, it was next tested whether Twist1 and TGFβ collaborate for EMT induction also in other tissues than the breast. For this purpose, the human lung carcinoma cell line A549 was transduced with the Twist1-ER construct (A549-Twist1-ER). In contrast to the results assessed in HMLE-Twist1-ER cells, it was observed that over a period of 16 days TGFβ was sufficient for the downregulation of E-cadherin expression (measured by RT-PCR) in A549-Twist1-ER cells (Fig. 16). In concordance with previous observations in this study, activating Twist1 by TAM in addition to TGFβ treatment further increased the transcriptional level of the mesenchymal markers fibronectin and Wnt5a, and significantly enhanced expression of EMT-TFs, such as ZEB1, ZEB2 and Slug compared to cells treated only with TGFβ (Fig. 16).
Taken together, these observations suggest that TGFβ controls the ability of Twist1 to promote mesenchymal transdifferentiation in a dose-dependent manner.

5.2.3 TGFβ regulates Twist1 binding to the ZEB1 promoter

Based on the changes in gene expression caused by treatment with TAM and TGFβ at time points as early as 3 days (Fig. 15B), it was most likely that Twist1 and TGFβ cooperate to activate transcription of EMT target genes. Since changes in transcriptional regulation can occur already within a few hours after growth factor

stimulation (Yamamoto and Alberts, 1976; Fowler et al., 2011), I performed short-term timecourses of HMLE-Twist1-ER cells treated with TAM, A83-01, TGFβ and combinations hereof for 6, 24, 48 and 72 hours. As assessed by RT-PCR, TAM-treatment resulted in transcriptional induction of ZEB1, ZEB2, fibronectin and Wnt5a (Fig. 17A). Thus, after 72 hours, ZEB1, ZEB2, Wnt5a and fibronectin were expressed 4 to 18-fold higher in TAM-treated cells compared to the untreated control (Fig. 17A). By contrast, cells treated with TAM and A83-01 displayed significantly lower mRNA levels of ZEB1, ZEB2 and fibronectin compared to TAM-treated cells (Fig. 17A), thereby corroborating the hypothesis that Twist1 requires TGFβ signaling for induction of EMT targets and effectors. Additionally, treatment with TGFβ alone resulted in the upregulation of mesenchymal markers, such as Wnt5a and fibronectin, but did not augment ZEB1 gene expression levels at any of the analyzed time points (Fig. 17A). Thus, it appears that even though TGFβ regulates transcription of mesenchymal markers, it is not sufficient to upregulate the EMT effector ZEB1. In contrast, the combination of exogenous TGFβ and TAM significantly enhanced transcript levels of ZEB1 and ZEB2. Notably, treatment with TAM and TGFβ for 72 hours increased ZEB1 mRNA expression 10-fold compared to cells treated with TAM alone (Fig. 17A). In congruence with these findings, by immunoblotting, at 72 hours, significantly more ZEB1 protein was detected in cells treated with TAM and TGFβ compared to TAM-treated cells (Fig. 17B). Since ZEB1 and the miR-200 family repress each other in a negative feedback loop (Burk et al., 2008), it was tested whether inhibition of TGFβ signaling reduces TAM-induced ZEB1 expression by upregulating miR-200 family members. However, TAM-treatment did not impact transcription of miR-141, miR-200b and miR-200c, independently of TGFβ signaling (Fig. 17C). Although addition of A83-01 partially suppressed Twist1-induced downregulation of miR-200a, addition of recombinant TGFβ did not further increase miR-200a transcript levels (Fig. 17C). This suggested that, at least during the early steps of Twist1-induced EMT, TGFβ signaling does not contribute to the induction of the Twist1 downstream effector ZEB1 by transcriptional suppression of miR-200 family members. Nevertheless, the negative feedback loop between the miR-200 family and ZEB1 is functional in HMLE-Twist1-ER cells, since after 16 days of TAM-treatment, transcript levels of miR-200 family members were strongly reduced compared to the non-treated control (Fig. 17D). At this time point, cells treated with both TAM and A83-01 showed higher transcript levels of all miR-200 family members

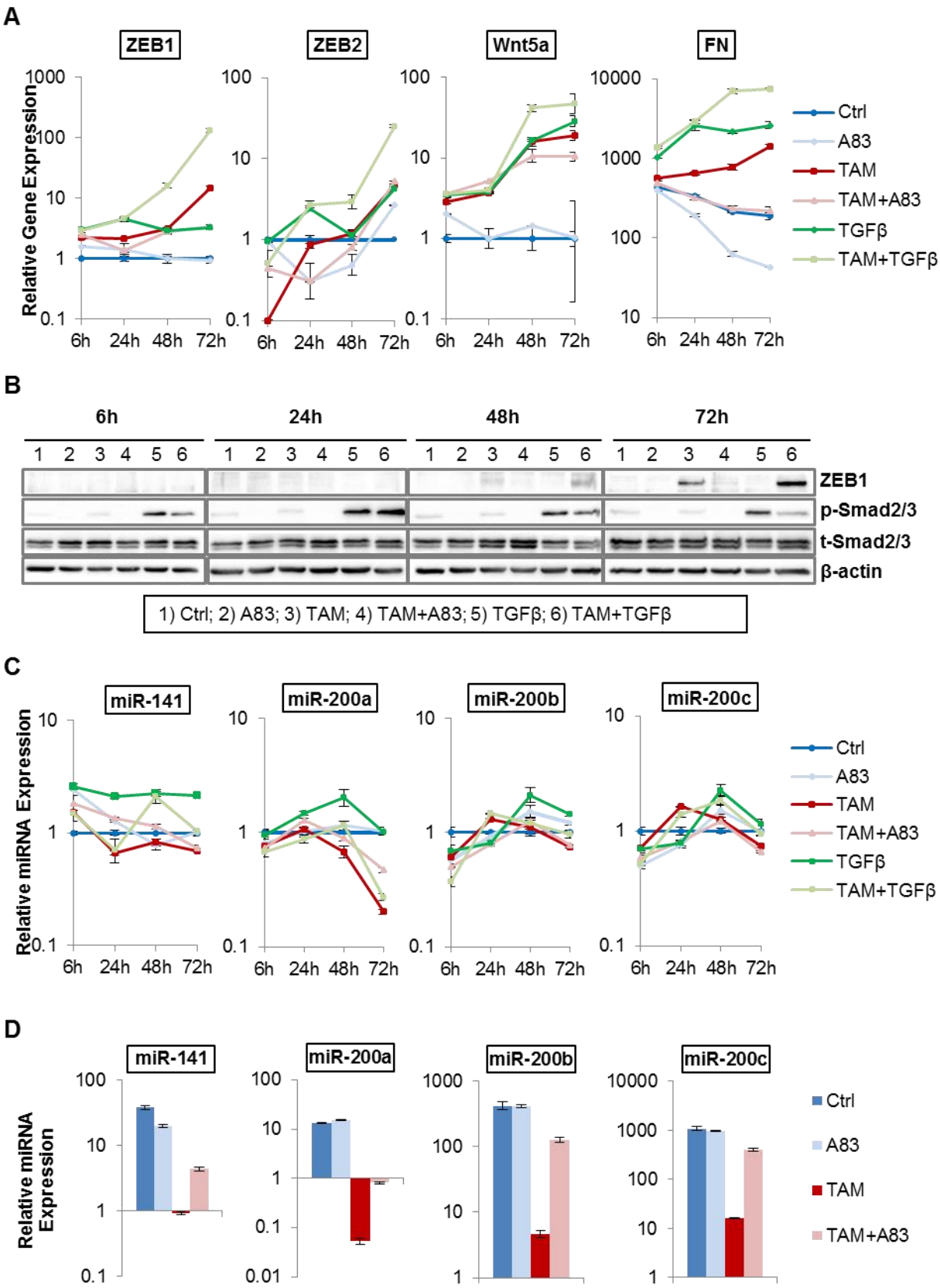
A
ZEB1
ZEB2
Wnt5a
FN
Relative Gene Expression
6h 24h 48h 72h
Ctrl
A83
TAM
TAM+A83
TGFβ
TAM+TGFβ
B
6h
24h
48h
72h
1 2 3 4 5 6
ZEB1
p-Smad2/3
t-Smad2/3
β-actin
1) Ctrl; 2) A83; 3) TAM; 4) TAM+A83; 5) TGFβ; 6) TAM+TGFβ
C
miR-141
miR-200a
miR-200b
miR-200c
Relative miRNA Expression
Ctrl
A83
TAM
TAM+A83
TGFβ
TAM+TGFβ
D
miR-141
miR-200a
miR-200b
miR-200c
Relative miRNA Expression
Ctrl
A83
TAM
TAM+A83

Figure 17: Twist1 and TGFβ cooperate during early time points of EMT induction.
A. RT-PCR analysis of ZEB1, ZEB2, Wnt5a and fibronectin (FN) mRNA expression at 6, 24, 48 and 72 h in HMLE-Twist1-ER cells treated every 24h with 4-hydroxytamoxifen(TAM), A83-01 (A83), TGFβ or combinations hereof. Control (Ctrl) = untreated. n=3. **B.** Western blot analysis of ZEB1, phosphorylated Smad2/3 (p-) and total Smad2/3 (t-) protein expression at 6, 24, 48 and 72 hours in HMLE-Twist1-ER cells treated as in (A). **C**. RT-PCR analysis of transcript levels of miR-200 family members at 6, 24, 48 and 72 hours in HMLE-Twist1-ER cells treated as in (A). n=3. **D.** RT-PCR analysis of transcript levels of miR-200 family members in HMLE-Twist1-ER cells treated every second day for 16 days with 4-hydroxytamoxifen (TAM), A83-01 (A83), or combinations hereof. Control (Ctrl) = untreated. n=3.

compared to TAM-treated cells, which correlates with previously assessed data showing that A83-01 reduces ZEB1 expression in these cells (Fig. 17D and Fig. 12C).

After ruling out postranscriptional regulators, it was next tested whether Twist1 and TGFβ collaborate on a transcriptional level for induction of Twist1 target genes. To this end, it was analyzed whether Twist1 and Smad2/3 co-localize to the nucleus during EMT induction for transcriptional target regulation. Therefore, HMLE-Twist1-ER cells were treated with TAM in the presence or absence of TGFβ and nuclear and cytoplasmic protein expression was assessed by Western blotting. As expected, Twist1 translocated to the nucleus upon TAM treatment after 24 hours. Additionally, an increase in nuclear phospho-Smad2/3 levels was observed upon treatment with exogenous TGFβ, which confirmed the activation of this pathway (Fig. 18A). In support of previous observations (Fig. 12E), cells treated with TAM and A83-01 showed hardly detectable nuclear phospho-Smad2/3, indicating an efficient inhibition of endogenous TGFβ signaling. The Twist1 downstream effector Slug was already expressed in control cells and was further augmented by treatment with TAM alone or in combination with TGFβ (Fig. 18A). Unlike Slug, ZEB1 nuclear expression was first induced by TAM-treatment after 3 days and was additionally boosted by concomitant treatment with exogenous TGFβ (Fig. 18A). By contrast, treatment with TAM and A83-01 for 3 days reduced the levels of nuclear Slug protein and completely abrogated ZEB1 expression compared to TAM-treated cells (Fig. 18A, right panel). These results reinforced the hypothesis stating that Twist1 requires TGFβ in a dose-dependent manner for induction of its downstream effector ZEB1. Importantly, once again TGFβ alone failed to upregulate nuclear ZEB1 protein (Fig. 18A). By contrast, treatment with recombinant TGFβ resulted in increased nuclear Slug levels compared to the control (Fig. 18A). Thus, it was concluded that Twist1

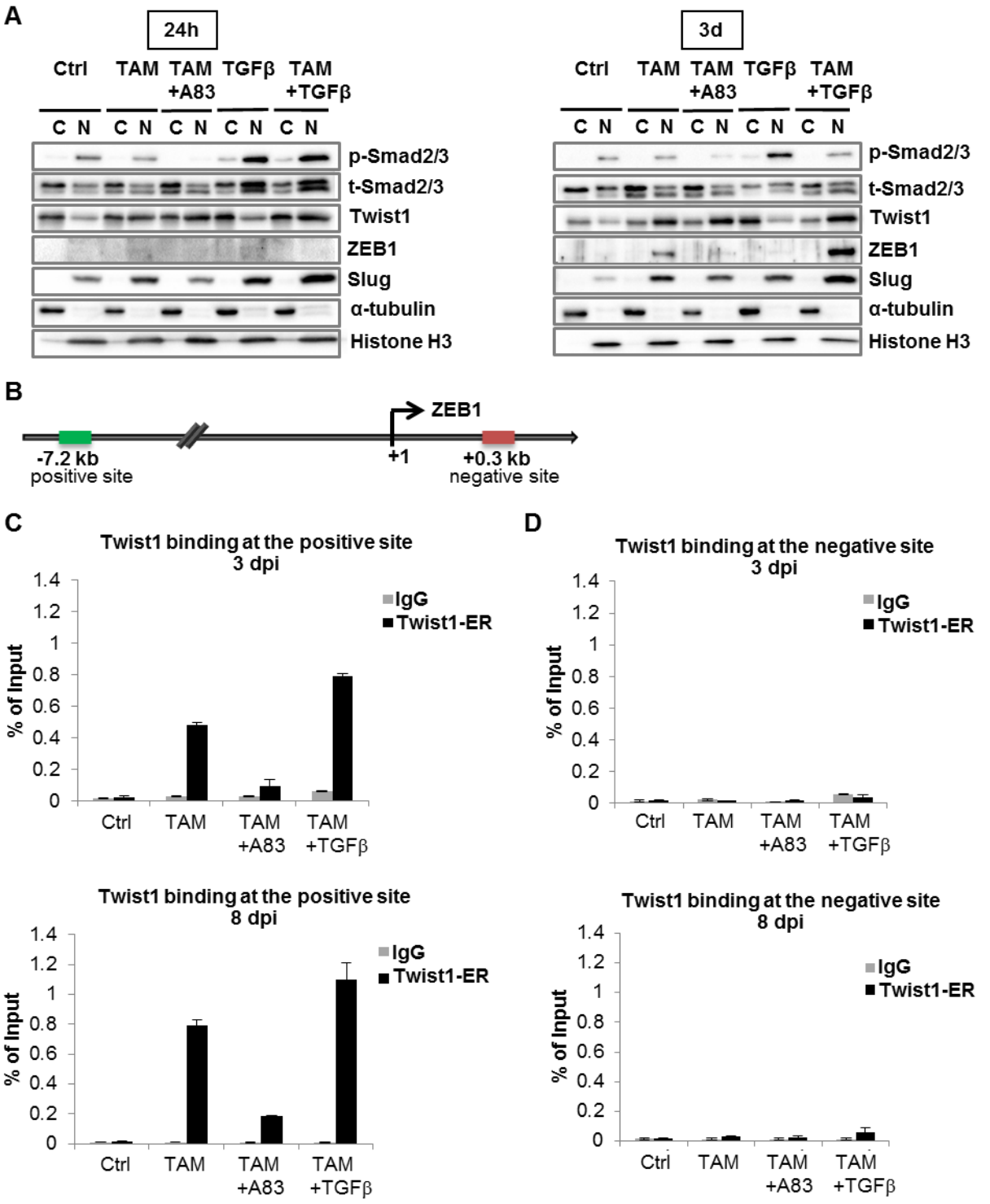

Figure 18: Twist1 requires TGFβ for induction ZEB1 transcription.
A. Western blot analysis of phosphorylated (p-) and total (t-) Smad2/3, Twist1, ZEB1 and Slug protein expression in cytoplasmic (C) and nuclear fractions (N) of HMLE-Twist1-ER cells treated every day with 4-hydroxytamoxifen(TAM), A83-01 (A83), TGFβ or combinations hereof for 24 hours or 3 days. Control (Ctrl) = untreated. α-tubulin and Histone H3 were used as cytosolic and nuclear loading control, respectively. **B.** Schematic representation of Twist1 binding to a *ZEB1* enhancer region (=positive site) or the coding region of the *ZEB1* gene (=negative site) **C.** ChIP analysis of Twist1 binding to the *ZEB1* positive site in HMLE-Twist1-ER cells treated with TAM, TAM+A83 or TAM+TGFβ. Cells were treated daily for 3 days (upper panel), or every second day for 8 days (lower panel). IgG was used as an antibody control. n=3. **D.** ChIP analysis of Twist1 binding to the *ZEB1* negative site in HMLE-Twist1-ER cells treated as in (C). IgG was used as an antibody control. n=3.

and TGFβ congregate and depend on each other for the regulation of ZEB1, but not of Slug expression.

Since the presence or absence of TGFβ did not influence the levels of nuclear Twist1 protein, it was most likely that TGFβ determines whether nuclear Twist1 can activate its target gene *ZEB1*. To test this hypothesis, the binding of Twist1 to a previously published (Chang et al., 2015) DNA-sequence 7.2 kb upstream of the transcription start site of *ZEB1* (=positive site) was investigated by ChIP analysis in the presence or absence of TGFβ (Fig. 18B and 18C). The coding sequence of *ZEB1* served as a control region (=negative site; Fig. 18B and 18D). ChIP analysis was done in collaboration with the Steven Johnsen Laboratory (University of Göttingen, Germany) and confirmed Twist1-binding to the positive site (Fig. 18C). In line with our hypothesis, Twist1-occupancy at the positive site was 5-fold less when cells were treated with TAM and A83-01 (Fig 18C). In reverse, Twist1-binding to the *ZEB1* positive site was 1.6-fold stronger in cells treated with TAM and TGFβ compared to TAM-treated cells (Fig. 18C). As a control, Twist1-binding was hardly detectable at the negative site of *ZEB1*, irrespective of the the analyzed conditions (Fig. 18D).

Together, these results suggest that Twist1 binds an enhancer region of *ZEB1*-transcription dependent on TGFβ signaling. Consequently, TGFβ determines the ability of Twist1 to induce EMT by regulating Twist1-binding to its target gene in a dose-dependent manner.

5.2.4 Twist1 generates cells with invasive properties independently of EMT

I next investigated whether other functions of Twist1 besides EMT induction, such as promotion of migration and invasion are also attenuated in response to TGFβ signaling inhibition. To assess invasive behavior, single-cell suspensions of HMLE-Twist1-ER cells treated with TAM or TAM and A83-01 for 16 days under adherent conditions were plated into 3D collagen gels, which mimic *in vivo* breast tissue environment (Linnemann et al., 2015). Because cell treatment resulted in a stable transcriptional profile, maintained even after drug-withdrawal (Fig. 19A; analysis was performed in collaboration with Anja Krattenmacher, a member of the Scheel group) cells were not treated further in 3D collagen gels. Corroborating these results, cells that were previously treated with TAM in 2D still exhibited strong nuclear localization of ZEB1 after 8 days of culture in 3D collagen gels (Fig. 19B). Likewise, consistent

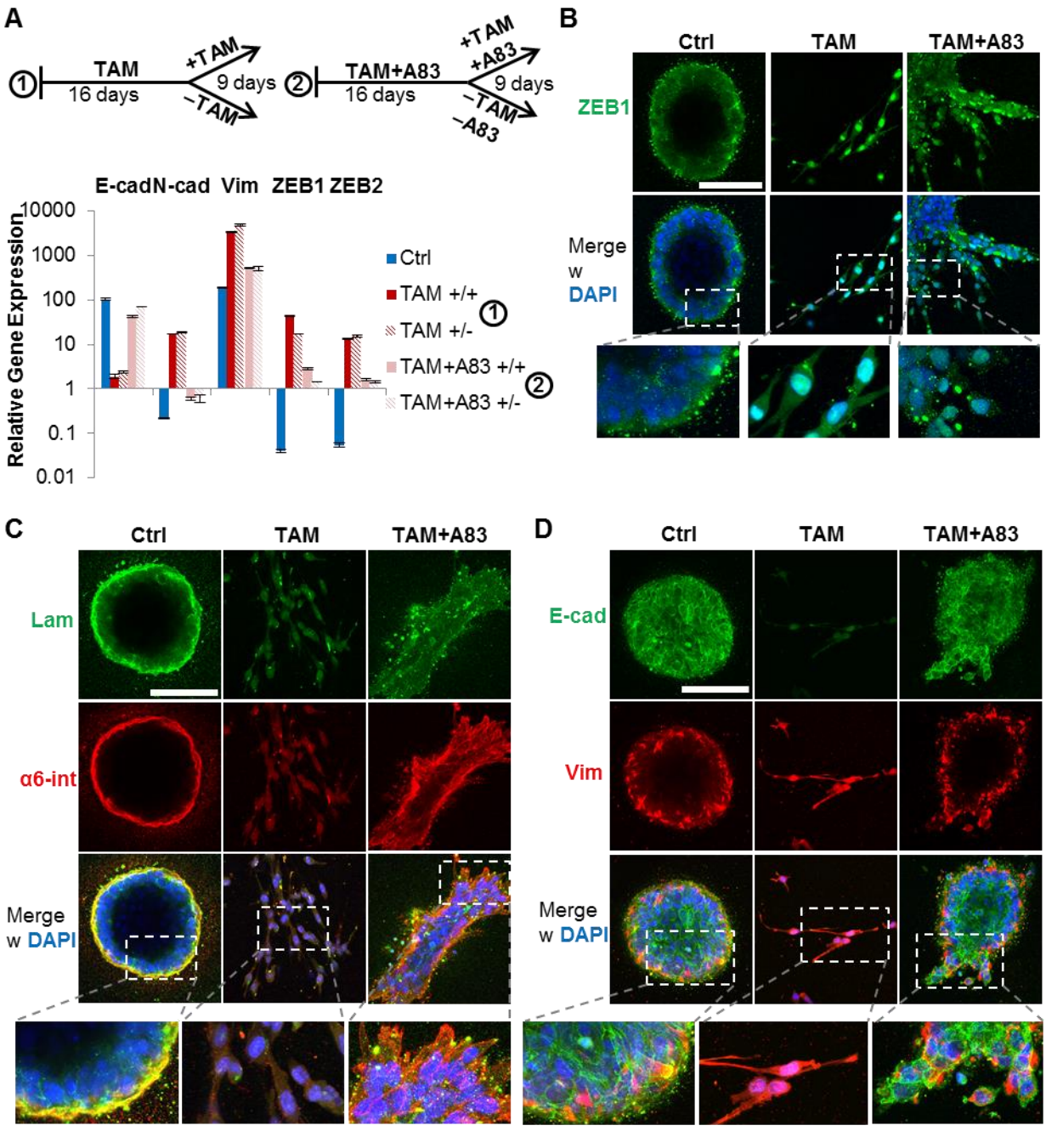
A
TAM
16 days
+TAM
9 days
−TAM
TAM+A83
16 days
+TAM
+A83
9 days
−TAM
−A83
E-cadN-cad Vim ZEB1 ZEB2
Relative Gene Expression
10000
1000
100
10
1
0.1
0.01
Ctrl
TAM +/+
TAM +/-
TAM+A83 +/+
TAM+A83 +/-
B
Ctrl
TAM
TAM+A83
ZEB1
Merge w DAPI
C
Ctrl
TAM
TAM+A83
Lam
α6-int
Merge w DAPI
D
Ctrl
TAM
TAM+A83
E-cad
Vim
Merge w DAPI
E
Ctrl
TAM+A83
Phalloidin/DAPI
F
Colonies/seeded cells (%)
20
18
16
14
12
10
8
6
4
2
0
*
invasive
non-invasive
Ctrl
TAM
TAM+A83

Figure 19: Twist1 generates cells with invasive properties in absence of TGFβ signaling and EMT.
A. RT-PCR analysis of HMLE-Twist1-ER cells treated every second day with TAM for 16 days and afterwards treated every second day with or w/o 4-hydroxytamoxifen (TAM) or with or w/o TAM and A83-01 for another 9 days. Control (Ctrl) = untreated. n=3. **B.** Immunofluorescence staining of HMLE-Twist1-ER cells treated every second day with 4-hydroxytamoxifen (TAM) or TAM and A83-01 (A83) for 16 days under adherent conditions and plated afterwards into collagen gels without further treatment. After another 8 days, cells were stained for ZEB1 expression. Nuclei were stained with DAPI. Control (Ctrl) = untreated. Scale bar: 100 µm. **C.** Immunofluorescence staining of HMLE-Twist1-ER cells treated as in (B). Cells were stained with antibodies against E-cadherin (E-cad) and vimentin (Vim). Nuclei were stained with DAPI. Scale bar: 100 µm. **D.** Immunofluorescence staining of the same conditions as described in (B). Cells were stained with antibodies against laminin-1 (Lam) and α6-integrin (α6-int). Nuclei were stained with DAPI. Scale bar: 100 µm. **E.** Phalloidin staining for detection of F-actin fibers in HMLE-Twist1-ER cells treated as indicated in (B). Yellow arrows in the condition TAM+A83 point out actin-rich invasive protrusions. Nuclei were stained with DAPI (blue). Scale bar: 100 µm. **F.** Quantification of invasive versus non-invasive structures based on stainings presented in (C) and (D). Percentage of colonies per seeded cells has been calculated for each condition based on the following colony-count: n=190 for Ctrl, n=40 for TAM and n=276 for TAM+A83. The p-value for invasive structures in the condition TAM+A83 versus Ctrl was *p<0.05.

with the results obtained under adherent conditions, cells previously treated with TAM and A83-01 displayed a faint ZEB1 nuclear signal compared to TAM-treated cells (Fig. 19B). With ZEB1 being an E-cadherin repressor (Eger et al., 2005) and a previous report showing that Twist1 induces collective migration without loss of E-cadherin expression (Shamir et al., 2014), the epithelial nature of these cells was investigated next.

Consistent with a non-invasive phenotype, control cells generated homogenous, cohesive multicellular spheres, showing an evenly distributed E-cadherin expression and basal localization of vimentin, accompanied by basal deposition of the basement membrane component laminin-1, which was co-localized with its cellular binding partner α6-integrin (Fig. 19C and 19D). In contrast, TAM-treated cells displayed a mesenchymal phenotype and distributed as single-cells throughout the gel (Fig. 19C and 19D). Remarkably, cells treated with both TAM and A83-01 generated invasive structures with diffused localization of laminin-1/α6-integrin and characterized by multicellular, invasive protrusions positively staining for E-cadherin (Fig. 19C and 19D). Moreover, unlike control cells, cells treated with TAM and A83-01 generated multicellular structures containing actin-rich protrusions, reminiscent of invadopodia (Fig. 19E). In line with these results, Twist1 has been shown to promote tumor metastasis by triggering the formation of invadopodia (Eckert et al., 2011). Consistently, structure quantification revealed that control cells generated only few invasive structures, whose amount was increased around 3-fold by activation of

Twist1 in absence of TGFβ signaling (Fig. 19F). TAM-treated cells, which remained as singly invading cells, generated 6 to 9-fold fewer structures compared to the two other conditions (Fig. 19F). Together, these findings suggested that Twist1 promotes either single-cell or collective invasion depending on whether TGFβ signaling is active.

These observations indicated that Twist1 only promotes collective but not single-cell invasion in absence of TGFβ signaling. To distinguish more precisely between collective and single-cell motility, the ability of single-cells to migrate through porous membranes was assessed. When counting migrated cells, a 97.4 % increase upon Twist1 activation by TAM was observed compared to the untreated control (Fig. 20A and 20B). This effect was entirely abrogated by simultaneous treatment with TAM and A83-01, where only very few cells had migrated through the pores (Fig. 20A and 20B). Subsequently, these findings were confirmed by monitoring single-cell movement via live cell imaging (performed in collaboration with Prof. Fabian Theis and Dr. Carsten Marr at the Institute for Computational Biology (ICB) at the Helmholtz Zentrum München). Single-cell tracking revealed that TAM-treated cells moved with higher velocity compared to the untreated control (Fig. 20C). In contrast, cells treated with TAM and A83-01 showed a lower cell speed compared to both TAM-treated and untreated cells (Fig. 20C). Moreover, we observed that

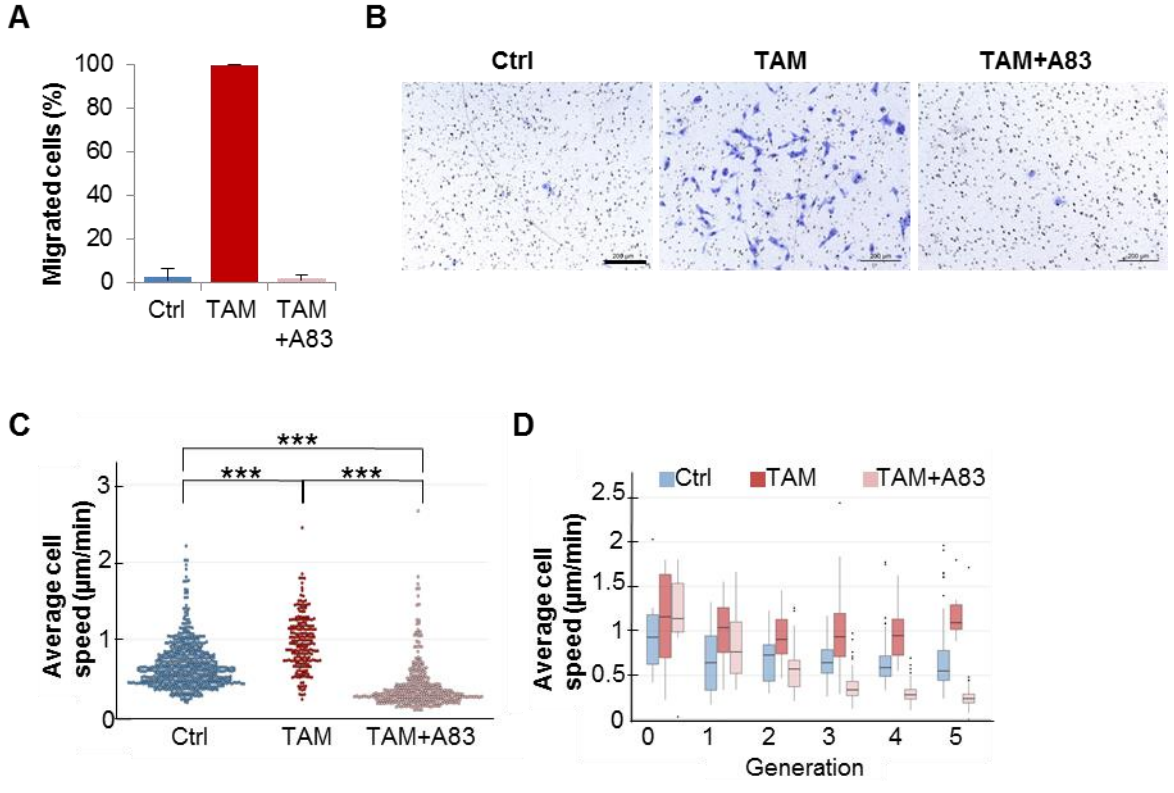

Figure 20: Twist1 requires TGFβ signaling to propagate single-cell migration.
A. Boyden chamber assay: quantification of migrated HMLE-Twist1-ER cells treated every second day with 4-hydroxytamoxifen (TAM) or TAM and A83-01 (A83) for 16 days. Control (Ctrl) = untreated. The number of cells migrated in the TAM condition was set as 100 % and the percentage of migrated cells from all other conditions were calculated relatively to the TAM condition. n=3. **B.** Boyden chamber assay: representative bright-field images of HMLE-Twist1-ER cells treated as indicated in (A). Scale bar: 200 µm. **C.** Live cell imaging: quantification of average cell speed of HMLE-Twist1-ER cells treated with 4-hydroxytamoxifen (TAM) or TAM and A83-01 (A83). Control (Ctrl) = untreated. Single-cells were tracked between 10 and 13 dpi. n=563 for Ctrl, n=210 for TAM, n=338 for TAM+A83; ***p<0.001. One representative experiment from 3 biological replicates is shown here. **D**. Live cell imaging: quantification of average cell speed over five generations of cells described in (C). n=563 for Ctrl, n=210 for TAM, n=338 for TAM+A83. One representative experiment from 3 biological replicates is shown here.

treatment with TAM and A83-01 decreased motility with each cell generation to levels even lower than in the untreated control (Fig. 20D).

These results suggest that Twist1 requires active TGFβ signaling for the generation of single migrating cells, but gives rise to collectively invading cells in its absence. Moreover, concomitant Twist1 activation and inhibition of TGFβ signaling leads to the generation of invasive cells, residing within a distinct and EMT-independent cell state, that is defined by low levels of ZEB1 and maintenance of epithelial identity.

5.2.5 Inhibition of TGFβ signaling prevents Twist1 from decelerating proliferation

The two most important requirements for metastatis to occur are invasion and proliferation. With respect to Twist1, our group (Schmidt et al., 2015) and others (Tsai et al., 2012) have reported before that high Twist1 levels contribute to the acquisition of migratory and invasive abilities during first steps of tumor spreading, but later on impair stemness features and metastatic potential due to an anti-proliferative effect. I therefore investigated whether inhibition of TGFβ signaling impacts the suppressive effects of Twist1 on cell proliferation. As done for invasion analysis, HMLE-Twist1-ER cells treated with TAM or TAM and A83-01 for 16 days under adherent conditions were plated into 3D collagen gels without further treatment. After 8 days, cell proliferation was quantified (Fig. 21A). In line with previous observations from our group, TAM-treated cells did not proliferate at all under 3D conditions, whereas untreated cells increased in cell number by 30-fold compared to the amount of originally plated cells (Fig. 21A). Most importantly, cells treated with both TAM and A83-01 proliferated at higher rates compared to TAM-treated cells (Fig. 21A),

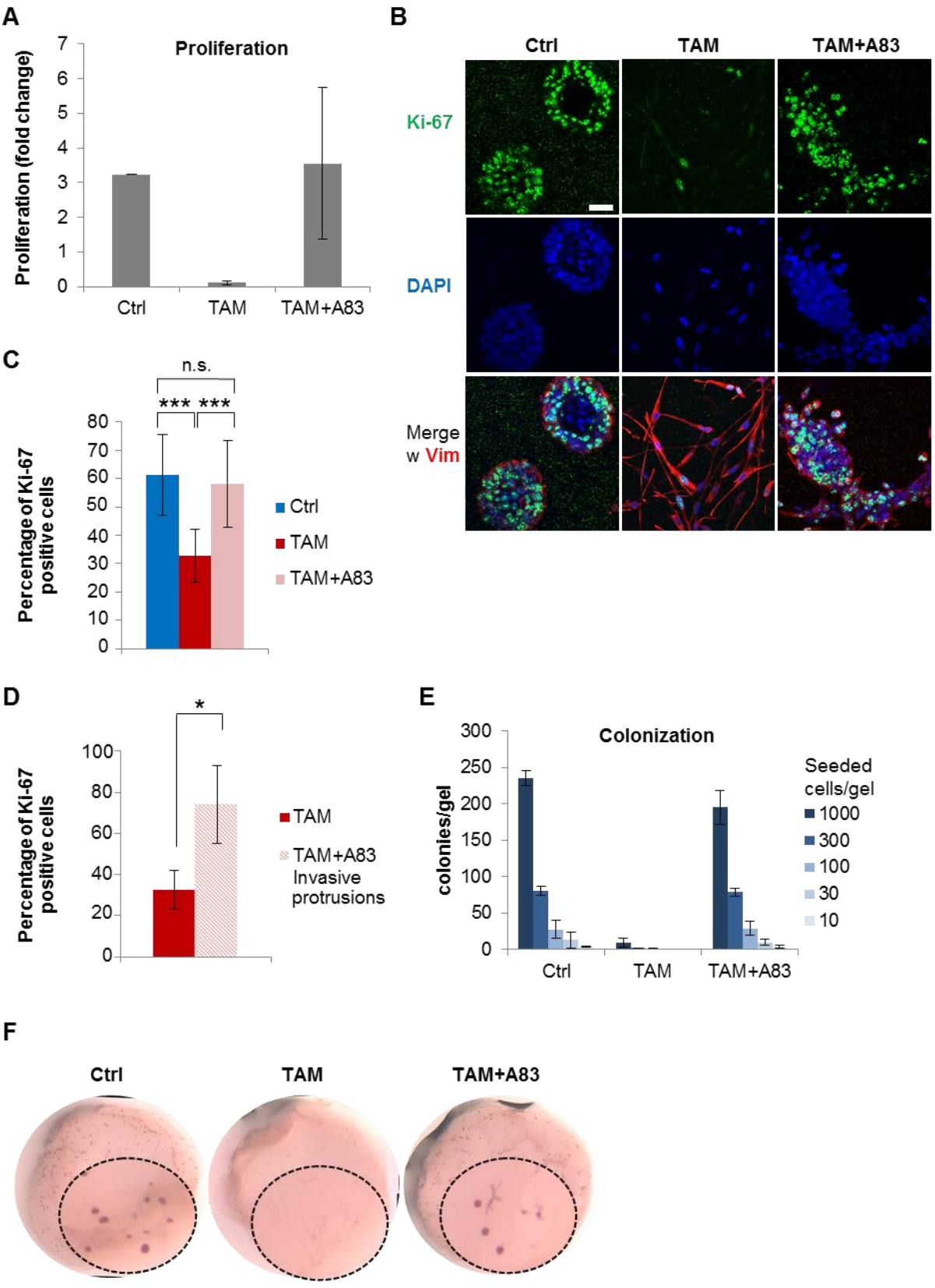
A
Proliferation
Proliferation (fold change)
7
6
5
4
3
2
1
0
Ctrl
TAM
TAM+A83
B
Ctrl
TAM
TAM+A83
Ki-67
DAPI
Merge w Vim
C
n.s.
*** ***
Percentage of Ki-67 positive cells
80
70
60
50
40
30
20
10
0
Ctrl
TAM
TAM+A83
D
*
Percentage of Ki-67 positive cells
100
80
60
40
20
0
TAM
TAM+A83 Invasive protrusions
E
Colonization
colonies/gel
300
250
200
150
100
50
0
Ctrl
TAM
TAM+A83
Seeded cells/gel
1000
300
100
30
10
F
Ctrl
TAM
TAM+A83

Figure 21: Twist1 reduces cell proliferation in a TGFβ dependent manner in 3D.
A. 3D collagen gels: proliferation relative to the number of originally plated cells per gel. HMLE-Twist1-ER cells were treated every second day with 4-hydroxytamoxifen (TAM) or TAM and A83-01 (A83) for 16 days under adherent conditions and plated afterwards into collagen gels without further treatment. Control (Ctrl) = untreated. n=3. **B.** 3D collagen gels: immunofluorescence staining for Ki-67 and vimentin (Vim). Cell nuclei were stained with DAPI. Cells were treated as in (A). Scale bar: 100 µM. **C.** Quantification of Ki-67 positive cells based on the conditions shown in (B). n=1732 for Ctrl, n=640 for TAM and n=1043 for TAM+A83. **D.** Quantification of Ki-67 positive cells within the TAM-treated population and the invasive cells from the TAM+A83 condition shown in (B). n=640 for TAM and n=175 for TAM+A83 invasive protrusions. **E.** 3D collagen gels: quantification of carmine-stained colonies generated by cells plated in densities ranging from 1000 to 10 per gel. Cells were treated as described in (A). n=3. **F.** 3D collagen gels: carmine staining of colonies generated by cells treated as in (A).

suggesting that Twist1 is not able to suppress proliferation in the absence of TGFβ signaling.

Corroborating these results, the condition TAM+A83 displayed higher amounts of cells positive for the proliferation marker Ki-67 compared to the TAM condition (Fig. 21B and 21C; this analysis was performed in collaboration with Anja Krattenmacher, a member of the Scheel group). Because it was reported before that only tumor cells which can both invade and proliferate are able to give rise to metastatic foci (Tsai et al., 2012; Giampieri et al., 2009) it was of great interest to determine whether the invading cells in the condition TAM+A83 actively proliferate. To this purpose, the amount of Ki-67 positive cells amongst protruding invasive cells from the condition TAM+A83 was quantified and compared to singly invading TAM-treated cells. Remarkably, the percentage of Ki-67 positive cells within the invading population previously treated with TAM and A83-01 was 2 to 3-fold higher compared to TAM-treated cells (Fig. 21D). Moreover, TAM-treated cells generated 25 to 45-fold less colonies compared to control cells (Fig. 21E and 21F). By contrast, cells treated with TAM and A83-01 colonized the gel very efficiently, at rates comparable to the untreated control (Fig. 21E and 21F). Therefore, it was concluded that in the absence of TGFβ signaling, Twist1 generates invasive cells with increased proliferative capacity.

Nevertheless, tracking single-cells for 3 days under 2D conditions by live cell imaging (in collaboration with the ICB, Helmholtz Zentrum München) revealed that activation of Twist1 by TAM slowed down cell proliferation only moderately compared to the untreated control (Fig. 22A). In contrast, inhibition of TGFβ signaling rescued the week anti-proliferative effect of Twist1 (Fig. 22A). At later time points (18 to 21 dpi), cells treated with both TAM and A83-01 proliferated at higher rates compared to cells

treated with TAM alone (Fig. 22B). However, Twist1-activation by TAM-treatment suppressed cell proliferation in 2D to a lower extent compared to 3D. Consequently, the maintenance of proliferative capacity caused by addition of A83-01 was less pronounced in 2D compared to 3D. It is most likely that 2D culturing conditions are not most suitable for investigations of metastatic outgrowth as they do not reflect the *in vivo* environment as well as 3D collagen gels.

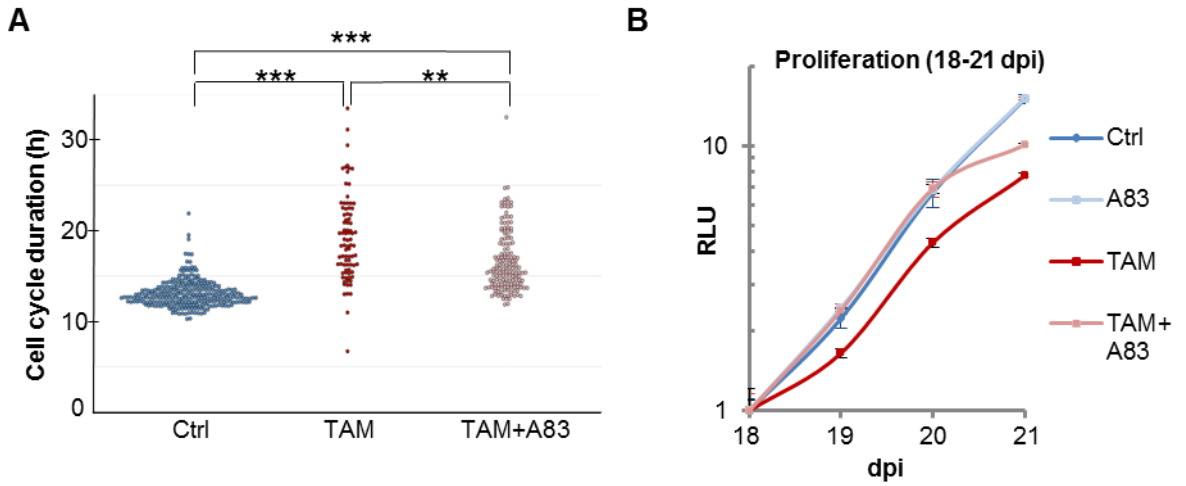

Figure 22: A83-01 treatment prevents Twist1 from decelerating proliferation in 2D.
A. Live cell imaging: quantification of duplication time of HMLE-Twist1-ER cells treated with 4-hydroxytamoxifen (TAM) or TAM and A83-01 (A83). Control (Ctrl) = untreated. Single-cells were tracked between 10 and 13 days post induction (dpi). n=274 for Ctrl, n=84 for TAM, n=158 for TAM+A83; **p<0.01, ***p<0.001. One representative experiment from 3 biological replicates is shown here. **B.** Luminescent cell viability assay of HMLE-Twist1-ER cells treated every second day with A83-01 (A83), 4-hydroxytamoxifen (TAM) or TAM+A83-01. Control (Ctrl) = untreated. Proliferation was measured between 18 and 21 days post induction (dpi). n=6.

Taken together, the acquired data showed that even though blocking TGFβ signaling impairs Twist1-induced EMT in 2D, in absence of TGFβ signaling Twist1 generates multicellular structures, which have the ability both to invade and proliferate in a 3D environment. By contrast, control cells mostly only proliferate, whereas TAM-treated mesenchymal cells only invade in 3D. Importantly, differences in proliferation and invasion induced by Twist1 dependent on TGFβ signaling are only revealed under 3D and not 2D culturing conditions.

5.3 Twist1 does not require TGFβ signaling for EMT maintenance

The results presented in section *5.2. Inhibition of developmental pathways during EMT induction* indicated that TGFβ signaling is required for Twist1-induced EMT.

However, it was still not clear why the mesenchymal cell line MDA-MB-231 displayed low sensitivity to inhibition of TGFβ signaling by A83-01. Therefore, I addressed the question whether cells acquire resistance to A83-01 directly after converting to a mesenchymal phenotype (done in collaboration with Lisa Meixner, an intern in our lab). To this end, HMLE-Twist1-ER cells were further treated with TAM beyond the 16 days required for EMT induction and A83-01 was added for another 6 days (Fig. 23A). By immunofluorescence stainig, it was observed that mesenchymal cells treated with A83-01 retained vimentin expression and did not re-express E-cadherin (Fig. 23A). These results indicated that cells that have completely transdifferentiated to a mesenchymal phenotype can maintain their identity independently of TGFβ signaling. Furthermore, to mimic the stable mesenchymal state of MDA-MB-231 cells, HMLE cells expressing a constitutively active Twist1 construct (HMLE-Twist1) were treated with A83-01 for 12 days. Corroborating the results obtained with MDA-MB-231 cells, HMLE-Twist1 cells did not display any phenotypical changes in response to prolonged treatment with A83-01 (Fig. 23B). Consequently, these data suggest that once cells have reached a stable mesenchymal state, they do not depend on TGFβ signaling for EMT maintenance.

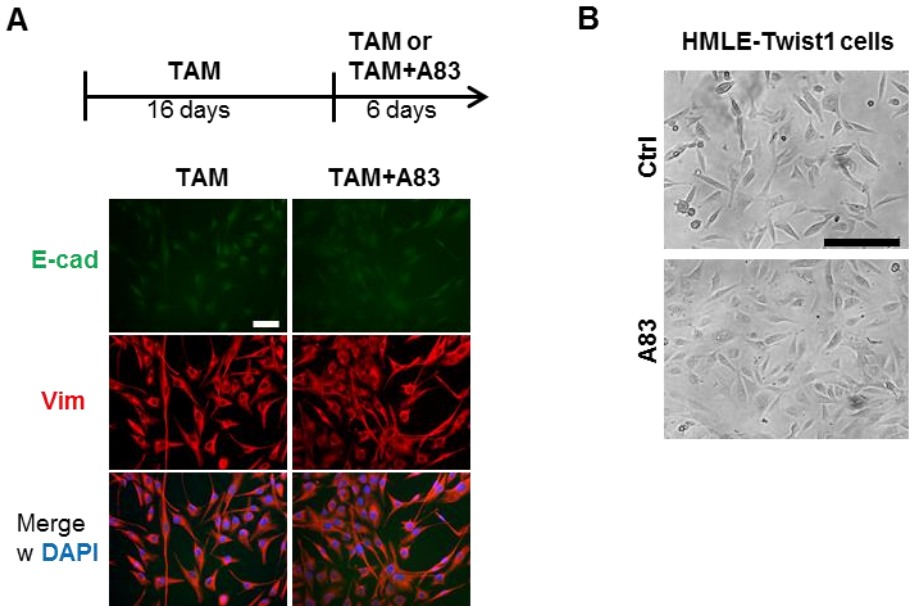

Figure 23: Cells that have undergone Twist1-induced EMT are resistant to A83-01 treatment.
A. Immunofluorescence staining of HMLE-Twist1-ER cells treated every second day with 4-hydroxytamoxifen (TAM) for 16 days and afterwards treated every second day with TAM or TAM and A83-01 (A83) for 6 days. Control (Ctrl) = untreated. Cells were stained for E-cadherin (E-cad) and vimentin (Vim). Nuclei were stained with DAPI. Scale bar: 100 µm. **B.** Brightfield pictures of HMLE-Twist1 cells treated every second day with A83-01 (A83) for 12 days. Control (Ctrl) = untreated. Scale bar: 200 µm.

6. Discussion

During the last 15 years, gene expression analysis of breast cancer tissues has greatly improved our knowledge regarding the different molecular subtypes of tumors in the mammary gland (Prat and Perou, 2010). Thus, it became possible to subdivide breast tumors in many more categories, compared to limited profiles provided by standard immunohistochemical markers. Most importantly, these molecular subtypes are different with respect to tumor recurrence and overall survival, thereby indicating that they represent distinct entities and should be approached as such when considering treatment strategies. Moreover, these studies have elucidated the genetic profile of TNBC, the only breast cancer subtype that does not profit from targeted therapies so far due to the lack of hormone receptor expression (Podo et al., 2010). The absence of efficient target therapies is also reflected by the poor clinical outcome associated with TNBC. Nevertheless, genetic profiling revealed that a subgroup of TNBC, termed ‘Claudin-low’, correlates with an EMT and stem cell-like signature (Herschkowitz et al., 2007). In addition, a mesenchymal gene expression profile relates also to another TNBC subgroup, basal-like breast cancers (Sarrió et al., 2008; Marchini et al., 2010). These findings suggest that targeting EMT is a promising strategy in the development of individualized therapies for TNBC patients.
This work focused on the inhibition of EMT signaling pathways both in the mesenchymal TNBC cell line MDA-MB-231, and during Twist1-induced EMT. More precisely, it was investigated whether blocking of EMT signaling pathways reduces tumorigenic features, such as migration, colonization and growth in anchorage-independence. In addition, the molecular mechanisms governing the interplay between the EMT-TF, Twist1 and the EMT inducer, TGFβ were dissected.

6.1 Biological read-out of the mammosphere assay

The mammosphere assay is widely used for identification and cultivation of healthy stem/progenitor cells and tumor initiating cells from the human mammary gland (Dontu et al., 2003). In the original protocol, human mammary cells are grown in anchorage-independence and in serum-free mammosphere medium without methylcellulose (Dontu et al., 2003). However, this study shows that addition of 10 % methylcellulose to the growth medium is required to ensure clonality of the

mammospheres (Fig. 4C). When using less than 10 % methylcellulose, the number of spheres did not linearly increase with higher amounts of plated cells (Fig. 4C). This indicated that under these conditions spheres were formed through cell aggregation rather than clonal growth. Indeed, others have shown that sphere formation can result from aggregation in the absence of methylcellulose, especially when increasing cell density (Kuch et al., 2012). Moreover, plating higher cell concentrations also facilitated aggregation, despite methylcellulose addition (Fig. 4D and 4E). It is very likely that higher cell concentrations force cells grown in suspension to physically interact. In concordance with published protocols (Dontu et al., 2003), this study reached the conclusion that plating more than 1000 cells/ml tampers with clonality and is therefore unsuitable for a reliable determination of sphere forming efficiency (Fig. 4D and 4E). Corroborating these findings, extensive studies performed with neurospheres, a mammosphere analog, suggest that a neurosphere can reliably be of clonal origin only when cells are plated at 1000 cells/ml or less (Pastrana et al., 2011).

It continues to be highly debated to which extent the ability to build mammospheres directly reflects stem-cell characteristics or tumor initiating capacity (Pastrana et al., 2011; Stingl, 2009). If only tumor initiating cells (TICs) would be able to grow under anchorage-independent conditions, as provided in the mammosphere assay, then, resulting from this study, every 3rd to 5th cell of the breast cancer cell lines MDA-MB-231 and MCF7-Ras should be able to give rise to *de novo* tumors (Fig. 4F and 4G). However, this scenario is highly unlikely and indeed, there has been reported before that sphere forming ability does not always correlate with tumor initiating properties *in vivo* (Kuch et al., 2013). Moreover, studies done with neurospheres predict that the neurosphere assay overestimates stem cell frequency by an order of magnitude (Pastrana et al., 2011).

Another read-out of the mammosphere assay that is critically viewed is that serial passaging enriches for stem cell-like properties (Dontu et al., 2003). Based on results in this study, it remains questionable whether this functional aspect also applies to TICs, since serial passaging of MDA-MB-231 and MCF7-Ras cells did not increase their sphere forming efficiency (Fig. 4F and 4G). These results are consistent with published work showing that cells serially cultivated as spheres do not display differences in tumor initiation compared to cells grown as adherent cultures (Kuch et al., 2013). In contrast, others have reported that cancer cells cultivated for one

passage as mammospheres could give rise to tumors more efficiently than cells grown under adherent conditions (Ponti et al., 2005; Cicalese et al., 2009). Interestingly, the sphere forming ability of MCF7-Ras cells decreased with each passage, while that of MDA-MB-231 remained unchanged (Fig. 4F and 4G). This suggests that the mammosphere assay may help distinguish between different tumorigenicity levels if cells are serially passaged.

6.2 Titration and choice of inhibitors

Small-molecule inhibitors were used in this study to block the main EMT inducing signaling pathways, TGFβ and Wnt (Lamouille et al., 2014). A83-01 has been described to be more potent in inhibiting the TGFRI compared to other compounds of the same class (Vogt et al., 2011). Titration of A83-01 revealed that 1 µM is sufficient to efficiently abrogate TGFβ signaling (Fig. 6A and 6B). By contrast, the commonly employed TGFRI inhibitors SB-431542 and SB-505124 allow 20-50 % residual kinase activity when used at 1 µM (Vogt et al., 2011). Similarly, the Wnt inhibitors, XAV939 and IWP-2 efficiently blocked canonical Wnt signaling at a concentration of 1 µM (Fig. 6C and 6D). Nevertheless, more recently another porcupine inhibitor more potent than IWP-2 was discovered, Wnt-C59 (Proffitt et al., 2013). Unlike IWP-2, Wnt-C59 is also bioavailable and should therefore be preferred to IWP-2 for future studies. Importantly, when employing inhibitors at the assessed effective concentrations, no general cytotoxic effects were observed (Fig. 5). Thus, any phenotypical changes caused by inhibitor treatments are most likely to reflect a specific inhibition of the targeted pathway.

6.3 TGFβ and Wnt signaling are not required for mammosphere formation, but potentially control cell motility in TNBC

Even though EMT is associated with acquisition of stem cell-like properties in breast cancer (Ansieu, 2013; Mani et al., 2008), inhibition of the EMT signaling pathways TGFβ and Wnt did not impact mammosphere formation of MDA-MB-231 cells (Fig. 7). There are two possible explanations for this. Either the mammosphere assay is not the most suitable assay for the read-out of stem cell features (previously discussed in *section 6.1. Biological read-out of the mammosphere assay*), or these

EMT inducing pathways are no longer required for sphere formation once cells have undergone EMT and reside in a stable mesenchymal state. Indeed, it has been reported before that EMT not only drives cancer stem cell formation, but is also associated with increased drug resistance (Singh and Settleman, 2010). It is therefore conceivable, that mesenchymal cells, like MDA-MB-231 retain a tumorigenic potential that overcomes growth factor dependency.

On the other hand, inhibition of either TGFβ or Wnt signaling resulted in a significant reduction of singly migrating cells, suggesting that TNBC cells at least partially employ these pathways for motility (Fig. 8). Thus, treatment of MDA-MB-231 cells with the TGFRI inhibitor A83-01 diminished the number of migrated cells by half compared to the control (Fig. 8B). Corroborating these findings, others have shown that expression of an inactive TGFRII mutant impaired single-cell migration of MDA-MB-231 cells (Dumont et al., 2003). In addition, inhibition of the non-canonical TGFβ pathway signaling through JNK also reduced single-cell migration (Fig. 8E). Nevertheless, SP60125 impaired migration to a lower extent than A83-01, indicating that both Smad-dependent and –independent TGFβ signaling are employed by motile cells. Mirroring these results, it has been reported before that MDA-MB-231 cells partially rely on Smad3 or JNK for migration (Dumont et al., 2003; Luwor et al., 2015). Similarly to treatment with A83-01, blocking Wnt signaling by incubation with IWP-2 or XAV939 halved the amount of migrated cells compared to the control (Fig. 8C and 8D). Indeed, it was shown that silencing of β-catenin impaired migratory abilities of MDA-MB-231 cells (Xu et al., 2015).

Since migration and invasion drive the first steps in the metastatic cascade (Scheel and Weinberg, 2012), it might be helpful to use TGFβ and Wnt inhibitors against tumorigenic TNBC cells. However, it should be considered, that blocking these pathways does not completely abrogate migratory abilities and those cells which escape drug treatment might still display cancer stem cell features and tumor initiating capacity.

Interestingly, blocking TGFβ, but not Wnt signaling, changed the morphology of MDA-MB-231 cells seeded into 3D collagen gels (Fig. 9A). Thus, cells treated with A83-01 formed invasive structures and expressed E-cadherin (Fig. 9B). By contrast, untreated MDA-MB-231 cells remained as singly invading cells (Fig. 9B). In conclusion, it appears that blocking TGFβ signaling produces a switch from single-cell to collective invasion. In fact, TGFβ signaling has been hold responsible for the

acquisition of single-cell motility at the invasive front of breast tumors and its inhibition resulted in a switch to collective invasion (Giampieri et al., 2009). Collectively invading cells were able to penetrate lymphatic vessels, but failed to enter the blood. While blocking TGFβ signaling reduced blood-borne metastasis, chronical activation of the pathway inhibited colonization of the lung. In contrast, a transient activation of TGFβ signaling with an initial TGFβ pulse, followed by retraction, lead to increased formation of distant metastases (Giampieri et al., 2009). Therefore, as targeted therapies evolving against TNBC include TGFβ inhibitors, it is crucial to consider that blocking TGFβ signaling in cells which have already disseminated might facilitate metastatic outgrowth.

6.4 EMT maintenance versus EMT induction

Because TGFβ signaling is one of the main EMT inducing pathways (Thiery et al., 2009), this study aimed to inhibit the TGFβ pathway in mesenchymal TNBC cells. However, treatment of MDA-MB-231 cells with the TGFRI inhibitor A83-01 did not reduce gene expression levels of mesenchymal markers and effectors (Fig. 10). This suggested that mesenchymal cells might reside within a stable state, where they do not depend on TGFβ signaling anymore for the maintenance of their mesenchymal phenotype. Thus, it might be necessary to re-express intracellular regulators of the mesenchymal state, such as members of the miR-200 family, to revert MDA-MB-231 cells to an epithelial phenotype (Park et al., 2008; Xie et al., 2014).

At this point, I postulated that TGFβ is only required for EMT induction in breast cancer, but once cells have become mesenchymal they overcome this growth factor dependency. To better understand the mechanism through which this independence is acquired, it was imperative to determine the molecular pathways controlled by TGFβ during EMT induction. To this purpose, I utilized Human Mammary Epithelial Cells (HMECs) which were immortalized by retroviral transduction of the human telomerase reverse transcriptase (hTERT) and the SV40 large-T antigen, a repressor of the p53 tumor suppressor protein (HMLE cells; Ellenbaas et al., 2001). In addition, to modulate mesenchymal transdifferentiation, HMLE cells were transduced with an inducible Twist1-ER construct, known to induce EMT upon activation by Tamoxifen treatment (HMLE-Twist1-ER cells) (Yang et al., 2004). According to gene expression profiling analysis, HMECs do not express ER, PR or HER2 and display a mixed

phenotype with both Claudin-low and basal-like breast cancer characteristics (Prat et al., 2013). Moreover, p53 inactivating mutations are frequently observed in basal-like breast cancer (Carey et al., 2006). Taken together, these genetic features of HMECs, HMLEs and their derivatives qualify them as a model for TNBC. Thus, HMLE-Twist1-ER cells might constitute a powerful tool for studying EMT induction in TNBC.

6.5 Twist1 requires autocrine TGFβ signaling for EMT induction

Activation of Twist1 by treatment with TAM for 16 days resulted in a complete EMT, accompanied by downregulation of the epithelial marker E-cadherin and upregulation of several mesenchymal markers and effectors (N-cadherin, vimentin, Fibronectin, Wnt5a, ZEB1/2, Slug, FoxC2) (Fig. 12B-D). Interestingly, blocking TGFβ, but not Wnt or JNK signaling inhibited Twist1-induced EMT to a large extent (Fig. 12A-D). This indicated that Twist1 specifically requires TGFβ signaling for EMT induction. Since inhibition of non-canonical TGFβ signaling through JNK did not impair Twist1-induced EMT, it is most likely that Twist1 depends on the TGFβ-Smad pathway for promoting mesenchymal transdifferentiation. Indeed, HMLE-Twist1-ER cells displayed autocrine, Smad-dependent TGFβ signaling required for Twist1-induced EMT (Fig. 12E). Although treatment with TAM and the TGFRI inhibitor A83-01 prevented the upregulation of mesenchymal markers and maintained E-cadherin expression, it only partially impaired the induction of some EMT effectors, such as ZEB1and ZEB2 (Fig. 12B-D). This suggested that even though Twist1 was not able to launch the mesenchymal program without TGFβ signaling, it might still induce other phenotypical changes which require intermediate levels of ZEB1/ZEB2.

Using A83-01 at a low dosage (1 µM) and assuring that it does not impact the activity of other kinases, such as RIPK2 and VEGFR greatly reduced the chance of off-target effects (Fig. 13 and 14). Nevertheless, knockdown of the TGFBR1 did not block Twist1-induced EMT to same extent as A83-01 (Fig. 12 and 13). Given the relatively high specificity of A83-01 (Vogt et al., 2011), it is most probable that this difference results from technical issues. Due to the fact that HMLE-Twist1-ER cells were previously transduced with a puromycin resistance gene, the same one as incorporated in the shRNA constructs targeting the TGFBRI, it was not possible to select successfully transduced cells by antibiotics. Therefore, it was necessary to purify positive cells by FACS. Unfortunately, sorted cells have lost the shRNA

constructs with passaging and thus, the efficiency of TGFBRI silencing dropped in time.

6.6 Twist1 and TGFβ collaborate to induce EMT target genes

Collaborations of TGFβ signaling and EMT-TFs, such as Snail, ZEB1 and ZEB2, have been previously reported to occur during EMT induction (Voncent et al., 2009; Postigo et al., 2003). However, to my knowledge, it has never been shown before that TGFβ potentiates Twist1-induced EMT. This study provides evidence that Twist1 not only requires TGFβ signaling for EMT induction, but it also synergizes with TGFβ for upregulation of several mesenchymal markers and effectors. Thus, cells treated with both TAM and TGFβ acquired a mesenchymal phenotype 8 days earlier compared to cells treated only with TAM (Fig. 15). Notably, treatment with TGFβ resulted in the upregulation of mesenchymal markers (N-cadherin, vimentin, fibronectin), but was not sufficient for a loss of the epithelial marker E-cadherin and therefore failed to induce a full EMT (Fig. 15). These data are consistent with published literature showing that TGFβ can directly induce transcription of N-cadherin, vimentin and fibronectin (Yang et al., 2015c; Nawshad et al., 2007). Nevertheless, in other cellular models, such as lung cancer, liver cancer or mouse mammary epithelial cells, TGFβ appears to be sufficient for an epithelial mesenchymal transdifferenciation (Fig. 16; Thuault et al., 2006; Yang et al., 2015c; Dang et al., 2011). Even so, concomitant activation of Twist1 in A549 lung carcinoma cells additionally boosted the effects of TGFβ on the upregulation of mesenchymal markers and effectors (Fig. 16). This indicates that the molecular collaboration between Twist1 and TGFβ in the EMT induction process might not be limited to breast tissue, but might also apply to other organs, such as the lung.

The effects of treatment with TAM, A83-01, TGFβ and combinations hereof were reflected in the gene expression levels of ZEB1, ZEB2, Wnt5a and fibronectin already after 48 hours (Fig. 17A and 17B). Since these results indicated that TGFβ might directly modulate the activation of Twist1 target genes, this work aimed to exemplify this hypothesis on the basis of *ZEB1*. Indeed, Twist1 binding to an enhancer region upstream of *ZEB1* was reduced in the absence of TGFβ signaling and was enhanced by addition of exogenous TGFβ (Fig. 18C). Thus, TGFβ signaling determined Twist1-occupancy at the *ZEB1* enhancer region in a dose-dependent

manner. However, blocking TGFβ signaling by A83-01 did not completely prevent Twist1-binding, thereby suggesting that other, TGFβ-independent mechanisms might regulate the transcriptional activity of Twist1. For example, Twist1 is known to recruit Bromodomain Containing 4 (BRD4) to the promoter of its target gene Wnt5a (Shi et al., 2014).

For further studies, it would be of great interest to determine whether Twist1 can still induce EMT in ZEB1-depleted cells. If so, this would indicate a hierarchical signaling cascade governing the EMT process, where Twist1 requires TGFβ signaling for transcriptional induction of ZEB1, which in turn downregulates E-cadherin and thereby triggers a mesenchymal transdifferentiation.

6.7 Twist1 promotes either single-cell or collective invasion dependent on TGFβ signaling

Even though blocking TGFβ signaling prevented Twist1 from upregulating several players of the mesenchymal program, ZEB1 and ZEB2 were moderately induced by treatment with TAM in the absence of TGFβ signaling (Fig. 12C and 12D). Moreover, this study showed that treatment with A83-01 did not completely impair Twist1-binding to a *ZEB1* enhancer region (Fig. 18C). Although the remaining ZEB1 expression was not sufficient for a full EMT induction, cells treated with TAM and A83-01 colectively invaded and proliferated in a 3D environment (Fig. 19 and 21). Thus, in the absence of TGFβ signaling, Twist1 might induce a distinct, EMT-independent cell-state. Underlying this hypothesis, in a manuscript under preparation we show that without an active TGFβ signaling Twist1 generates cells which express endothelial markers, such as CD31, CD99 and VEGFR2. Consistently, it has been reported that Twist1 promotes vasculogenic mimicry in breast cancer (Zhang et al., 2014). Moreover, circulating tumor cell clusters (CTC-clusters) resulting from collectively invading tumor cells may display an advantage at colonizing distant tissues by “bringing their own soil”, i.e. platelets and endothelial cells (Aceto et al., 2015). Although CTCs are much rarer in the blood, they demonstrate increased metastatic potential compared to single CTCs (Aceto et al., 2014). In addition, the observation of epithelial cells displaying an invasive phenotype is corroborated by clinical data showing that distant metastasis of invasive breast carcinomas consistently express E-cadherin (Kowalski et al., 2003; Bukholm et al., 2000).

To confirm tumor initiating and metastatic ability *in vivo*, it would be imperative to transplant cells treated with TAM and A83-01 into immunocompromised mice.

6.8 Inhibition of TGFβ signaling overcomes the Twist1-induced proliferation barrier

It has been reported before that constitutive activation of Twist1 results in growth inhibition and inability of metastatic colonization (Schmidt et al., 2015; Tsai et al., 2012). This study shows that concomitant inhibition of TGFβ signaling overcomes this barrier and maintains the proliferative capacity and colonization ability (Fig. 21). Interestingly, members of the TGFβ pathway are frequently mutated in invasive breast cancers and a disabled TGFβ signaling is associated with increased metastasis (Chen et al., 1998; Chen et al., 2006; Yang et al., 2008). Considering the growth inhibitory effect of TGFβ (Massague, 2008), it is highly likely that inactivating mutations of the pathway represent an advantage for colonization of distant sites and metastatic outgrowth.

6.9 TGFβ signaling is required for EMT induction, but not for EMT maintenance

Once HMLE-Twist1-ER cells have undergone EMT upon TAM-treatment, they were able to maintain a mesenchymal phenotype independently of TGFβ signaling (Fig. 23A). Similarly, prolonged treatment of HMLE cells constitutively expressing Twist1 (HMLE-Twist1) with A83-01 did not result in re-epithelialization (Fig. 23B). Since TGFβ signaling was required for induction of ZEB1 in a dose-dependent manner, it is highly likely that ZEB1 levels within a cell decide whether this cell undergoes an EMT or retains an epithelial identity. Usually, the miR-200 family represses ZEB1 expression within a negative feedback-loop (Fig. 17D; Burk et al., 2008). Nevertheless, it is conceivable that the miR-200 – ZEB1 regulatory mechanism is no longer functional once cells have reached a stable mesenchymal state. Thus, Twist1 might require TGFβ during EMT induction to boost ZEB1 transcription to levels sufficient to break the miR-200 – ZEB1 negative feedback loop. Consequently, once ZEB1 is stably expressed, Twist1 does not depend on TGFβ signaling anymore for the propagation of the mesenchymal phenotype. The same evasion mechanism might explain also the resistance of mesenchymal MDA-MB-231 cells to A83-01

treatment. These cells might have reached ZEB1 levels high enough to disperse the miR-200 – ZEB1 negative feedback loop and therefore reside in a stable, TGFβ-independent mesenchymal state. In line with this hypothesis, it has been shown before that overexpression of miR-200c in MDA-MB-231 resulted in a MET (Xie et al., 2014). Moreover, as a direct repressor of E-cadherin, ZEB1 has been demonstrated to be indinspensible for the maintenance of the mesenchymal phenotype. Thus, ZEB1 depletion in MDA-MB-231 cells was sufficient to induce E-cadherin expression (Aigner et al., 2007).

Beyond directly suppressing transcription of E-cadherin, ZEB1 was shown to promote methylation and silencing of the E-cadherin promoter in MDA-MB-231 cells (Fukagawa et al., 2015). Consequently, ZEB1 knock-down restored E-cadherin expression and induced re-epithelialization of MDA-MB-231 cells (Fukagawa et al., 2015).

6.10 Closing remarks

The results of this study suggest that using inhibitors of the TGFβ pathway in therapy against breast cancer prone to EMT might promote metastasis and tumor recurrence. More precisely, in tumors with active Twist1, inhibition of TGFβ signaling might result in a switch from single-cell to collective invasion. If these cell clusters enter blood vessels and are systemically disseminated, they will likely be able to establish actively growing metastases, since they retain proliferative capacity. These considerations are important for ongoing therapeutic strategies, as inhibitors of the TGFβ pathway are currently being used in various clinical trials against patients suffering from advanced or metastatic breast cancer (Buijis et al., 2012; Calone and Souchelnytskyi, 2012).

7. Summary

The Epithelial-Mesenchymal Transition (EMT) is a developmental process, through which epithelial cells transdifferentiate to a mesenchymal and highly migratory state. Beyond its implications in embryogenesis, EMT has been proposed to promote tumor cell dissemination and metastasis. Nevertheless, for the last step of the metastatic cascade, i.e. colonization, cells have to revert to an epithelial state to regain proliferative capacity. The cellular signaling pathways employed by cancer-related EMT programs for regulation of invasion and proliferation have not yet been extensively analyzed. Therefore, the aim of my doctoral thesis was to study the role of developmental signaling pathways, such as TGFβ, Wnt and JNK signaling during both EMT-induction and EMT-maintenance. For the latter approach, I have treated the mesenchymal, triple negative breast cancer (TNBC) cell line MDA-MB-231 with small-molecule inhibitors of the TGFβ, Wnt and JNK signaling pathways. I have found that all these pathways support single-cell migratory abilities of MDA-MB-231 cells, but they are not required for the maintenance of the mesenchymal phenotype. Moreover, treatment of MDA-MB-231 cells with the TGFRI inhibitor A83-01 switched cells from a singly to a collectively invading phenotype in 3D.

In contrast to maintenance of the mesenchymal state, TGFβ signaling was indispensable for induction of EMT in immortalized human mammary epithelial cells (HMLE), mediated by the EMT transcription factor Twist1. Thus, without autocrine TGFβ signaling Twist1 was unable to induce mesenchymal transdifferentiation, while addition of exogenous TGFβ greatly accelerated Twist1-induced EMT. Mechanistically, this was explained by the fact that TGFβ signaling promoted Twist1-occupancy on an enhancer region of the crucial downstream effector for EMT, ZEB1, in a dose-dependent manner. In the absence of TGFβ signaling, Twist1 promoted a distinct, EMT-independent cell-state, characterized by low levels of ZEB1 and maintenance of an epithelial phenotype. On a functional level, cells in this state were able to invade collectively and retained the ability to generate multicellular structures in 3D, whereas mesenchymal cells invaded as single cells and were greatly attenuated in their ability to proliferate in 3D.

In conclusion, this study shows that inhibition of TGFβ signaling in TNBC cells and during Twist1-induced EMT generates collectively invading cells with proliferative capacities. Since collective invasion has been reported to contribute to metastatic

dissemination, inhibition of TGFβ signaling in cancer-related EMT might result in increased metastatic outgrowth. Thus, this study provides novel insights into the signaling context governing tumorigenic invasion and colonization, and cautions against therapeutic approaches using TGFβ inhibitors against EMT-related breast cancer.

8. Bibliography

Aceto N, Bardia A, Miyamoto DT, Donaldson MC, Wittner BS, Spencer JA, Yu M, Pely A, Engstrom A, Zhu H, Brannigan BW, Kapur R, Stott SL, Shioda T, Ramaswamy S, Ting DT, Lin CP, Toner M, Haber DA, Maheswaran S. Circulating tumor cell clusters are oligoclonal precursors of breast cancer metastasis. Cell 2014; 158: 1110-22.

Aceto N, Toner M, Maheswaran S, Haber DA. En Route to Metastasis: Circulating Tumor Cell Clusters and Epithelial-to-Mesenchymal Transition. Trends in Cancer 2015; 1: 44-52.

Acloque H, Adams MS, Fishwick K, Bronner-Fraser M, Nieto MA. Epithelial-mesenchymal transitions: the importance of changing cell state in development and disease. J Clin Invest 2009; 119: 1438-49.

Aigner K, Dampier B, Descovich L, Mikula M, Sultan A, Schreiber M, Mikulits W, Brabletz T, Strand D, Obrist P, Sommergruber W, Schweifer N, Wernitznig A, Beug H, Foisner R, Eger A. Oncogene 2007; 26: 6979-88.

Alcorn JF, Guala AS, van der Velden J, McElhinney B, Irvin CG, Davis RJ, Janssen-Heininger YM. Jun N-terminal kinase 1 regulates epithelial-to-mesenchymal transition induced by TGFβ1. J Cell Sci 2008; 121: 1036-45.

Alves CC, Carneiro F, Hoefler H, Becker KF. Role of the epithelial-mesenchymal transition regulator Slug in primary human cancers. Front Biosci (Landmark Ed) 2009; 14: 3035-50.

Amos KD, Adamo B, Anders CK. Triple-negative breast cancer: an update on neoadjuvant clinical trials. Int J Breast Cancer 2012; 2012: 385978.

Ansieau S, Bastid J, Doreau A, Morel AP, Bouchet BP, Thomas C, Fauvet F, Puisieux I, Doglioni C, Piccinin S, Maestro R, Voeltzel T, Selmi A, Valsesia-Wittmann S, Caron de Fromentel C, Puisieux A. Induction of EMT by twist proteins as a collateral effect of tumor-promoting inactivation of premature senescence. Cancer Cell 2008; 14: 79-89.

Ansieau S. EMT in breast cancer stem cell generation. Cancer Lett 2013; 338: 63-8.

Asiedu MK, Ingle JN, Behrens MD, Radisky DC, Knutson KL. TGFbeta/TNF(alpha)-mediated epithelial-mesenchymal transition generates breast cancer stem cells with a claudin-low phenotype. Cancer Res 2011; 71: 4707-19.

Bachelder RE, Yoon SO, Franci C, de Herreros AG, Mercurio AM. Glycogen synthase kinase-3 is an endogenous inhibitor of Snail transcription: implications for the epithelial-mesenchymal transition. J Cell Bio. 2005; 168: 29-33.

Barrallo-Gimeno A, Nieto MA. The Snail genes as inducers of cell movement and survival: implications in development and cancer. Development 2005; 132: 3151-61.

Bartel DP. MicroRNAs: target recognition and regulatory functions. Cell 2009; 136: 215-33.

Bartis D, Mise N, Mahida RY, Eickelberg O, Thickett DR. Epithelial-mesenchymal transition in lung development and disease: does it exist and is it important? Thorax 2014; 69: 760-5.

Bindels S, Mestdagt M, Vandewalle C, Jacobs N, Volders L, Noël A, van Roy F, Berx G, Foidart JM, Gilles C. Regulation of vimentin by SIP1 in human epithelial breast tumor cells. Oncogene 2006; 25: 4975-85.

Bouquet F, Pal A, Pilones KA, Demaria S, Hann B, Akhurst RJ, Babb JS, Lonning SM, DeWyngaert JK, Formenti SC, Barcellos-Hoff MH. TGFβ1 inhibition increases the radiosensitivity of breast cancer cells in vitro and promotes tumor control by radiation in vivo. Clin Cancer Res 2011; 17: 6754-65.

Boussif O, Lezoualc'h F, Zanta MA, Mergny MD, Scherman D, Demeneix B, Behr JP. A versatile vector for gene and oligonucleotide transfer into cells in culture and in vivo: polyethylenimine. Proc Natl Acad Sci U S A 1995; 92: 7297-301.

Boutet A, De Frutos CA, Maxwell PH, Mayol MJ, Romero J, Nieto MA. Snail activation disrupts tissue homeostasis and induces fibrosis in the adult kidney. EMBO J 2006; 25: 5603-13.

Brabletz T, Jung A, Reu S, Porzner M, Hlubek F, Kunz-Schughart LA, Knuechel R, Kirchner T. Variable beta-catenin expression in colorectal cancers indicates tumor progression driven by the tumor environment. Proc Natl Acad Sci U S A 2001; 98: 10356-61.

Brinkley BR, Beall PT, Wible LJ, Mace ML, Turner DS, Cailleau RM. Variations in cell form and cytoskeleton in human breast carcinoma cells in vitro. Cancer Res 1980; 40: 3118-29.

Buijs JT, Stayrook KR, Guise TA. The role of TGF-β in bone metastasis: novel therapeutic perspectives. Bonekey Rep 2012; 1: 96.

Bukholm IK, Nesland JM, Børresen-Dale AL. Re-expression of E-cadherin, alpha-catenin and beta-catenin, but not of gamma-catenin, in metastatic tissue from breast cancer patients. J Pathol 2000; 190: 15-9.

Burk U, Schubert J, Wellner U, Schmalhofer O, Vincan E, Spaderna S, Brabletz T. A reciprocal repression between ZEB1 and members of the miR-200 family promotes EMT and invasion in cancer cells. EMBO Rep 2008; 9: 582-9.

Calone I, Souchelnytskyi S. Inhibition of TGFβ signaling and its implications in anticancer treatments. Exp Oncol 2012; 34: 9-16.

Carey LA, Perou CM, Livasy CA, Dressler LG, Cowan D, Conway K, Karaca G, Troester MA, Tse CK, Edmiston S, Deming SL, Geradts J, Cheang MC, Nielsen TO, Moorman PG, Earp HS, Millikan RC. Race, breast cancer subtypes, and survival in the Carolina Breast Cancer Study. JAMA 2006; 295: 2492-502.

Carey LA, Dees EC, Sawyer L, Gatti L, Moore DT, Collichio F, Ollila DW, Sartor CI, Graham ML, Perou CM. The triple negative paradox: primary tumor chemosensitivity of breast cancer subtypes. Clin Cancer Res 2007; 13: 2329-34.

Carlsson P, Mahlapuu M. Forkhead transcription factors: key players in development and metabolism. Dev Biol 2002; 250: 1-23.

Carmona-Fontaine C, Matthews HK, Kuriyama S, Moreno M, Dunn GA, Parsons M, Stern CD, Mayor R. Contact inhibition of locomotion in vivo controls neural crest directional migration. Nature 2008; 456: 957-61.

Casas E, Kim J, Bendesky A, Ohno-Machado L, Wolfe C.J, and Yang J. Snail2 is an essential mediator of Twist1-induced epithelial mesenchymal transition and metastasis. Cancer Res 2011; 71: 245-254.

Chang AT, Liu Y, Ayyanathan K, Benner C, Jiang Y, Prokop JW, Paz H, Wang D, Li HR, Fu XD, Rauscher FJ 3rd, Yang J. An evolutionarily conserved DNA architecture determines target specificity of the TWIST family bHLH transcription factors. Genes Dev 2015; 29: 603-16.

Chen B, Dodge ME, Tang W, Lu J, Ma Z, Fan CW, Wei S, Hao W, Kilgore J, Williams NS, Roth MG, Amatruda JF, Chen C, Lum L. Small molecule-mediated disruption of Wnt-dependent signaling in tissue regeneration and cancer. Nat Chem Biol 2009; 5: 100-7.

Chen HH, Zhou XL, Shi YL, Yang J. Roles of p38 MAPK and JNK in TGF-β1-induced human alveolar epithelial to mesenchymal transition. Arch Med Res 2013 Feb; 44: 93-8.

Chen T, Carter D, Garrigue-Antar L, Reiss M. Transforming growth factor beta type I receptor kinase mutant associated with metastatic breast cancer. Cancer Res 1998; 58: 4805-10.

Chen T, Jackson CR, Link A, Markey MP, Colligan BM, Douglass LE, Pemberton JO, Deddens JA, Graff JR, Carter JH. Int7G24A variant of transforming growth factorβ receptor type I is associated with invasive breast cancer. Clin Cancer Res 2006; 12: 392-7.

Chen ZF, Behringer RR. twist is required in head mesenchyme for cranial neural tube morphogenesis. Genes Dev 1995; 9: 686-99.

Cheung KJ, Gabrielson E, Werb Z, Ewald AJ. Collective invasion in breast cancer requires a conserved basal epithelial program. Cell 2013 Dec; 155: 1639-51.

Cheung KJ, Ewald AJ. Illuminating breast cancer invasion: diverse roles for cell-cell interactions. Curr Opin Cell Biol 2014; 30: 99-111.

Cicalese A, Bonizzi G, Pasi CE, Faretta M, Ronzoni S, Giulini B, Brisken C, Minucci S, Di Fiore PP, Pelicci PG. The tumor suppressor p53 regulates polarity of self-renewing divisions in mammary stem cells. Cell 2009; 138: 1083-95.

Comijn J, Berx G, Vermassen P, Verschueren K, van Grunsven L, Bruyneel E, Mareel M, Huylebroeck D, van Roy F. The two-handed E box binding zinc finger protein SIP1 downregulates E-cadherin and induces invasion. Mol Cell 2001; 7: 1267-78.

Cornell RA, Eisen JS. Notch in the pathway: the roles of Notch signaling in neural crest development. Semin Cell Dev Biol 2005; 16: 663-72.

Dang H, Ding W, Emerson D, Rountree CB. Snail1 induces epithelial-to-mesenchymal transition and tumor initiating stem cell characteristics. BMC Cancer 2011; 11: 396.

Dave N, Guaita-Esteruelas S, Gutarra S, Frias À, Beltran M, Peiró S, de Herreros AG. Functional cooperation between Snail1 and twist in the regulation of ZEB1 expression during epithelial to mesenchymal transition. J Biol Chem 2011; 286: 12024-32.

De Craene B, Berx G. Regulatory networks defining EMT during cancer initiation and progression. Nat Rev Cancer 2013; 13:97-110.

Dent R, Trudeau M, Pritchard KI, Hanna WM, Kahn HK, Sawka CA, Lickley LA, Rawlinson E, Sun P, Narod SA. Triple-negative breast cancer: clinical features and patterns of recurrence. Clin Cancer Res 2007; 13: 4429-34.

Derynck R, Akhurst RJ. Differentiation plasticity regulated by TGFβ family proteins in development and disease. Nat Cell Biol 2007; 9: 1000-4.

Derynck R, Zhang YE. Smad-dependent and Smad-independent pathways in TGFβ family signalling. Nature 2003; 425: 577-84.

Dontu G, Abdallah WM, Foley JM, Jackson KW, Clarke MF, Kawamura MJ, Wicha MS. In vitro propagation and transcriptional profiling of human mammary stem/progenitor cells. Genes Dev 2003; 17: 1253-70.

Du C, Zhang C, Hassan S, Biswas MH, Balaji KC. Protein kinase D1 suppresses epithelial-to-mesenchymal transition through phosphorylation of snail. Cancer Res 2010; 70: 7810-9.

Dumont N, Bakin AV, Arteaga CL. Autocrine transforming growth factorβ signaling mediates Smad-independent motility in human cancer cells. J Biol Chem 2003; 278: 3275-85.

Early Breast Cancer Trialists' Collaborative Group. Tamoxifen for early breast cancer: an overview of the randomised trials. Lancet 1998; 351: 1451-67.

Eckert MA, Lwin TM, Chang AT, Kim J, Danis E, Ohno-Machado L, Yang J. Twist1-induced invadopodia formation promotes tumor metastasis. Cancer Cell 2011; 19: 372-86.

Eger A, Aigner K, Sonderegger S, Dampier B, Oehler S, Schreiber M, Berx G, Cano A, Beug H, Foisner R. DeltaEF1 is a transcriptional repressor of E-cadherin and

regulates epithelial plasticity in breast cancer cells. Oncogene 2005; 24: 2375-85.

Eilken HM, Nishikawa S-I, Schroeder T. Continuous single-cell imaging of blood generation from haemogenic endothelium. Nature 2009; 457: 896-900.

Elenbaas B, Spirio L, Koerner F, Fleming M.D, Zimonjic D.B, Donaher J.L, Popescu N.C, Hahn W.C, and Weinberg R.A. Human breast cancer cells generated by oncogenic transformation of primary mammary epithelial cells. Genes Dev 2001; 15: 50-65.

el Ghouzzi V, Le Merrer M, Perrin-Schmitt F, Lajeunie E, Benit P, Renier D, Bourgeois P, Bolcato-Bellemin AL, Munnich A, Bonaventure J. Mutations of the TWIST gene in the Saethre-Chotzen syndrome. Nat Genet 1997; 15: 42-6.

Fillmore CM, Kuperwasser C. Human breast cancer cell lines contain stem-like cells that self-renew, give rise to phenotypically diverse progeny and survive chemotherapy. Breast Cancer Res 2008; 10: R25.

Fowler T, Sen R, Roy AL. Regulation of primary response genes. Mol Cell 2011; 44: 348-60.

Fukagawa A, Ishii H, Miyazawa K, Saitoh M. δEF1 associates with DNMT1 and maintains DNA methylation of the E-cadherin promoter in breast cancer cells. Cancer Med 2015; 4: 125-35.

García-Castro MI, Marcelle C, Bronner-Fraser M. Ectodermal Wnt function as a neural crest inducer. Science 2002; 297: 848-51.

Geyer FC, Lacroix-Triki M, Savage K, Arnedos M, Lambros MB, MacKay A, Natrajan R, Reis-Filho JS. β-Catenin pathway activation in breast cancer is associated with triple-negative phenotype but not with CTNNB1 mutation. Mod Pathol 2011 Feb; 24: 209-31.

Giampieri S, Manning C, Hooper S, Jones L, Hill CS, Sahai E. Localized and reversible TGFbeta signalling switches breast cancer cells from cohesive to single-cell motility. Nat Cell Biol 2009; 11: 1287-96.

Giard DJ, Aaronson SA, Todaro GJ, Arnstein P, Kersey JH, Dosik H, Parks WP. In vitro cultivation of human tumors: establishment of cell lines derived from a series of solid tumors. J Natl Cancer Inst 1973; 51: 1417-23.

Gonzalez DM, Medici D. Signaling mechanisms of the epithelial-mesenchymal transition. Sci Signal 2014; 7: re8.

Gonzalez-Moreno O, Lecanda J, Green JE, Segura V, Catena R, Serrano D, Calvo A. VEGF elicits epithelial-mesenchymal transition (EMT) in prostate intraepithelial neoplasia (PIN)-like cells via an autocrine loop. Exp Cell Res 2010 ; 316: 554-67.

Gradl D, Kühl M, Wedlich D. The Wnt/Wg signal transducer beta-catenin controls fibronectin expression. Mol Cell Biol 1999; 19: 5576-87.

Graessel A, Hauck SM, von Toerne C, Kloppmann E, Goldberg T, Koppensteiner H, Schindler M, Knapp B, Krause L, Dietz K, Schmidt-Weber CB, Suttner K. A Combined Omics Approach to Generate the Surface Atlas of Human Naive CD4+ T Cells during Early T-Cell Receptor Activation. Mol Cell Proteomics 2015; 14: 2085-2102.

Gras B, Jacqueroud L, Wierinckx A, Lamblot C, Fauvet F, Lachuer J, Puisieux A, Ansieau S. Snail family members unequally trigger EMT and thereby differ in their ability to promote the neoplastic transformation of mammary epithelial cells. PLoS One 2014; 9: e92254.

Gregory PA, Bracken CP, Smith E, Bert AG, Wright JA, Roslan S, Morris M, Wyatt L, Farshid G, Lim YY, Lindeman GJ, Shannon MF, Drew PA, Khew-Goodall Y, Goodall GJ. An autocrine TGFβ/ZEB/miR-200 signaling network regulates establishment and maintenance of epithelial-mesenchymal transition. Mol Biol Cell 2011; 22: 1686-98.

Guaita S, Puig I, Franci C, Garrido M, Dominguez D, Batlle E, Sancho E, Dedhar S, De Herreros AG, Baulida J. Snail induction of epithelial to mesenchymal transition in tumor cells is accompanied by MUC1 repression and ZEB1 expression. J Biol Chem 2002 Oct; 277: 39209-16.

Gujral TS, Chan M, Peshkin L, Sorger PK, Kirschner MW, MacBeath G. A noncanonical Frizzled2 pathway regulates epithelial-mesenchymal transition and metastasis. Cell 2014; 159: 844-56.

Habas R, Dawid IB. Dishevelled and Wnt signaling: is the nucleus the final frontier? J Biol 2005; 4: 2.

Han XY, Wei B, Fang JF, Zhang S, Zhang FC, Zhang HB, Lan TY, Lu HQ, Wei HB. Epithelial-mesenchymal transition associates with maintenance of stemness in spheroid-derived stem-like colon cancer cells. PLoS One 2013; 8: e73341.

Hartwell KA, Muir B, Reinhardt F, Carpenter AE, Sgroi DC, Weinberg RA. The Spemann organizer gene, Goosecoid, promotes tumor metastasis. Proc Natl Acad Sci U S A 2006; 103: 18969-74.

Hauck SM, Dietter J, Kramer RL, Hofmaier F, Zipplies JK, Amann B, Feuchtinger A, Deeg CA, Ueffing M. Deciphering membrane-associated molecular processes in target tissue of autoimmune uveitis by label-free quantitative mass spectrometry. Mol Cell Proteomics 2010; 9: 2292-305.

Hay ED. Organization and fine structure of epithelium and mesenchyme in the developing chick embryos. In *Epithelial-Mesenchymal Interactions: 18th Hahnemann Symposium* 1968; ed. R Fleischmajer, RE Billingham, pp. 31-35. Baltimore: Williams&Wilkins.

Hay ED. Collagen and other matrix glycoproteins in embryogenesis. In *Cell Biology of Extracellular Matrix* 1991; ed. ED Hay, pp. 419-62. New York: Plenum.

Hay ED, Zuk A. Transformations between epithelium and mesenchyme: normal, pathological, and experimentally induced. Am J Kidney Dis 1995; 26: 678-90.

Hayashi M, Nimura K, Kashiwagi K, Harada T, Takaoka K, Kato H, Tamai K, Kaneda Y. Comparative roles of Twist-1 and Id1 in transcriptional regulation by BMP signaling. J Cell Sci 2007; 120: 1350-7.

Hemavathy K, Guru SC, Harris J, Chen JD, Ip YT. Human Slug is a repressor that localizes to sites of active transcription. Mol Cell Biol 2000; 20: 5087-95.

Herschkowitz JI, Simin K, Weigman VJ, Mikaelian I, Usary J, Hu Z, Rasmussen KE, Jones LP, Assefnia S, Chandrasekharan S, Backlund MG, Yin Y, Khramtsov AI, Bastein R, Quackenbush J, Glazer RI, Brown PH, Green JE, Kopelovich L, Furth PA, Palazzo JP, Olopade OI, Bernard PS, Churchill GA, Van Dyke T, Perou CM. Identification of conserved gene expression features between murine mammary carcinoma models and human breast tumors. Genome Biol 2007; 8: R76.

Hocevar BA, Brown TL, Howe PH. TGFβ induces fibronectin synthesis through a c-Jun N-terminal kinase-dependent, Smad4-independent pathway. EMBO J 1999; 18: 1345-56.

Hong J, Zhou J, Fu J, He T, Qin J, Wang L, Liao L, Xu J. Phosphorylation of serine 68 of Twist1 by MAPKs stabilizes Twist1 protein and promotes breast cancer cell invasiveness. Cancer Res 2011; 71: 3980-90.

Howard TD, Paznekas WA, Green ED, Chiang LC, Ma N, Ortiz de Luna RI, Garcia Delgado C, Gonzalez-Ramos M, Kline AD, Jabs EW. Mutations in TWIST, a basic helix-loop-helix transcription factor, in Saethre-Chotzen syndrome. Nat Genet 1997; 15: 36-41.

Howe LR, Watanabe O, Leonard J, Brown AM. Twist is up-regulated in response to Wnt1 and inhibits mouse mammary cell differentiation. Cancer Res 2003; 63: 1906-13.

Huang SM, Mishina YM, Liu S, Cheung A, Stegmeier F, Michaud GA, Charlat O, Wiellette E, Zhang Y, Wiessner S et al. Tankyrase inhibition stabilizes axin and antagonizes Wnt signalling. Nature 2009; 461: 614-20.

Ip YT, Park RE, Kosman D, Yazdanbakhsh K, Levine M. dorsal-twist interactions establish snail expression in the presumptive mesoderm of the Drosophila embryo. Genes Dev 1992; 6: 1518-30.

Iwano M, Plieth D, Danoff TM, Xue C, Okada H, Neilson EG. Evidence that fibroblasts derive from epithelium during tissue fibrosis. J Clin Invest 2002; 110: 341-50.

Jamora C, DasGupta R, Kocieniewski P, Fuchs E. Links between signal transduction, transcription and adhesion in epithelial bud development. Nature 2003; 422:317-22.

Jeong H, Ryu YJ, An J, Lee Y, Kim A. Epithelial-mesenchymal transition in breast cancer correlates with high histological grade and triple-negative phenotype. Histopathology 2012; 60: E87-95.

Jordà M, Olmeda D, Vinyals A, Valero E, Cubillo E, Llorens A, Cano A, Fabra A. Upregulation of MMP-9 in MDCK epithelial cell line in response to expression of the Snail transcription factor. J Cell Sci 2005; 118: 3371-85.

Kalluri R, Weinberg RA. The basics of epithelial-mesenchymal transition. J Clin Invest 2009; 119: 1420-8.

Kang Y, Chen CR, Massagué J. A self-enabling TGFbeta response coupled to stress signaling: Smad engages stress response factor ATF3 for Id1 repression in epithelial cells. Mol Cell 2003; 11: 915-26.

Kasid A, Lippman ME, Papageorge AG, Lowy DR, Gelmann EP. Transfection of v-rasH DNA into MCF-7 human breast cancer cells bypasses dependence on estrogen for tumorigenicity. Science 1985; 228: 725-8.

Kenny PA, Lee GY, Myers CA, Neve RM, Semeiks JR, Spellman PT, Lorenz K, Lee EH, Barcellos-Hoff MH, Petersen OW, Gray JW, Bissell MJ. The morphologies of breast cancer cell lines in three-dimensional assays correlate with their profiles of gene expression. Mol Oncol 2007; 1: 84-96.

Khew-Goodall Y, Wadham C. A perspective on regulation of cell-cell adhesion and epithelial-mesenchymal transition: known and novel. Cells Tissues Organs 2005; 179: 81-6.

Khramtsov AI, Khramtsova GF, Tretiakova M, Huo D, Olopade OI, Goss KH. Wnt/beta-catenin pathway activation is enriched in basal-like breast cancers and predicts poor outcome. Am J Pathol 2010; 176: 2911-20.

Kim SJ, Jeang KT, Glick AB, Sporn MB, Roberts AB. Promoter sequences of the human transforming growth factorβ 1 gene responsive to transforming growth factorβ 1 autoinduction. J Biol Chem 1989; 264: 7041-5.

Kim S, Lee J, Jeon M, Nam SJ, Lee JE. Elevated TGF-β1 and -β2 expression accelerates the epithelial to mesenchymal transition in triple-negative breast cancer cells. Cytokine 2015; 75: 151-8.

Klenova E, Chernukhin I, Inoue T, Shamsuddin S, Norton J. Immunoprecipitation techniques for the analysis of transcription factor complexes. Methods 2002; 26: 254-9.

Kondo M, Cubillo E, Tobiume K, Shirakihara T, Fukuda N, Suzuki H, Shimizu K, Takehara K, Cano A, Saitoh M, Miyazono K. A role for Id in the regulation of TGFβ-induced epithelial-mesenchymal transdifferentiation. Cell Death Differ 2004; 11: 1092-101.

Korpal M, Lee ES, Hu G, Kang Y. The miR-200 family inhibits epithelial-mesenchymal transition and cancer cell migration by direct targeting of E-cadherin transcriptional repressors ZEB1 and ZEB2. J Biol Chem 2008; 283: 14910-4.

Kowalski PJ, Rubin MA, Kleer CG. E-cadherin expression in primary carcinomas of the breast and its distant metastases. Breast Cancer Res 2003; 5: R217-22.

Kuch V, Schreiber C, Thiele W, Umansky V, Sleeman JP. Tumor-initiating properties of breast cancer and melanoma cells in vivo are not invariably reflected by spheroid formation in vitro, but can be increased by long-term culturing as adherent monolayers. Int J Cancer 2013; 132: E94-105.

Kühl M. Non-canonical Wnt signaling in Xenopus: regulation of axis formation and gastrulation. Semin Cell Dev Biol 2002; 13: 243-9.

Lamouille S, Subramanyam D, Blelloch R, Derynck R. Regulation of epithelial-mesenchymal and mesenchymal-epithelial transitions by microRNAs. Curr Opin Cell Biol 2013; 25: 200-7.

Lamouille S, Xu J, Derynck R. Molecular mechanisms of epithelial-mesenchymal transition. Nat Rev Mol Cell Biol 2014; 15: 178-96.

Laursen KB, Mielke E, Iannaccone P, Fuchtbauer EM. Mechanism of transcriptional activation by the proto-oncogene Twist1. J Biol Chem 2007; 282: 34623-34633.

LeBleu VS, O'Connell JT, Gonzalez Herrera KN, Wikman H, Pantel K, Haigis MC, de Carvalho FM, Damascena A, Domingos Chinen LT, Rocha RM, Asara JM, Kalluri R. PGC-1α mediates mitochondrial biogenesis and oxidative phosphorylation in cancer cells to promote metastasis. Nat Cell Biol 2014; 16: 992-1003.

Le Du F, Eckhardt BL, Lim B, Litton JK, Moulder S, Meric-Bernstam F, Gonzalez-Angulo AM, Ueno NT. Is the future of personalized therapy in triple-negative breast cancer based on molecular subtype? Oncotarget 2015; 6: 12890-908.

Liedtke C, Mazouni C, Hess KR, André F, Tordai A, Mejia JA, Symmans WF, Gonzalez-Angulo AM, Hennessy B, Green M, Cristofanilli M, Hortobagyi GN, Pusztai L. Response to neoadjuvant therapy and long-term survival in patients with triple-negative breast cancer. J Clin Oncol 2008; 26: 1275-81.

Liu J, Pan S, Hsieh MH, Ng N et al. Targeting Wnt-driven cancer through the inhibition of Porcupine by LGK974. Proc Natl Acad Sci U S A 2013; 110: 20224-9.

Liu L, Chen X2, Wang Y1, Qu Z1, Lu Q3, Zhao J3, Yan X3, Zhang H1, Zhou Y3. Notch3 is important for TGF-β-induced epithelial-mesenchymal transition in non-small cell lung cancer bone metastasis by regulating ZEB-1. Cancer Gene Ther 2014; 21: 364-72.

Liu P, Wakamiya M, Shea MJ, Albrecht U, Behringer RR, Bradley A. Requirement for Wnt3 in vertebrate axis formation. Nat Genet 1999; 22: 361-5.

Liu YN, Yin JJ, Abou-Kheir W, Hynes PG, Casey OM, Fang L, Yi M, Stephens RM, Seng V, Sheppard-Tillman H, Martin P, Kelly K. MiR-1 and miR-200 inhibit EMT via Slug-dependent and tumorigenesis via Slug-independent mechanisms. Oncogene 2013; 32: 296-306.

Lo HW, Hsu SC, Xia W, Cao X, Shih JY, Wei Y, Abbruzzese JL, Hortobagyi GN, Hung MC. Epidermal growth factor receptor cooperates with signal transducer

and activator of transcription 3 to induce epithelial-mesenchymal transition in cancer cells via up-regulation of TWIST gene expression. Cancer Res 2007 ; 67: 9066-76.

Long J, Zuo D, Park M. Pc2-mediated sumoylation of Smad-interacting protein 1 attenuates transcriptional repression of E-cadherin. J Biol Chem 2005; 280: 35477-89.

Lowry OH, Rosebrough NJ, Farr AL, Randall RJ. Protein measurement with the Folin phenol reagent. J Biol Chem 1951; 193: 265-75.

Lu Z, Ghosh S, Wang Z, Hunter T. Downregulation of caveolin-1 function by EGF leads to the loss of E-cadherin, increased transcriptional activity of beta-catenin, and enhanced tumor cell invasion. Cancer Cell 2003; 4: 499-515.

Luwor RB, Hakmana D, Iaria J, Nheu TV, Simpson RJ, Zhu HJ. Single live cell TGF-β signalling imaging: breast cancer cell motility and migration is driven by sub-populations of cells with dynamic TGF-β-Smad3 activity. Mol Cancer 2015; 14: 50.

Ma L, Teruya-Feldstein J, Weinberg RA. Tumour invasion and metastasis initiated by microRNA-10b in breast cancer. Nature. 2007; 449: 682-8.

Mani SA, Yang J, Brooks M, Schwaninger G, Zhou A, Miura N, Kutok JL, Hartwell K, Richardson AL, Weinberg RA. Mesenchyme Forkhead 1 (FOXC2) plays a key role in metastasis and is associated with aggressive basal-like breast cancers. Proc Natl Acad Sci U S A 2007; 104: 10069-74.

Marchini C, Montani M, Konstantinidou G, Orrù R, Mannucci S, Ramadori G, Gabrielli F, Baruzzi A, Berton G, Merigo F, Fin S, Iezzi M, Bisaro B, Sbarbati A, Zerani M, Galiè M, Amici A. Mesenchymal/stromal gene expression signature relates to basal-like breast cancers, identifies bone metastasis and predicts resistance to therapies. PLoS One 2010; 5: e14131.

Massagué J. TGFbeta in Cancer. Cell 2008; 134: 215-30.

Massari ME, Murre C. Helix-loop-helix proteins: regulators of transcription in eucaryotic organisms. Mol Cell Biol 2000; 20: 429-40.

Mauri D, Pavlidis N, Polyzos NP, Ioannidis JP. Survival with aromatase inhibitors and inactivators versus standard hormonal therapy in advanced breast cancer: meta-analysis. J Natl Cancer Inst 2006; 98: 1285-91.

Meijer L, Skaltsounis AL, Magiatis P, Polychronopoulos P, Knockaert M, Leost M, Ryan XP, Vonica CA, Brivanlou A, Dajani R, Crovace C, Tarricone C, Musacchio A, Roe SM, Pearl L, Greengard P. GSK-3-selective inhibitors derived from Tyrian purple indirubins. Chem Biol 2003; 10: 1255-66.

Mercado-Pimentel ME, Hubbard AD, Runyan RB. Endoglin and Alk5 regulate epithelial-mesenchymal transformation during cardiac valve formation. Dev Biol 2007; 304: 420-32.

Meylan E, Tschopp J. The RIP kinases: crucial integrators of cellular stress. Trends Biochem Sci 2005; 30: 151-9.

Miettinen PJ, Ebner R, Lopez AR, Derynck R. TGFβ-induced transdifferentiation of mammary epithelial cells to mesenchymal cells: involvement of type I receptors. J Cell Biol 1994; 127: 2021-2036.

Miller DG, Adam MA, Miller AD. Gene transfer by retrovirus vectors occurs only in cells that are actively replicating at the time of infection. Mol Cell Biol 1990; 10: 4239-42.

Moes M, Le Béchec A, Crespo I, Laurini C, Halavatyi A, Vetter G, Del Sol A, Friederich E. A novel network integrating a miRNA-203/SNAI1 feedback loop which regulates epithelial to mesenchymal transition. PLoS One 2012; 7: e35440.

Molyneux G, Geyer FC, Magnay FA, McCarthy A, Kendrick H, Natrajan R, Mackay A, Grigoriadis A, Tutt A, Ashworth A, Reis-Filho JS, Smalley MJ. BRCA1 basal-like breast cancers originate from luminal epithelial progenitors and not from basal stem cells. Cell Stem Cell 2010; 7: 403-17.

Moody SE, Perez D, Pan TC, Sarkisian CJ, Portocarrero CP, Sterner CJ, Notorfrancesco KL, Cardiff RD, Chodosh LA. The transcriptional repressor Snail promotes mammary tumor recurrence. Cancer Cell 2005;8: 197-209.

Morel AP, Hinkal GW, Thomas C, Fauvet F, Courtois-Cox S, Wierinckx A, Devouassoux-Shisheboran M, Treilleux I, Tissier A, Gras B, Pourchet J, Puisieux I, Browne GJ, Spicer DB, Lachuer J, Ansieau S, Puisieux A. EMT inducers catalyze malignant transformation of mammary epithelial cells and drive tumorigenesis towards claudin-low tumors in transgenic mice. PLoS Genet 2012; 8: e1002723.

Moreno-Bueno G, Cubillo E, Sarrió D, Peinado H, Rodríguez-Pinilla SM, Villa S, Bolós V, Jordá M, Fabra A, Portillo F, Palacios J, Cano A. Genetic profiling of epithelial cells expressing E-cadherin repressors reveals a distinct role for Snail, Slug, and E47 factors in epithelial-mesenchymal transition. Cancer Res 2006; 66: 9543-56.

Morita T, Mayanagi T, Sobue K. Dual roles of myocardin-related transcription factors in epithelial mesenchymal transition via slug induction and actin remodeling. J Cell Biol 2007; 179: 1027-42.

Moustakas A, Heldin CH. Non-Smad TGFβ signals. J Cell Sci 2005; 118: 3573-84.

Nagarajan S, Hossan T, Alawi M, Najafova Z, Indenbirken D, Bedi U, Taipaleenmäki H, Ben-Batalla I, Scheller M, Loges S, Knapp S, Hesse E, Chiang CM, Grundhoff A, Johnsen SA. Bromodomain protein BRD4 is required for estrogen receptor-dependent enhancer activation and gene transcription. Cell Rep 2014; 8: 460-9.

Nahta R, Yu D, Hung MC, Hortobagyi GN, Esteva FJ. Mechanisms of disease: understanding resistance to HER2-targeted therapy in human breast cancer. Nat Clin Pract Oncol 2006; 3: 269-80.

Nawshad A, Medici D, Liu CC, Hay ED. TGFbeta3 inhibits E-cadherin gene expression in palate medial-edge epithelial cells through a Smad2-Smad4-LEF1 transcription complex. J Cell Sci. 2007; 120: 1646-53.

Nelson WJ, Nusse R. Convergence of Wnt, beta-catenin, and cadherin pathways. Science. 2004; 303: 1483-7.

Niessen K, Fu Y, Chang L, Hoodless PA, McFadden D, Karsan A. Slug is a direct Notch target required for initiation of cardiac cushion cellularization. J Cell Biol 2008; 182: 315-25.

Nieto MA, Sargent MG, Wilkinson DG, Cooke J. Control of cell behavior during vertebrate development by Slug, a zinc finger gene. Science 1994; 264: 835-9.

Nieto MA. The snail superfamily of zinc-finger transcription factors. Nat Rev Mol Cell Biol 2002; 3: 155-66.

Nieto MA. The Ins and Outs of the Epithelial to Mesenchymal Transition in Health and Disease. Annu Rev Cell Dev Biol 2011; 27: 347-76.

Nieto MA. Epithelial plasticity: a common theme in embryonic and cancer cells. Science 2013; 342: 1234850.

Ning Q, Liu C, Hou L, Meng M, Zhang X, Luo M, Shao S, Zuo X, Zhao X. Vascular endothelial growth factor receptor-1 activation promotes migration and invasion of breast cancer cells through epithelial-mesenchymal transition. PLoS One 2013; 8: e65217.

Nishimura G, Manabe I, Tsushima K, Fujiu K, Oishi Y, Imai Y, Maemura K, Miyagishi M, Higashi Y, Kondoh H, Nagai R. DeltaEF1 mediates TGFβ signaling in vascular smooth muscle cell differentiation. Dev Cell. 2006; 11: 93-104.

Nishita M, Hashimoto MK, Ogata S, Laurent MN, Ueno N, Shibuya H, Cho KW. Interaction between Wnt and TGFβ signalling pathways during formation of Spemann's organizer. Nature 2000; 403: 781-5.

Norton JD. ID helix-loop-helix proteins in cell growth, differentiation and tumorigenesis. J Cell Sci 2000; 113: 3897-905.

Ocaña OH, Córcoles R, Fabra A, Moreno-Bueno G, Acloque H, Vega S, Barrallo-Gimeno A, Cano A, Nieto MA. Metastatic colonization requires the repression of the epithelial-mesenchymal transition inducer Prrx1. Cancer Cell 2012 ; 22: 709-24.

O'Connor JW, Gomez EW. Biomechanics of TGFβ-induced epithelial-mesenchymal transition: implications for fibrosis and cancer. Clin Transl Med 2014; 3: 23.

Oft M, Heider KH, Beug H. TGFbeta signaling is necessary for carcinoma cell invasiveness and metastasis. Curr Biol 1998; 8: 1243-52.

Ohba S, Hirose Y, Kawase T, Sano H. Inhibition of c-Jun N-terminal kinase enhances temozolomide-induced cytotoxicity in human glioma cells. J Neurooncol 2009; 95: 307-16.

Parise CA, Caggiano V. Breast Cancer Survival Defined by the ER/PR/HER2 Subtypes and a Surrogate Classification according to Tumor Grade and Immunohistochemical Biomarkers. J Cancer Epidemiol 2014; 2014: 469251.

Park SM, Gaur AB, Lengyel E, Peter ME. The miR-200 family determines the epithelial phenotype of cancer cells by targeting the E-cadherin repressors ZEB1 and ZEB2. Genes Dev 2008; 22: 894-907.

Pastrana E, Silva-Vargas V, Doetsch F. Eyes wide open: a critical review of sphere-formation as an assay for stem cells. Cell Stem Cell 2011; 8: 486-98.

Peinado H, Ballestar E, Esteller M, Cano A. Snail mediates E-cadherin repression by the recruitment of the Sin3A/histone deacetylase 1 (HDAC1)/HDAC2 complex. Mol Cell Biol 2004; 24: 306-19.

Peinado H, Del Carmen Iglesias-de la Cruz M, Olmeda D, Csiszar K, Fong KS, Vega S, Nieto MA, Cano A, Portillo F. A molecular role for lysyl oxidase-like 2 enzyme in snail regulation and tumor progression. EMBO J 2005; 24: 3446-58.

Peinado H, Olmeda D, Cano A. Snail, Zeb and bHLH factors in tumour progression: an alliance against the epithelial phenotype? Nat Rev Cancer 2007; 7: 415-28.

Perdigão-Henriques R, Petrocca F, Altschuler G, Thomas MP, Le MT, Tan SM, Hide W, Lieberman J. miR-200 promotes the mesenchymal to epithelial transition by suppressing multiple members of the Zeb2 and Snail1 transcriptional repressor complexes. Oncogene 2015. [Epub ahead of print]

Perez EA, Romond EH, Suman VJ, Jeong JH, Sledge G, Geyer CE Jr, Martino S, Rastogi P, Gralow J, Swain SM, Winer EP, Colon-Otero G, Davidson NE, Mamounas E, Zujewski JA, Wolmark N. Trastuzumab plus adjuvant chemotherapy for human epidermal growth factor receptor 2-positive breast cancer: planned joint analysis of overall survival from NSABP B-31 and NCCTG N9831. J Clin Oncol 2014; 32: 3744-52.

Perez-Moreno MA, Locascio A, Rodrigo I, Dhondt G, Portillo F, Nieto MA, Cano A. A new role for E12/E47 in the repression of E-cadherin expression and epithelial-mesenchymal transitions. J Biol Chem 2001; 276: 27424-31.

Perou CM, Sørlie T, Eisen MB, van de Rijn M, Jeffrey SS, Rees CA, Pollack JR, Ross DT, Johnsen H, Akslen LA, Fluge O, Pergamenschikov A, Williams C, Zhu SX, Lønning PE, Børresen-Dale AL, Brown PO, Botstein D. Molecular portraits of human breast tumours. Nature 2000; 406: 747-52.

Piccart-Gebhart MJ, Procter M, Leyland-Jones B, Goldhirsch A et al. Trastuzumab after adjuvant chemotherapy in HER2-positive breast cancer. N Engl J Med 2005; 353: 1659-72.

Piek E, Moustakas A, Kurisaki A, Heldin CH, ten Dijke P. TGF-(beta) type I receptor/ALK-5 and Smad proteins mediate epithelial to mesenchymal transdifferentiation in NMuMG breast epithelial cells. J Cell Sci 1999 ; 112: 4557-68.

Podo F, Buydens LM, Degani H, Hilhorst R, Klipp E, Gribbestad IS, Van Huffel S, van Laarhoven HW, Luts J, Monleon D, Postma GJ, Schneiderhan-Marra N, Santoro F, Wouters H, Russnes HG, Sørlie T, Tagliabue E, Børresen-Dale AL; FEMME Consortium. Triple-negative breast cancer: present challenges and new perspectives. Mol Oncol 2010; 4: 209-29.

Polyak K, Weinberg RA. Transitions between epithelial and mesenchymal states: acquisition of malignant and stem cell traits. Nat Rev Cancer 2009; 9: 265-73.

Ponti D, Costa A, Zaffaroni N, Pratesi G, Petrangolini G, Coradini D, Pilotti S, Pierotti MA, Daidone MG. Isolation and in vitro propagation of tumorigenic breast cancer cells with stem/progenitor cell properties. Cancer Res 2005; 65: 5506-11.

Portella G, Cumming SA, Liddell J, Cui W, Ireland H, Akhurst RJ, Balmain A. Transforming growth factor beta is essential for spindle cell conversion of mouse skin carcinoma in vivo: implications for tumor invasion. Cell Growth Differ 1998; 9: 393-404.

Postigo AA. Opposing functions of ZEB proteins in the regulation of the TGFbeta/BMP signaling pathway. EMBO J 2003; 22: 2443-52.

Postigo AA, Depp JL, Taylor JJ, Kroll KL. Regulation of Smad signaling through a differential recruitment of coactivators and corepressors by ZEB proteins. EMBO J. 2003; 22: 2453-62.

Potenta S, Zeisberg E, Kalluri R. The role of endothelial-to-mesenchymal transition in cancer progression. Br J Cancer 2008; 99: 1375-9.

Prall F. Tumour budding in colorectal carcinoma. Histopathology 2007; 50: 151-62.

Prat A, Parker JS, Karginova O, Fan C, Livasy C, Herschkowitz JI, He X, Perou CM. Phenotypic and molecular characterization of the claudin-low intrinsic subtype of breast cancer. Breast Cancer Res 2010;12: R68.

Prat A, Perou CM. Deconstructing the molecular portraits of breast cancer. Mol Oncol 2011; 5: 5-23.

Prat A, Karginova O, Parker JS, Fan C, He X, Bixby L, Harrell JC, Roman E, Adamo B, Troester M, Perou CM. Characterization of cell lines derived from breast cancers and normal mammary tissues for the study of the intrinsic molecular subtypes. Breast Cancer Res Treat 2013; 142: 237-55.

Prenzel T, Begus-Nahrmann Y, Kramer F, Hennion M, Hsu C, Gorsler T, Hintermair C, Eick D, Kremmer E, Simons M, Beissbarth T, Johnsen SA. Estrogen-dependent gene transcription in human breast cancer cells relies upon

proteasome-dependent monoubiquitination of histone H2B. Cancer Res 2011; 71: 5739-53.

Qi L, Sun B, Liu Z, Li H, Gao J, Leng X. Dickkopf-1 inhibits epithelial-mesenchymal transition of colon cancer cells and contributes to colon cancer suppression. Cancer Sci 2012; 103: 828-35.

Qin L, Yin YT, Zheng FJ, Peng LX, Yang CF, Bao YN, Liang YY, Li XJ, Xiang YQ, Sun R, Li AH, Zou RH, Pei XQ, Huang BJ, Kang TB, Liao DF, Zeng YX, Williams BO, Qian CN. WNT5A promotes stemness characteristics in nasopharyngeal carcinoma cells leading to metastasis and tumorigenesis. Oncotarget 2015; 6: 10239-52.

Qin Q, Xu Y, He T, Qin C, Xu J. Normal and disease-related biological functions of Twist1 and underlying molecular mechanisms. Cell Res 2012; 22: 90-106.

Rota LM, Lazzarino DA, Ziegler AN, LeRoith D, Wood TL. Determining mammosphere-forming potential: application of the limiting dilution analysis. J Mammary Gland Biol Neoplasia 2012; 17: 119-23.

Remacle JE, Kraft H, Lerchner W, Wuytens G, Collart C, Verschueren K, Smith JC, Huylebroeck D. New mode of DNA binding of multi-zinc finger transcription factors: deltaEF1 family members bind with two hands to two target sites. EMBO J 1999; 18: 5073-84.

Rieger MA, Hoppe PS, Smejkal BM, Eitelhuber AC, Schroeder T. Hematopoietic cytokines can instruct lineage choice. Science 2009; 325: 217-218.

Ru P, Steele R, Newhall P, Phillips NJ, Toth K, Ray RB. miRNA-29b suppresses prostate cancer metastasis by regulating epithelial-mesenchymal transition signaling. Mol Cancer Ther 2012; 11: 1166-73.

Sahu SK, Garding A, Tiwari N, Thakurela S, Toedling J, Gebhard S, Ortega F, Schmarowski N, Berninger B, Nitsch R, Schmidt M, Tiwari VK. JNK-dependent gene regulatory circuitry governs mesenchymal fate. EMBO J 2015 [Epub ahead of print]

Sánchez-Tilló E, Lázaro A, Torrent R, Cuatrecasas M, Vaquero EC, Castells A, Engel P, Postigo A. ZEB1 represses E-cadherin and induces an EMT by recruiting the SWI/SNF chromatin-remodeling protein BRG1. Oncogene 2010 ; 29: 3490-500.

Santibañez JF. JNK mediates TGFβ1-induced epithelial mesenchymal transdifferentiation of mouse transformed keratinocytes. FEBS Lett 2006; 580: 5385-91.

Sarrió D, Rodriguez-Pinilla SM, Hardisson D, Cano A, Moreno-Bueno G, Palacios J. Epithelial-mesenchymal transition in breast cancer relates to the basal-like phenotype. Cancer Res 2008; 68: 989-97.

Savagner P. The epithelial-mesenchymal transition (EMT) phenomenon. Ann Oncol 2010;21 Suppl 7: vii89-92.

Scheel C, Eaton EN, Li SH, Chaffer CL, Reinhardt F, Kah KJ, Bell G, Guo W, Rubin J, Richardson AL, Weinberg RA. Paracrine and autocrine signals induce and maintain mesenchymal and stem cell states in the breast. Cell 2011; 145: 926-40.

Schmidt JM, Panzilius E, Bartsch HS, Irmler M, Beckers J, Kari V, Linnemann JR, Dragoi D, Hirschi B, Kloos UJ et al. Stem-cell-like properties and epithelial plasticity arise as stable traits after transient Twist1 activation. Cell Rep 2015; 10: 131-9.

Schmittgen TD, Livak KJ. Analyzing real-time PCR data by the comparative C(T) method. Nat Protoc 2008; 3: 1101-8.

Sethi S, Sarkar FH, Ahmed Q, Bandyopadhyay S, Nahleh ZA, Semaan A, Sakr W, Munkarah A, Ali-Fehmi R. Molecular markers of epithelial-to-mesenchymal transition are associated with tumor aggressiveness in breast carcinoma. Transl Oncol 2011; 4: 222-6.

Shamir ER, Pappalardo E, Jorgens DM, Coutinho K, Tsai WT, Aziz K, Auer M, Tran PT, Bader JS, Ewald AJ. Twist1-induced dissemination preserves epithelial identity and requires E-cadherin. J Cell Biol 2014; 204: 839-56.

Shao S, Zhao X, Zhang X, Luo M, Zuo X, Huang S, Wang Y, Gu S, Zhao X. Notch1 signaling regulates the epithelial-mesenchymal transition and invasion of breast cancer in a Slug-dependent manner. Mol Cancer 2015 ; 14: 28.

Shi Y, Massagué J. Mechanisms of TGFβ signaling from cell membrane to the nucleus. Cell 2003; 113: 685-700.

Shi J, Wang Y, Zeng L, Wu Y, Deng J, Zhang Q, Lin Y, Li J, Kang T, Tao M et al. Disrupting the interaction of BRD4 with diacetylated Twist suppresses tumorigenesis in basal-like breast cancer. Cancer Cell 2014; 25: 210-25.

Shipitsin M, Campbell LL, Argani P, Weremowicz S, Bloushtain-Qimron N, Yao J, Nikolskaya T, Serebryiskaya T, Beroukhim R, Hu M, Halushka MK, Sukumar S, Parker LM, Anderson KS, Harris LN, Garber JE, Richardson AL, Schnitt SJ, Nikolsky Y, Gelman RS, Polyak K. Molecular definition of breast tumor heterogeneity. Cancer Cell 2007; 11: 259-73.

Shirakihara T, Saitoh M, Miyazono K. Differential regulation of epithelial and mesenchymal markers by deltaEF1 proteins in epithelial mesenchymal transition induced by TGFβ. Mol Biol Cell 2007; 18: 3533-44.

Siemens H, Jackstadt R, Hünten S, Kaller M, Menssen A, Götz U, Hermeking H. miR-34 and SNAIL form a double-negative feedback loop to regulate epithelial-mesenchymal transitions. Cell Cycle 2011; 10: 4256-71.

Simpson P. Maternal-Zygotic Gene Interactions during Formation of the Dorsoventral Pattern in Drosophila Embryos. Genetics 1983 ; 105: 615-32.

Singh A, Settleman J. EMT, cancer stem cells and drug resistance: an emerging axis of evil in the war on cancer. Oncogene 2010; 29: 4741-51.

Skromne I, Stern CD. Interactions between Wnt and Vg1 signalling pathways initiate primitive streak formation in the chick embryo. Development 2001; 128: 2915-27.

Sørlie T, Perou CM, Tibshirani R, Aas T, Geisler S, Johnsen H, Hastie T, Eisen MB, van de Rijn M, Jeffrey SS, Thorsen T, Quist H, Matese JC, Brown PO, Botstein D, Lønning PE, Børresen-Dale AL. Gene expression patterns of breast carcinomas distinguish tumor subclasses with clinical implications. Proc Natl Acad Sci U S A 2001; 98: 10869-74.

Spaderna S, Schmalhofer O, Wahlbuhl M, Dimmler A, Bauer K, Sultan A, Hlubek F, Jung A, Strand D, Eger A, Kirchner T, Behrens J, Brabletz T. The transcriptional repressor ZEB1 promotes metastasis and loss of cell polarity in cancer. Cancer Res 2008; 68: 537-44.

Spring J, Yanze N, Middel AM, Stierwald M, Groger H, Schmid V. The mesoderm specification factor twist in the life cycle of jellyfish. Dev Biol 2000; 228: 363-375.

Stingl J. Detection and analysis of mammary gland stem cells. J Pathol 2009; 217: 229-41.

Taki M, Verschueren K, Yokoyama K, Nagayama M, Kamata N. Involvement of Ets-1 transcription factor in inducing matrix metalloproteinase-2 expression by epithelial-mesenchymal transition in human squamous carcinoma cells. Int J Oncol 2006; 28: 487-96.

Thiery JP. Epithelial-mesenchymal transitions in development and pathologies. Curr Opin Cell Biol 2003; 15: 740-6.

Thiery JP, Acloque H, Huang RY, Nieto MA. Epithelial-mesenchymal transitions in development and disease. Cell 2009; 139: 871-90.

Thuault S, Valcourt U, Petersen M, Manfioletti G, Heldin CH, Moustakas A. Transforming growth factorβ employs HMGA2 to elicit epithelial-mesenchymal transition. J Cell Biol. 2006; 174: 175-83.

Thuault S, Tan EJ, Peinado H, Cano A, Heldin CH, Moustakas A. HMGA2 and Smads co-regulate SNAIL1 expression during induction of epithelial-to-mesenchymal transition. J Biol Chem 2008; 283: 33437-46.

Timmerman LA, Grego-Bessa J, Raya A, Bertrán E, Pérez-Pomares JM, Díez J, Aranda S, Palomo S, McCormick F, Izpisúa-Belmonte JC, de la Pompa JL. Notch promotes epithelial-mesenchymal transition during cardiac development and oncogenic transformation. Genes Dev 2004; 18: 99-115.

Tojo M, Hamashima Y, Hanyu A, Kajimoto T, Saitoh M, Miyazono K, Node M, Imamura T. The ALK-5 inhibitor A-83-01 inhibits Smad signaling and epithelial-to-mesenchymal transition by transforming growth factorβ. Cancer Sci 2005; 96: 791-800.

Torre LA, Bray F, Siegel RL, Ferlay J, Lortet-Tieulent J, Jemal A. Global cancer statistics, 2012. CA Cancer J Clin 2015; 65: 87-108.

Tsai JH, Donaher JL, Murphy DA, Chau S, Yang J. Spatiotemporal regulation of epithelial-mesenchymal transition is essential for squamous cell carcinoma metastasis. Cancer Cell 2012; 22: 725-36.

Tun NM, Villani G, Ong K, Yoe L, Bo ZM. Risk of having BRCA1 mutation in high-risk women with triple-negative breast cancer: a meta-analysis. Clin Genet 2014; 85: 43-8.

Valcourt U, Kowanetz M, Niimi H, Heldin CH, Moustakas A. TGFβ and the Smad signaling pathway support transcriptomic reprogramming during epithelial-mesenchymal cell transition. Mol Biol Cell 2005; 16: 1987-2002.

Valentin MD, da Silva SD, Privat M, Alaoui-Jamali M, Bignon YJ. Molecular insights on basal-like breast cancer. Breast Cancer Res Treat 2012; 134: 21-30.

Vallin J, Thuret R, Giacomello E, Faraldo MM, Thiery JP, Broders F. Cloning and characterization of three Xenopus slug promoters reveal direct regulation by Lef/beta-catenin signaling. J Biol Chem 2001; 276: 30350-8.

Van de Putte T, Maruhashi M, Francis A, Nelles L, Kondoh H, Huylebroeck D, Higashi Y. Mice lacking ZFHX1B, the gene that codes for Smad-interacting protein-1, reveal a role for multiple neural crest cell defects in the etiology of Hirschsprung disease-mental retardation syndrome. Am J Hum Genet 2003; 72: 465-70.

Vandewalle C, Comijn J, De Craene B, Vermassen P, Bruyneel E, Andersen H, Tulchinsky E, Van Roy F, Berx G. SIP1/ZEB2 induces EMT by repressing genes of different epithelial cell-cell junctions. Nucleic Acids Res 2005; 33: 6566-78.

van Grunsven LA, Michiels C, Van de Putte T, Nelles L, Wuytens G, Verschueren K, Huylebroeck D. Interaction between Smad-interacting protein-1 and the corepressor C-terminal binding protein is dispensable for transcriptional repression of E-cadherin. J Biol Chem 2003; 278: 26135-45.

Veeman MT, Slusarski DC, Kaykas A, Louie SH, Moon RT. Zebrafish prickle, a modulator of noncanonical Wnt/Fz signaling, regulates gastrulation movements. Curr Biol 2003; 13: 680-5.

Vincent T, Neve EP, Johnson JR, Kukalev A, Rojo F, Albanell J, Pietras K, Virtanen I, Philipson L, Leopold PL, Crystal RG, de Herreros AG, Moustakas A, Pettersson RF, Fuxe J. A SNAIL1-SMAD3/4 transcriptional repressor complex promotes TGFβ mediated epithelial-mesenchymal transition. Nat Cell Biol 2009; 11: 943-50.

Vogt J, Traynor R, Sapkota GP. The specificities of small molecule inhibitors of the TGFß and BMP pathways. Cell Signal 2011; 23: 1831-42.

Wang J, Kuiatse I, Lee AV, Pan J, Giuliano A, Cui X. Sustained c-Jun-NH2-kinase activity promotes epithelial-mesenchymal transition, invasion, and survival of breast cancer cells by regulating extracellular signal-regulated kinase activation. Mol Cancer Res 2010; 8: 266-77.

Wang K, Zhang Q, Li D, Ching K, Zhang C, Zheng X, Ozeck M, Shi S, Li X, Wang H, Rejto P, Christensen J, Olson P3. PEST domain mutations in Notch receptors comprise an oncogenic driver segment in triple-negative breast cancer sensitive to a γ-secretase inhibitor. Clin Cancer Res 2015; 21: 1487-96.

Wang X, Zheng M, Liu G, Xia W, McKeown-Longo PJ, Hung MC, Zhao J. Krüppel-like factor 8 induces epithelial to mesenchymal transition and epithelial cell invasion. Cancer Res 2007; 67: 7184-93.

Wang X, Lu H, Urvalek AM, Li T, Yu L, Lamar J, DiPersio CM, Feustel PJ, Zhao J. KLF8 promotes human breast cancer cell invasion and metastasis by transcriptional activation of MMP9. Oncogene 2011; 30: 1901-11.

Wei SC, Fattet L, Tsai JH, Guo Y, Pai VH, Majeski HE, Chen AC, Sah RL, Taylor SS, Engler AJ, Yang J. Matrix stiffness drives epithelial-mesenchymal transition and tumour metastasis through a TWIST1-G3BP2 mechanotransduction pathway. Nat Cell Biol 2015; 17: 678-88.

Wellner U, Schubert J, Burk UC, Schmalhofer O, Zhu F, Sonntag A, Waldvogel B, Vannier C, Darling D, zur Hausen A, Brunton VG, Morton J, Sansom O, Schüler J, Stemmler MP, Herzberger C, Hopt U, Keck T, Brabletz S, Brabletz T. The EMT-activator ZEB1 promotes tumorigenicity by repressing stemness-inhibiting microRNAs. Nat Cell Biol 2009; 11: 1487-95.

Weston CR, Davis RJ. The JNK signal transduction pathway. Curr Opin Genet Dev 2002; 12: 14-21.

Xie M, Zhang L, He CS, Xu F, Liu JL, Hu ZH, Zhao LP, Tian Y. Activation of Notch-1 enhances epithelial-mesenchymal transition in gefitinib-acquired resistant lung cancer cells. J Cell Biochem 2012; 113: 1501-13.

Xie G, Ji A, Yuan Q, Jin Z, Yuan Y, Ren C, Guo Z, Yao Q, Yang K, Lin X, Chen L. Tumour-initiating capacity is independent of epithelial-mesenchymal transition status in breast cancer cell lines. Br J Cancer 2014; 110: 2514-23.

Xu J, Lamouille S, Derynck R. TGFβ-induced epithelial to mesenchymal transition. Cell Res 2009; 19: 156-72.

Yamamoto KR, Alberts BM. Steroid receptors: elements for modulation of eukaryotic transcription. Annu Rev Biochem 1976; 45: 721-46.

Yamamoto-Ibusuki M, Arnedos M, André F. Targeted therapies for ER+/HER2-metastatic breast cancer. BMC Med 2015; 13: 137.

Yamashita M, Fatyol K, Jin C, Wang X, Liu Z, Zhang YE. TRAF6 mediates Smad-independent activation of JNK and p38 by TGFβ. Mol Cell 2008; 31: 918-24.

Yang F, Sun L, Li Q, Han X, Lei L, Zhang H, Shang Y. SET8 promotes epithelial-mesenchymal transition and confers TWIST dual transcriptional activities. EMBO J 2012 ; 31: 110-23.

Yang J, Mani SA, Donaher JL, Ramaswamy S, Itzykson RA, Come C, Savagner P, Gitelman I, Richardson A, Weinberg RA. Twist, a master regulator of morphogenesis, plays an essential role in tumor metastasis. Cell 2004; 117: 927-39.

Yang L, Lin C, Liu ZR. P68 RNA helicase mediates PDGF-induced epithelial mesenchymal transition by displacing Axin from beta-catenin. Cell 2006 ; 127: 139-55.

Yang L, Huang J, Ren X, Gorska AE, Chytil A, Aakre M, Carbone DP, Matrisian LM, Richmond A, Lin PC, Moses HL. Abrogation of TGF beta signaling in mammary carcinomas recruits Gr-1+CD11b+ myeloid cells that promote metastasis. Cancer Cell 2008; 13: 23-35.

Yang MH, Hsu DS, Wang HW, Wang HJ, Lan HY, Yang WH, Huang CH, Kao SY, Tzeng CH, Tai SK, Chang SY, Lee OK, Wu KJ. Bmi1 is essential in Twist1-induced epithelial-mesenchymal transition. Nat Cell Biol 2010; 12: 982-92.

Yang X, Li L, Huang Q, Xu W, Cai X, Zhang J, Yan W, Song D, Liu T, Zhou W, Li Z1, Yang C, Dang Y, Xiao J. Wnt signaling through Snail1 and Zeb1 regulates bone metastasis in lung cancer. Am J Cancer Re. 2015a; 5: 748-55.

Yang L, Tang H, Kong Y, Xie X, Chen J, Song C, Liu X, Ye F, Li N, Wang N, Xie X. LGR5 Promotes Breast Cancer Progression and Maintains Stem-Like Cells Through Activation of Wnt/β-Catenin Signaling. Stem Cells 2015b [Epub ahead of print].

Yang H, Wang L, Zhao J, Chen Y, Lei Z, Liu X, Xia W, Guo L, Zhang HT. TGF-β-activated SMAD3/4 complex transcriptionally upregulates N-cadherin expression in non-small cell lung cancer. Lung Cancer 2015c; 87: 249-57.

Zavadil J, Cermak L, Soto-Nieves N, Böttinger EP. Integration of TGFβ/Smad and Jagged1/Notch signalling in epithelial-to-mesenchymal transition. EMBO J 2004; 23: 1155-65.

Zawel L, Dai JL, Buckhaults P, Zhou S, Kinzler KW, Vogelstein B, Kern SE. Human Smad3 and Smad4 are sequence-specific transcription activators. Mol Cell 1998; 1: 611-7.

Zhang D, Lin J, Han J. Receptor-interacting protein (RIP) kinase family. Cell Mol Immunol 2010; 7: 243–249.

Zhang J, Zhang H, Liu J, Tu X, Zang Y, Zhu J, Chen J, Dong L, Zhang J. miR-30 inhibits TGF-β1-induced epithelial-to-mesenchymal transition in hepatocyte by targeting Snail1. Biochem Biophys Res Commun 2012; 417: 1100-5.

Zhang D, Sun B1, Zhao X, Ma Y, Ji R, Gu Q, Dong X, Li J, Liu F, Jia X, Leng X, Zhang C, Sun R, Chi J. Twist1 expression induced by sunitinib accelerates

tumor cell vasculogenic mimicry by increasing the population of CD133+ cells in triple-negative breast cancer. Mol Cancer 2014; 13: 207.

Zhang X, Zhao X, Shao S, Zuo X, Ning Q, Luo M, Gu S, Zhao X. Notch1 induces epithelial-mesenchymal transition and the cancer stem cell phenotype in breast cancer cells and STAT3 plays a key role. Int J Oncol 2015; 46: 1141-8.

Zhou BP, Deng J, Xia W, Xu J, Li YM, Gunduz M, Hung MC. Dual regulation of Snail by GSK-3β-mediated phosphorylation in control of epithelial–mesenchymal transition. Nat Cell Biol 2004; 6: 931-940.

Zhou W, Wang G, Guo S. Regulation of angiogenesis via Notch signaling in breast cancer and cancer stem cells. Biochim Biophys Acta 2013; 1836: 304-20.

Zhuge X, Kataoka H, Tanaka M, Murayama T, Kawamoto T, Sano H, Togi K, Yamauchi R, Ueda Y, Xu Y, Nishikawa S, Kita T, Yokode M. Expression of the novel Snai-related zinc-finger transcription factor gene Smuc during mouse development. Int J Mol Med 2005; 15: 945-8.

9. Acknowledgements

I wish to thank several people who made this thesis possible and supported me throughout its course.

First, I would like to thank Dr. Christina Scheel for the opportunity to complete my PhD thesis in a state-of-the-art research environment in her lab. I am grateful for her support, her scientific advice and for everything she has taught me during my PhD.

My thanks also belong to all members of the Scheel group (Johanna Schmidt, Anja Krattenmacher, Elena Panzilius, Jelena Linnemann, Lisa Meixner and Uwe Kloos) for fruitful discussions and a very pleasant working environment. I would also like to acknowledge members of the Institute of Stem Cell Research at the Helmholtz Zentrum München. Special thanks to Stefania Petricca, Melanie Push and Miriam Esgleas for sharing their protocols and technical knowledge.

Furthermore, I want to express my gratitude to our collaborators: Prof. Steven Johnsen and Vivek Mishra at the University of Göttingen for conducting ChIP experiments and finding the enhancer region of ZEB1 where Twist1 binds; Dr. Carsten Marr, Felix Buggenthin and Daniel Schwarz at the ICB – Helmholtz Zentrum München for setting up and analyzing life cell imaging.

I would like to acknowledge the members of my thesis committee, Prof. Heiko Lickert and Prof. Fabian Theis, for great discussions and input.

I wish to thank the German Cancer Aid organization for financial funding and facilitation of this study.

My very special thanks go to my family and friends who have supported me emotionally and motivated me throughout my doctoral thesis.